

INFORMATION TO USERS

This material was produced from a microfilm copy of the original document. While the most advanced technological means to photograph and reproduce this document have been used, the quality is heavily dependent upon the quality of the original submitted.

The following explanation of techniques is provided to help you understand markings or patterns which may appear on this reproduction.

1. The sign or "target" for pages apparently lacking from the document photographed is "Missing Page(s)". If it was possible to obtain the missing page(s) or section, they are spliced into the film along with adjacent pages. This may have necessitated cutting thru an image and duplicating adjacent pages to insure you complete continuity.
2. When an image on the film is obliterated with a large round black mark, it is an indication that the photographer suspected that the copy may have moved during exposure and thus cause a blurred image. You will find a good image of the page in the adjacent frame.
3. When a map, drawing or chart, etc., was part of the material being photographed the photographer followed a definite method in "sectioning" the material. It is customary to begin photoing at the upper left hand corner of a large sheet and to continue photoing from left to right in equal sections with a small overlap. If necessary, sectioning is continued again - beginning below the first row and continuing on until complete.
4. The majority of users indicate that the textual content is of greatest value, however, a somewhat higher quality reproduction could be made from "photographs" if essential to the understanding of the dissertation. Silver prints of "photographs" may be ordered at additional charge by writing the Order Department, giving the catalog number, title, author and specific pages you wish reproduced.
5. PLEASE NOTE: Some pages may have indistinct print. Filmed as received.

Xerox University Microfilms

300 North Zeeb Road
Ann Arbor, Michigan 48106

76-3114

LIN, Chorng-Jen, 1945-
KINETICS AND MECHANISM OF THE OLEFIN
DISPROPORTIONATION REACTION OVER
SUPPORTED RHENIUM OXIDE CATALYSTS.

The University of Oklahoma, Ph.D., 1975
Engineering, chemical

Xerox University Microfilms, Ann Arbor, Michigan 48106

THE UNIVERSITY OF OKLAHOMA
GRADUATE COLLEGE

KINETICS AND MECHANISM OF THE OLEFIN DISPROPORTIONATION
REACTION OVER SUPPORTED RHENIUM OXIDE CATALYSTS

A DISSERTATION
SUBMITTED TO THE GRADUATE FACULTY
in partial fulfillment of the requirements for the
degree of
DOCTOR OF PHILOSOPHY

BY
CHORNG-JEN LIN
Norman, Oklahoma

1975

KINETICS AND MECHANISM OF THE OLEFIN DISPROPORTIONATION
REACTION OVER SUPPORTED RHENIUM OXIDE CATALYSTS

APPROVED BY

Robert Clark
Lucy W. Alder
R. C. Jernier
K. E. Stalling
Stanley C. Kober
DISSERTATION COMMITTEE

ABSTRACT

The kinetics and mechanism of the olefin disproportionation reaction over supported rhenium oxide catalysts were investigated using a fixed bed flow reactor. The catalysts of varying weight percentage of rhenium oxide have been prepared by impregnation, using both γ -alumina and silica as supports.

The steady state kinetics of the disproportionation of mono-deuterated ethylene over 10% $\text{Re}_2\text{O}_7/\text{Al}_2\text{O}_3$ catalyst were measured. The amount of dideuterated ethylene product was determined by the mass spectrograph. This simple reaction has the advantages that the adsorbabilities of reactant and product ethylene are essentially equal, gas phase - surface phase equilibrium exists at all times, and the elucidation of the kinetic picture is much simplified.

The adsorptions of regular ethylene on the catalysts of varying weight percentages of rhenium heptoxide were measured. For the fully oxidized catalysts, probably Re_2O_7 , on both silica and alumina the ethylene adsorption is reversible, with the amount of ethylene adsorbed tending to zero as the ethylene pressure tends to zero. On both silica and alumina supported catalysts which have been partially reduced in hydrogen, the adsorption of ethylene at room temperature becomes slow and partially irreversible. However, with further reduction, the results for alumina supported catalysts differ significantly from those of the

silica supported catalysts. After 15 hours of hydrogen reduction at 500°C, ethylene adsorption on silica supported catalysts again becomes reversible whereas on alumina supported catalysts there is always a significant amount of strong irreversibly held ethylene.

On the alumina supported catalyst the amount of ethylene adsorbed increases with the increase of Re_2O_7 content to about 5%, and then decreases with further increase of rhenium content, due probably to the blocking of the pores.

On the silica supported catalyst the amount of ethylene adsorbed decreases with the increase of Re_2O_7 percentage. The amount adsorbed for the supported catalyst never exceed that of the support alone.

There are indications of the interaction between rhenium oxide and alumina. Rhenium oxide is reduced with greater difficulty on the alumina support. Catalysts supported on silica are inactive for propylene disproportionation up to 180°C whereas the reaction proceed readily on the alumina supported catalysts at room temperature with an activity that decays with time, and is a function of level of prerduction of the oxide.

The isosteric heat of adsorption of ethylene on the unreduced catalyst is in the range of physical adsorption. The entropy change calculated from the isotherms indicates that the adsorption of ethylene is somewhat mobil. At high temperatures the Freundlich type of isotherm fits data better than that of the Langmuir type.

The rates of propylene disproportionation on the reduced catalyst decrease rapidly with reaction time. The initial rates increase with the increase of the time of reduction. With a catalyst reduced for

15 hours, the initial rate at room temperature is about five times that of the unreduced catalyst, the two rates become essentially the same after two hours. On the reduced catalyst the ratio of the product trans-2-butene to cis-2-butene decreases with time, while on the unreduced catalyst the ratio has no appreciable change with time.

It is believed that the irreversible adsorption of both reactant and product is responsible for the rapid decay of activity. Experiments show that reduced catalysts have lower initial rates of propylene disproportionation if the catalyst is exposed to ethylene longer prior to the introduction of propylene. The experiments also show that the reversible part of the ethylene adsorption is independent of the extent of reduction of the reduced catalyst. The ethylene held irreversibly by the reduced catalyst is supposed to be situated on the anion vacancies created by reduction.

All the kinetic data on propylene disproportionation are taken on 10% $\text{Re}_2\text{O}_7/\text{Al}_2\text{O}_3$ catalyst. There is a significant mass transfer effect on the 20% catalyst at room temperature in the flow range studied.

On the disproportionation of propylene, the Langmuir-Hinshelwood mechanism fits data better than the Rideal mechanism which is in agreement with other studies.

On the disproportionation of monodeuterated ethylene, a refined Langmuir Hinshelwood reaction mechanism has been deduced and applied fairly accurately to the experimental results. The reaction is extremely slow at room temperature. The reaction kinetics are obtained at 75 and 95°C.

At high pressures the isotope effect on the adsorption of

ethylene is relatively small. The fact that the adsorption equilibrium exists in this steady state kinetics made possible the correlation between the rate of reaction and the amount of adsorption.

ACKNOWLEDGMENTS

The author would like to express his sincere appreciation to Dr. Alfred Clark and Dr. Arthur W. Aldag, Jr. for their continued guidance during the course of this investigation. The author is also indebted to the other members of his advisory committee, Dr. K. E. Starling, Dr. S. C. Neely and Dr. R. C. Jerner for their interest in this program and review of this work.

Acknowledgment is made to the Donors of the Petroleum Research Fund administered by the American Chemical Society, for the support of this research.

Finally, the author wishes to thank his grandparents, parents, and his wife for their encouragement throughout this work.

TABLE OF CONTENTS

	Page
LIST OF TABLES.....	x
LIST OF FIGURES	xiii
Chapter	
I. INTRODUCTION.....	1
II. LITERATURE REVIEW.....	4
A. Disproportionation Reaction.....	4
B. Disproportionation Catalysts.....	5
C. Disproportionation Mechanism.....	7
D. Rhenium Oxide Catalyst.....	16
E. Catalyst Support.....	22
F. Adsorption of Ethylene.....	26
G. C ₂ H ₃ D Disproportionation Over MoO ₃ /Al ₂ O ₃ Catalyst.....	33
III. THEORETICAL BACKGROUND.....	35
A. Adsorption Isotherms.....	35
B. Heat of Adsorption.....	37
C. Entropy of Adsorption.....	38
D. Mass Transfer Effects.....	39
E. Reaction Rate and Reaction Mechanism.....	40
F. Mechanistic Equations.....	43
G. Reaction Rate Versus the Amount of Adsorption.....	46

Chapter	Page
IV. EXPERIMENTAL APPARATUS.....	48
V. EXPERIMENTAL PROCEDURE.....	55
A. Preparation of the Supported Rhenium Oxide Catalysts...	55
B. Activation of the Catalyst.....	56
C. Procedure of Ethylene Adsorption.....	56
D. Procedure of the Measurement of the Reaction Rate.....	57
VI. RESULTS AND DISCUSSION.....	59
A. Adsorption of Ethylene on the Supported Rhenium Oxide Catalysts.....	59
B. Disproportionation of Propylene.....	77
C. Disproportionation of Monodeuterated Ethylene on Unreduced Catalyst.....	90
VII. CONCLUSION AND RECOMMENDATION.....	104
NOMENCLATURE.....	107
BIBLIOGRAPHY.....	110
APPENDICES.....	115
A. Gas Chromatographic Analysis of the Products From the Disporportionation of Propylene.....	116
B. Mass Spectrographic Analysis of the Products From the Disproportionation of Monodeuterated Ethylene.....	119
C. Least Square Fitting of the Adsorption Data to the Various Adsorption Isotherms.....	122

LIST OF TABLES

TABLE	PAGE
1. Physical Properties and Oxidation States of Oxides and Sulfides of Rhenium and its Neighboring Elements.....	18
2. Classification of Metals and Semimetals Based on Adsorption Properties.....	31
3. A Selection of Adsorption Isotherms.....	36
4. The Adsorption of Ethylene at Room Temperature with the Blank Adsorption Cell.....	60
5. The Heats of Adsorption and the Entropies of Adsorption of Ethylene on Alumina.....	67
6. The Heats of Adsorption and the Entropies of Adsorption of Ethylene on 10.95% $\text{Re}_2\text{O}_7/\text{Al}_2\text{O}_3$ Catalyst.....	67
7. The Heats of Adsorption and the Entropies of Adsorption of Ethylene on 10.81% $\text{Re}_2\text{O}_7/\text{Al}_2\text{O}_3$ Catalyst.....	68
8. The Heats of Adsorption and the Entropies of Adsorption of Ethylene on 11.06% $\text{Re}_2\text{O}_7/\text{SiO}_2$ Catalyst.....	68
9. The Adsorbabilities of the Reused Catalysts.....	75
10. The Amount of Irreversible Adsorption of Ethylene on the Alumina Supported Rhenium Oxide Catalysts.....	75
11. Results for the Disproportionation of Propylene at Room Temperature and 1 Atmosphere on 21.39% $\text{Re}_2\text{O}_7/\text{Al}_2\text{O}_3$ Catalyst....	80

TABLE	PAGE
12. Results for the Disproportionation of Propylene at Room Temperature and 1 Atmosphere on 9.94% $\text{Re}_2\text{O}_7/\text{Al}_2\text{O}_3$ Catalyst....	80
13. Effect of Catalyst Particle Size on Reaction Rate.....	83
14. Activities of the 10.95% $\text{Re}_2\text{O}_7/\text{Al}_2\text{O}_3$ Catalyst Versus Time in Propylene Stream.....	83
15. Rates of Reaction of Propylene Disproportionation on 10.95% $\text{Re}_2\text{O}_7/\text{Al}_2\text{O}_3$ at 25°C, and 1 Atmosphere Pressure.....	85
16. Rates of Reaction of Propylene Disproportionation on 10.95% $\text{Re}_2\text{O}_7/\text{Al}_2\text{O}_3$ at 40°C, and 1 Atmosphere Pressure.....	85
17. Rates of Reaction of Propylene Disproportionation on 10.95% $\text{Re}_2\text{O}_7/\text{Al}_2\text{O}_3$ at 68°C, and 1 Atmosphere Pressure.....	85
18. Results of the Least Square Fitting of the Rate Data for Propylene Disproportionation on 10.95% $\text{Re}_2\text{O}_7/\text{Al}_2\text{O}_3$ Catalyst...	86
19. Effect of Time of Reduction on the Initial Rate of the Disproportionation of Propylene.....	89
20. Effect of Pre-adsorption of Ethylene on the Initial Rate of the Disproportionation of Propylene at Room Temperature.....	89
21. Adsorption of C_2H_4 and $\text{C}_2\text{H}_3\text{D}$ at 22°C on 10.81% $\text{Re}_2\text{O}_7/\text{Al}_2\text{O}_3$ Catalyst.....	91
22. Isotope Effect on the Adsorption of Ethylene at 22°C.....	91
23. The Composition of the Equilibrium Products of the Disproportionation of $\text{C}_2\text{H}_3\text{D}$ on 10.81% $\text{Re}_2\text{O}_7/\text{Al}_2\text{O}_3$	93
24. Results for the disproportionation of $\text{C}_2\text{H}_3\text{D}$ over Unreduced 10.81% $\text{Re}_2\text{O}_7/\text{Al}_2\text{O}_3$ Catalyst at 75°C, and 95°C.....	93

TABLE	PAGE
25. Results of the Least Square Fitting of the Rate Data for the Disproportionation of C_2H_3D on 10.81% Re_2O_7/Al_2O_3 Catalyst at 75°C, and 95°C.....	94
26. Adsorption of C_2H_4 at 75°C on 10.81% Re_2O_7/Al_2O_3	95
27. Adsorption of C_2H_4 at 95°C on 10.81% Re_2O_7/Al_2O_3	96
28. Correlation of the Reaction Rate of the Disproportionation of C_2H_3D with the Amount of Adsorption at 75°C on 10.81% Re_2O_7/Al_2O_3	98
29. Correlation of the Reaction Rate of the Disproportionation of C_2H_3D with the Amount of Adsorption at 95°C on 10.81% Re_2O_7/Al_2O_3	99
30. Substance-Specific Correction Factors for Thermoconductivity Cells Using Helium as Carrier Gas.....	118

LIST OF FIGURES

FIGURE	PAGE
1. Structure of a Molybdenum-Diolefin Complex.....	11
2. Surface Complex of Ethylene Disproportionation.....	12
3. The Structure of ReO_2 , ReO_3 , and Re_2O_7	21
4. Five Types of Isotherms According to Brunauer et al.....	26
5. Apparatus for the Adsorption of Ethylene and the Disproportionation of Propylene.....	49
6. Apparatus for the Disproportionation of Deuterated Ethylene...	53
7. Adsorption of Ethylene at Room Temperature on the Unreduced Alumina-Supported Catalysts.....	61
8. Adsorption of Ethylene at Room Temperature on the Unreduced Silica-Supported Catalysts.....	63
9. Adsorption of Ethylene at Various Temperatures on the Unreduced Alumina-Supported Catalysts.....	65
10. Adsorption of Ethylene at 1°C and 25°C on the Unreduced and the Reduced 11.06% $\text{Re}_2\text{O}_7/\text{SiO}_2$ Catalysts.....	66
11. Adsorption of Ethylene at Room Temperature on the Reduced Silica-Supported Catalysts.....	70
12. Adsorption of Ethylene at Room Temperature on 10% $\text{Re}_2\text{O}_7/\text{Al}_2\text{O}_3$ Catalysts of Different Times of Reduction at 500°C	71

FIGURE	PAGE
13. Adsorption of Ethylene at Room Temperature on the 15 hours Reduced Alumina-Supported Catalysts.....	72
14. The Rate of Adsorption of Ethylene at Room Temperature on the 15 hours Reduced 10.95% $\text{Re}_2\text{O}_7/\text{Al}_2\text{O}_3$ Catalyst.....	74
15. Reversible Adsorption of Ethylene at Room Temperature on the Reduced 10.95% $\text{Re}_2\text{O}_7/\text{Al}_2\text{O}_3$ Catalysts.....	78
16. Percent Conversion of Propylene Versus W/F for 21.39% and 9.94% $\text{Re}_2\text{O}_7/\text{Al}_2\text{O}_3$ Catalysts.....	81
17. The Rate of Propylene Disproportionation Versus Time on 10.95% $\text{Re}_2\text{O}_7/\text{Al}_2\text{O}_3$ Catalyst.....	87
18. The Ratio of Trans-2-Butene to Cis-2-Butene Versus Time for the Disproportionation of Propylene on 10.95% $\text{Re}_2\text{O}_7/\text{Al}_2\text{O}_3$ Catalyst.....	87

CHAPTER I.

INTRODUCTION

The kinetic study of chemical reactions is not only interesting from a scientific point of view, but is also very important for the rational design and operation of chemical processes in the laboratory as well as in the plant. Moreover, kinetic analysis is a working tool that may lead the way to new paths of chemical synthesis. The kinetic analysis elucidates in detail the mode of activation of chemical systems and establishes the intimate mechanism of the fundamental chemical reaction. Thus it provides the basic information required to develop new reactions. Without it, this must be left to chance or to laborious experimentation.

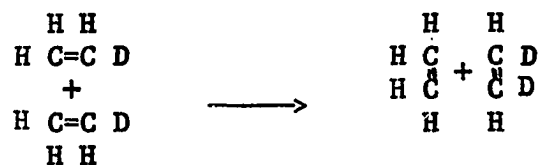
Surface catalysis is a phenomenon which is difficult to observe and measure. One of the most important application of the kinetic study of the catalytic reaction is the determination of reaction mechanism. No matter how well a given mechanism fits the basic observations and specific tests, it is always possible that some different mechanism, which represents the data just as well, will be discovered later. The confidence which can be placed in the correctness of a mechanism increases with the number, variety, and accuracy of the measurements upon which it is based.

Most of the catalytic reactions are complex, and difficult to predict and explain. During the past two decades tremendous efforts have

been made to study both the interaction of gas molecules and atoms at the catalyst surface and the structure of the catalyst itself. The establishment of an adequate theory is still in its scientific infancy, but all the research tools of science have been brought to bear on the continuing search for a better understanding of the detailed mechanisms through which catalysts are able to function.

The object of this work is to study the kinetics and mechanism of the olefin disproportionation reaction over supported rhenium oxide catalysts. The reaction proceeds in a highly specific and efficient manner, and therefore is a good one for the kinetic study.

In this work ethylene tagged with deuterium is used to study the disproportionation reaction. The reaction proceeds as follow:



Olefin disproportionation has been investigated rather extensively in both homogeneous and heterogeneous systems, but there is no report on the kinetics using tagged ethylene. The use of ethylene has the following advantages:

- (1). Ethylene is the simplest olefin molecule.
- (2). Complications from side reactions, such as double bond isomerization which occurs with 1-butene, are absent.
- (3). Gas phase - surface phase equilibrium exists at all times.
- (4). Surface concentrations of ethylene are known during the reaction.
- (5). Adsorbabilities of reactant and product ethylene are equal, within the limits of an isotope effect which is estimated to be small.

The supported rhenium oxide catalyst is active at room temperature and even lower, making adsorption studies simpler than similar studies on molybdena and tungsten oxide catalysts both of which become active only at much higher temperatures.

The adsorption isotherms of ethylene are determined volumetrically over catalysts of different concentrations of rhenium oxide on alumina or on silica. A high vacuum adsorption system was constructed. The disproportionation reaction proceeds during the adsorption measurements, but it can be observed for ethylene only when tagged molecules are used. Adsorption at various temperatures have been measured in order to calculate the isosteric heat of adsorption, and the entropy change during adsorption. The adsorptions on the catalysts of different extent of reduction have also been investigated. Catalysts with different supports behave differently.

Due to the high cost of the tagged ethylene, propylene is used first for the study of the kinetics of the disproportionation reaction over the supported rhenium oxide catalysts. The reaction rates are measured at various temperatures with catalysts of varying percentage of rhenium oxide. Mass transfer effect has been taken into consideration. The effect of oxidation state of the catalyst on the kinetics of propylene disproportionation is also studied.

The disproportionation of monodeuterated ethylene is investigated at 75 and 95°C. A refined Langmuir-Hinshelwood mechanism is deduced, and a correlation between the reaction rate and the amount of adsorption has been established.

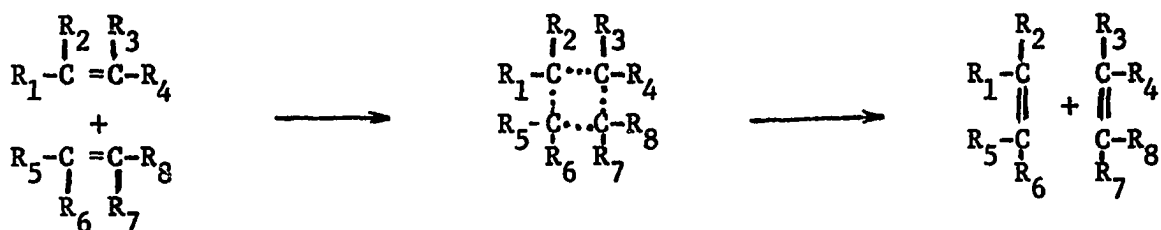
CHAPTER II

LITERATURE REVIEW

A. Disproportionation Reaction:

A new catalytic reaction of olefins was discovered by Banks and Baily in 1964, which they called olefin disproportionation.² By this reaction linear olefins were converted into homologs of shorter and longer chains in a highly specific manner. Olefin dismutation⁸ or olefin metathesis^{12,13} are other names for this reaction used by other investigators.

For acyclic mono-olefins the reaction can be depicted as follows:



where the R is hydrogen or hydrocarbon group.¹⁵ If both reactant molecules are identical and symmetrical about the double bond, no disproportionation will be observed. Disproportionation reactions have also been reported for diolefins, acetylenes, and cyclic olefins.¹ A non-catalytic counterpart of this reaction was reported by Schneider and Frolich in 1931 for the pyrolysis of propylene.⁵⁹

B. Disproportionation Catalysts:

Both homogeneous and heterogeneous catalysts have been reported to be active for olefin disproportionation. A homogeneous catalyst system was disclosed by Calderon et al. in 1967.¹² The catalyst was obtained by the interaction of tungsten hexachloride, ethanol, and ethylaluminum dichloride. None of the components alone was active for disproportionation or double bond isomerization of the olefin. Equilibrium conversions were obtained in two minutes or less at room temperature. Wang and Menapace⁶⁶ use a mixture of tungsten hexachloride and n-butyl lithium to study 2-pentene disproportionation. Another homogeneous system was reported by Zuech.⁶⁴ Treatment of the green nitrosyl complexes $L_2Cl_2(NO)_2M$ (M= Mo or W, L= Ph_3P , C_5H_5N , Ph_3PO etc.) with a variety of alkylaluminum halides in chlorobenzene yields brown homogeneous solutions, which are very active catalysts for disproportionation at low temperatures (0-50°C.).

In the heterogeneous catalyst system a wide variety of solid materials were active for olefin disproportionation. They fall into the category of supported catalysts, comprising a high surface area refractory support on which a promoter is deposited. Useful supports include oxides of silicon, aluminum, thorium, zirconium, magnesium, and titanium; phosphates of aluminum, zirconium, magnesium, and titanium; phosphates of aluminum, zirconium, titanium, magnesium, and calcium; and mixed oxides of some of these metals.²⁸ Active promoters include hexacarbonyls, oxides, and sulfides of molybdenum and tungsten; and oxides of rhenium, lanthanum, tin, iridium, ruthenium, osmium, niobium, tantalum, and tellurium.^{28,10} The various combinations differ somewhat in activity. Compositions having highest activities were tungsten and molybdenum oxides

on silica, alumina, or aluminum phosphate.²⁸ Activation of either the support or the finished catalyst is necessary, presumably to remove water and other adsorbed compounds that acts as poisons, and possibly to promote the formation of specific atomic configurations on the surface.

In the preparation of the tungsten, molybdenum, and rhenium hexacarbonyl catalysts, the alumina support was preactivated and allowed to contact only inert materials during impregnation with the promoter.² In most other preparations, the finished catalyst was activated by passing a stream of inert gas, optionally containing oxygen, over the catalyst at elevated temperatures. Wide ranges of temperatures and times have been reported but in a high proportion of the examples the catalysts were activated at 540 to 595°C for several hours. Since water and other polar compounds are reported to be poisons²⁶ these must be removed during activation. Some chemical interaction of promoter and support may be necessary in the case of oxides, and this reaction may be facilitated by the high activation temperature.

Activity and selectivity were increased by a controlled treatment after activation with reducing gases; such as carbon monoxide or hydrogen, however, such treatment was not necessary to obtain good activity.

Water, air, acetone, carbon monoxide, hydrogen, and methanol in the feed were temporary poisons. They decreased the catalyst activity, but on introduction of pure feed the original activity was recovered.²⁶

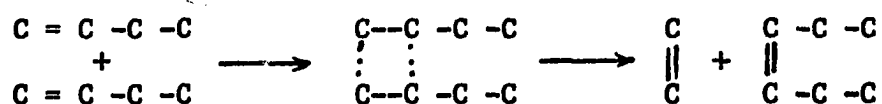
The catalyst activity could be increased by treating the feed. Heckelsberg²⁹ showed that treating a feed with tributyl phosphine increased the conversion of 2-pentene over a tungsten oxide-silica catalyst. Alkema and Van Helden found that the activity and life of molybdenum oxide-alumina and rhenium oxide alumina catalysts were increased by adding

molecular hydrogen to the olefin feed. Pennella and Banks⁵⁵ also reported the higher conversion of propylene over a tungsten oxide on silica catalyst through the addition of small amounts of polyolefins to the propylene feed.

Catalysts that were deactivated during use were regenerated by repeating the activation procedure with a controlled amount of oxygen to burn off accumulated coke.

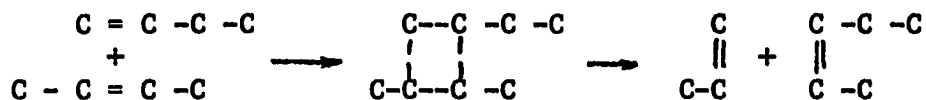
C. Disproportionation Mechanism:

Bradshaw, Howman, and Turner⁸ were the first to publish a four-center type of intermediate to explain olefin disproportionation. They conducted a series of experiments on the disproportionation of 1-butene using cobalt molybdate catalyst. The clue to the mechanism came from the observation that selectivity to ethylene and hexene varied inversely as the isomerization of 1-butene to 2-butene. They then treated the catalyst with varying amounts of sodium bicarbonate to poison isomerization sites and made a series of runs with these catalysts under identical conditions. The results showed even more clearly the effect of isomerization on selectivity to ethylene and hexenes. They also studied the reaction of ethylene with cis-2-butene and with 4-methyl-2-pentene over the catalyst. All of their results were consistent with a mechanistic scheme which they pictured as following for the 1-butene reactions:

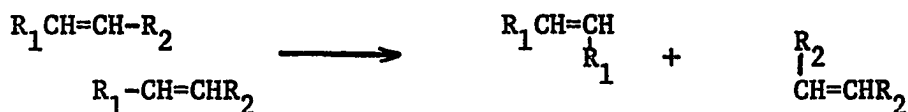


They called the intermediate compound "quasi-cyclobutane".

Further reactions may follow by isomerization of 1-butene to 2-butene and disproportionation of the two isomers:



As an alternative to the transalkylidenation mechanism described above, Calderon et al.¹³ also considered the possibility of a transalkylation mechanism which they described as involving the interchange of alkyl groups via scission α to the double bond:



where R_1 and R_2 are alkyl groups.

They conducted experiments with 2-butene- d_8 designed to distinguish between transalkylation and transalkylidenation. 2-butene- d_8 was reacted with 2-butene and 3-hexene in the presence of the homogeneous tungsten complex catalyst. In both cases only one new product was found, and it had a mass consistent with the four-center mechanism.

Further evidences in support of the four center, quasi-cyclobutane intermediate were obtained by Mol, Monlijn, and Boelhouwer,⁵² and by Clark¹⁵ through application of the radioactive carbon isotope C^{14} .

Mol and co-workers reported that they reacted propylene labeled with C^{14} in each of the three positions, over rhenium oxide-alumina catalyst at moderate temperatures. With 2- C^{14} -propylene, the ethylene formed showed no radio-activity at all, in contrast with the butenes, which showed a specific radioactivity twice as much as that of the starting material. A linear mechanism, as suggested by Dowden,²²

$$2 \text{C} = \text{C}^* - \text{C} \longrightarrow (\text{C} - \text{C}^* - \text{C} - \text{C} - \text{C}^* - \text{C}) \longrightarrow \text{C} = \text{C}^* + \text{C} - \text{C} = \text{C}^* - \text{C}$$

is excluded by this experimental result.

Experiments with 1-C¹⁴-propylene and 3-C¹⁴-propylene showed that the two methyl groups retain their identity throughout the disproportionation. This excluded an allylic intermediate as has been proved for the oxidation reaction of propylene.

Clark used propylene labeled in the one and two positions and cobalt-molybdate catalyst. With 1-C¹⁴-propylene, only the ethylene product showed radioactivity. To carry out the experiment successfully, it was necessary to avoid isomerization of the 1-C¹⁴-propylene to 3-C¹⁴-propylene. For this reason, the temperature was kept as low as possible (80°C), consistent with sufficient reaction products for accurate detection. The results support the postulated four center mechanism. As the temperature of the reaction is increased above 80°C, disproportionation of 1-C¹⁴-propylene yields products with an increasing amount of radioactivity in the butenes as a result of isomerization to 3-C¹⁴-propylene, until, at 160°C, nearly as much C¹⁴ is present in the butenes as in the ethylene.

Mol and co-workers⁵¹ later proposed that a four-center intermediate forms with the abstraction of hydrogen atoms by the catalyst, so that a cyclobutadiene intermediate is formed instead of the cyclobutane structure. The experiment of Calderon and co-workers¹³ with butene plus deuterated butene would appear to rule out that mechanism for the homogeneous catalyst system because it should give a random distribution of hydrogen and deuterium on carbon atoms 2 and 3 of butene which was not observed. Experiments by Craine¹⁹ also indicated that the cyclobutadiene mechanism was not likely to occur with heterogeneous catalysts. He passed ethylene with 2,3-dimethyl-2-butene over a molybdena-alumina catalyst

treated with potassium hydroxide and obtained isobutene as the only product. The cyclobutadiene mechanism would require the migration of two methyl groups and two hydrogen atoms to the catalyst and their return to the same carbon atoms. The inability to detect methylbutenes, propylene, or n-butenes in the product makes the possibility of a cyclobutadiene intermediate remote.

There are many other reactions in which the evidence for a four center mechanism is favorable. Among them are the dehydrogenation of 1-butene over chromia-alumina catalyst and the polymerization of propylene over nickel oxide-silica alumina catalyst.

A more detailed picture of the intermediate complex has been proposed recently by Hughes³² for the homogeneous system, and by Lewandos and Pettit³⁹ for the heterogeneous system.

Hughes³² studied the kinetics and mechanism of the homogeneous disproportionation of 2-pentene to 2-butene and 3-hexene using a $L_2Mo(NO)_2Cl_2 - R_xAlCl_{3-x}$ catalyst. It was shown that the rate of disappearance of 2-pentene was first order in catalyst and variable order in olefin. At low olefin catalyst ratios the order was greater than one; at higher olefin catalyst ratios the order was approximately one. These results were interpreted in terms of a mechanism involving stepwise, rapid reversible olefin complexation followed by a rate-determining disproportionation step. It was suggested that the disproportionation of two olefins occurred via a molybdenum-diolefin complex of the structure shown in Fig. 1.

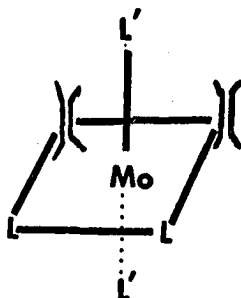


Fig. 1. Structure of a molybdenum-diolefin complex.

A cis-diolefin complex intermediate has been proposed for the tungsten-catalyzed reaction.¹³ The metal-olefin bonding was depicted with the olefinic bonds perpendicular to the plane of the molybdenum and the ligand L. The sigma component of the Mo-olefin bond was formed by overlap of metal sigma type acceptor orbitals with olefin pi-orbitals. Disproportionation occurred by a disrotation of the two complexed olefins which resulted in positive overlap of the pi orbitals which eventually became the product olefin sigma bonds. At the same time the sigma bonds of the reactant olefins were broken and rehybridization to p-pi orbitals which formed the product pi-bonds.

Using the concepts of molecular orbital symmetry conservation which had been applied successfully by Hoffman and Woodward⁶⁸ to various types of electrocyclic reactions, an interpretation of the role of the metal in the catalyzed olefin cyclodimerization reaction had been offered.⁴⁵ A similar rationale would apply to the disproportionation reaction. The important point was that the function of the metal was to provide, through complex formation, low energy molecular orbitals of the proper symmetry.

Lewandos and Pettit³⁹ studied the disproportionation of ethylene over molybdena on alumina catalyst. It was supposed that if the disproportionation of ethylene with itself were to proceed via a transition

state resembling cyclobutane, then cyclobutane should be one of the products. Treatment of ethylene with the catalyst does indeed produce cyclobutane but only in extremely low yields ($< 0.1\%$). In contrast, under similar conditions, ethylene undergoes the disproportionation with itself to an extent that at least 35% of the molecules present enter into reaction which leads to the disproportionation products. This value was obtained through the use of monodeuteroethylene and by measuring the amount of $C_2H_2D_2$ produced. Furthermore, cyclobutane reacts with the catalyst under similar conditions to produce ethylene but again only in extremely low yields (3%). It was clear that the activation energy for the two reactions (disproportionation versus cyclobutane formation and cleavage) are different and that different transition states must therefore be involved.

It was suggested that the four carbon atoms of the intermediate are not to be considered as a cyclobutane ring. They proposed that the ethylene molecules first react with the metal to form a bis-ethylene pi-complex I which reorganizes to a multicentered organometallic system II in which the bonding is most conveniently described as resulting from the interaction of a basic set of metal atomic orbitals and form methylenic units. A more detailed description is given in Fig. 2.

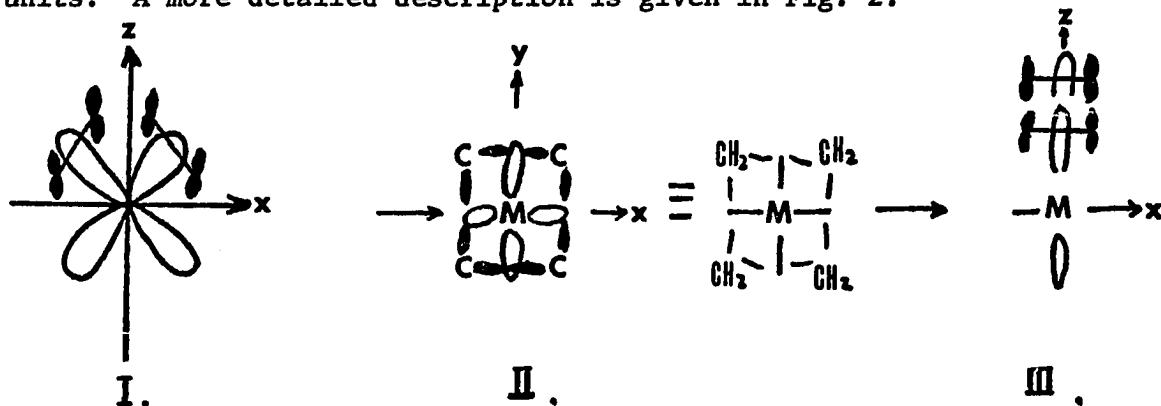


Fig. 2. Surface complex of ethylene disproportionation.

The carbon-carbon sigma bonds of the initial olefins are ruptured concurrently with the pi bonds, so that a cyclobutane molecule is never realized. An orbital symmetry correlation diagram for a concerted reaction is presented to illustrate that an allowed pathway exists to reach the tetramethylene-metal intermediate.

The disproportionation was slightly stereospecific under some conditions, but sufficient data have not been reported for a conformational interpretation. The results of Banks and Bailey for disproportionation over cobaltmolybdate showed that with 1-pentene feed at 95°C, the cis/trans ratio of 2-butene in the product (resulting from disproportionation of isomerized feed or product) was greater than equilibrium. The cis/trans ratio of 2-pentene was less than equilibrium in the product made by disproportionation of propylene or butenes.

Calderon and co-workers¹³ reported that with $WCl_6 \cdot EtOH \cdot EtAlCl_2$ catalyst, regardless of the structure of the starting 2-pentene, the initially formed butenes and hexenes were somewhat higher in cis-content than the equilibrium values. Working with $WCl_6 \cdot BuLi$ catalyst, Wang and Menapace⁶⁶ formed a higher ratio of trans/cis butene in the product from trans-2-pentene than from cis-2-pentene. Hughes³¹ studied the disproportionation of 2-pentene with a soluble molybdenum catalyst. The results in marked contrast to those obtained in the tungsten system, reveal that the molybdenum catalyst exhibits a high degree of stereoselectivity. The distribution of cis- and trans-isomers of the three olefins, namely, 2-pentene, 2-butene, and 3-hexene, attains an equilibrium value independent of the nature of the starting 2-pentene; which indicates that the final composition is thermodynamically controlled. However, examination of the

reactions in their early stages reveals that the initial isomer distribution in the product is dependent upon the isomeric nature of the starting 2-pentene, i.e., they are kinetically controlled. Cis-2-pentene disproportionates preferentially to cis-2-butene and cis-3-hexene and that trans-2-pentene reacts to yield preferentially trans-2-butene and trans-3-hexene. It was also found that the rate of disproportionation and the rate of isomerization decrease simultaneously which implies that the two processes are intimately connected and probably occur on the same catalyst. The stereoselectivity was rationalized in terms of a molybdenum-diolefin complex intermediate. It also suggested that isomerization should proceed at a slower rate than disproportionation due to the sterically unfavorable configuration that led to isomerization.

Davie, Whan and Kemball²¹ reported the disproportionation reactions of the three linear butenes on a supported molybdenum hexacarbonyl catalyst. They suggested different mechanism for the interconversion of cis- and trans-2-butenes, and for the interconversion of 1-butene and the 2-butenes. Cis-trans isomerization is shown to occur by a bimolecular reaction of the disproportionation type, while the double bond shift process displays characteristics of a monomolecular reaction where a vacant site is required adjacent to the site on which the reacting molecule is adsorbed.

Kinetic studies of the disproportionation of propylene over molybdena-alumina catalyst both by Lewis⁴¹ and by Moffat⁴⁷ indicate that the reaction proceeds by a Langmuir-Hinshelwood mechanism in which both interacting olefin molecules are adsorbed.

The true surface kinetics of olefin disproportionation over tungsten oxide-silica catalyst are clouded by diffusion-controlled

reaction under all conditions studied.^{48,49} Begley and Wilson⁴ studied the propylene disproportionation using an integral reactor and found that the Rideal model correlate the data better than the Langmuir-Hinshelwood model. But later others have shown that the system of Begley and Wilson had severe mass transfer limitation. Luckner and co-workers⁴³ also studied the disproportionation of propylene over 10% WO_3/SiO_2 catalyst. The initial rate data were taken under the condition where the interphase and intraparticle mass transfer effects were negligible. It appeared that the experimental data were well correlated by the Langmuir-Hinshelwood mechanism.

Olefin disproportionation over molybdena-alumina catalyst reveals an unusual kinetic phenomena:⁴⁷ a rate-temperature maximum at constant space velocity and pressure of reactant. The phenomena is reversible. The reaction is not well understood, but it is consistent with a Langmuir-Hinshelwood model applied to a surface with a spectrum of adsorption-site energies.

Luckner and Wills⁴⁴ also reported the transient kinetics of the disproportionation of propylene over a tungsten oxide on silica catalyst. The catalyst exhibits a "break in" period before reaching the steady state. It was shown that the initial oxidation state of the tungsten influenced the rate of break-in, but that break-in was not merely a result of reduction. Catalyst with lower oxidation state of tungsten shows higher rate of disproportionation. Some data are presented to establish that both a reduction of the catalyst and the irreversible adsorption of propylene accompany the period of transient activity.

Moulijn²¹ had proposed another mechanism on disproportionation:



His proposal is based on the recent work of Cassar et al.¹⁴ who studied the valence isomerization of cubane to syntricyclooctadiene where a non-concerted reaction that proceeds via a five-member ring was suggested. Very recently Grubbs and Brunck²⁵ reported also experimental evidence for this scheme.

D. Rhenium Oxide Catalyst:

Catalysts consisting of rhenium oxide on alumina are notable for their disproportionation activity at relatively low temperatures. Typical catalysts studied by British Petroleum Company Ltd. were made by impregnating alumina with an aqueous solution of ammonium perrhenate, drying and then activating in a stream of dry air for two hours at 550°C followed by dry nitrogen for one hour.⁹ Suitable concentrations of rhenium oxide were said to range from about 0.1 to 30%. Typical catalysts contained 14-20% rhenium oxide. Reaction temperatures in the range 20-100°C were preferred. At 25°C, atmospheric pressure, and a 1600 gas hourly space velocity, 38% of a 1-butene feed was converted into ethylene and hexene with 95.5% efficiency.

Rhenium oxide on silica prepared by mechanical mixing was reported by Heckelsberg, Banks and Bailey.²⁸ This catalyst was unusual in showing activity maxima in two separate temperature regions, 200 and 480°C.

The increased availability of rhenium and greater knowledge of its chemistry have stimulated increased research on its catalytic applications.²⁰ World production is about five metric tons a year.⁵⁴ Rhenium falls below manganese and technetium in Group VII of the periodic table.

However, rhenium differs considerably from manganese in its chemical and catalytic properties, just as tungsten differs from chromium. Rhenium is most stable in the +7 state. Some of the physical properties and oxidation states of oxides and sulfides of rhenium and its neighboring elements were summarized in Table 1.

In many respects rhenium occupies an intermediate position between tungsten and the platinum metals. In mixed oxides³⁴ rhenium has been found in all oxidation states from +3 to +7; e.g. $\text{NaRe}^{+7}\text{O}_4$, $\text{Ba}_2\text{MgRe}^{+6}\text{O}_6$, $\text{Cd}_2\text{Re}_2^{+5}\text{O}_6$, $\text{Na}_2\text{Re}^{+4}\text{O}_3$, and $\text{LiRe}^{+3}\text{O}_2$. Compounds where rhenium formally has a fractional oxidation state are also known, e.g. $\text{La}_4\text{Re}_6^{+4.3}\text{O}_{19}$, $\text{Na}_{0.9}\text{Re}^{+5.1}\text{O}_3$, and $\text{K}_{0.3}\text{Re}^{+5.7}\text{O}_3$. However, in the binary Re-O system,⁵⁷ ReO_2 , ReO_3 , and Re_2O_7 are well characterized and examined in detail. A tetragonal Re_2O_5 has been reported by Trabalat et al. Other forms which have been reported are:²³ Re_3O_8 , $\text{Re}_2\text{O}_3 \cdot x\text{H}_2\text{O}$, $\text{ReO} \cdot \text{H}_2\text{O}$, $\text{Re}_2\text{O} \cdot 2\text{H}_2\text{O}$. The di- and sesqui-oxides are stable ionic compounds.

Chemically, Re_2O_7 is extremely sensitive to moisture, and early reports of a peroxide Re_2O_8 seem to have been occasioned by the presence of trace of water in the heptoxide.⁶³ Re_2O_7 is always produced when rhenium compounds are ignited in oxygen; it can be made by heating metallic rhenium in oxygen at any temperature above 150°C, or by evaporating an aqueous solution of perrhenic acid HReO_4 to dryness. The ordinary form is yellow and melts at 304°C and boils at 350°C. It is mostly covalent and is easily soluble in water. The heptoxide is reduced by hydrogen at 300°C to the dioxide, and at 500°C to the metal. CO and SO_2 reduce Re_2O_7 slowly in the cold, and rapidly on heating to the coloured lower oxides.

Re_2O_7 is orthorhombic at room temperature, and is supposed to have polymeric structure in the solid state. Its vapor is monomeric; this

Table 1. Physical Properties and Oxidation States of Oxides and Sulfides of Rhenium and its neighboring Elements.²⁰

Group	VI	VII	VIII		
Element	Tungsten	Rhenium	Osmium	Iridium	Platinum
Atomic No.	74	75	76	77	78
Electronic Structure:					
Hafnium Core					
+					
5d	4	5	6	7	8
6s	2	2	2	2	2
Density	19.3	21.0	22.6	22.6	21.4
M.P. (°C)	3140	3170	3045	2440	1770
B.P. (°C)	5927	5630	5000	4500	3800
Atomic Radius (Å)	1.41	1.37	1.35	1.36	1.39
Oxidation States of Oxides	6,4	7,6,4,3	8,4	6,4,3	4,3,2
Oxidation State of Sulfides	6,4	7,4	2	6,4,3,2	4,2

implies that in this phase the metal atom is in a tetrahedral environment.

Anhydrous $\text{Al}(\text{ReO}_4)_3$ is obtained by heating Re_2O_7 with Al_2O_3 in a sealed tube, and they dissociate to the same oxides in air above 300°C . All the known hydrates of $\text{Al}(\text{ReO}_4)_3$ are readily soluble in water, ethanol, and acetone, and may be dehydrated without hydrolysis.

Rhenium trioxide is made by allowing the heptoxide to react with powdered rhenium or rhenium dioxide at about 300°C or by burning the metal in a slight deficiency of oxygen. Better methods of preparation are the decomposition of the rhenium heptoxide-dioxane adduct, or the reaction between carbon monoxide and rhenium heptoxide at 300°C . It has a small temperature independent paramagnetism of 0.086×10^{-6} emu/gm,²⁴ and its property is similar to sodium bronze (Na_xWO_3 as $x \rightarrow 1$). The conduction band state of ReO_3 and Na_xWO_3 are identical and predominantly d-like.

The colour of ReO_3 is said to vary with the state of division of material; it is usually red, but blue and purple specimens have been obtained. The crystal structure is closely related to perovskite with cubic close packing of the oxygen atoms. Each oxygen atom is linked to two metal atoms and the metal atoms are octahedrally coordinated ($\text{Re} - \text{O} = 1.87\text{\AA}$). CrO_3 and WO_3 have structures closely related to this simple type. According to vapor pressure measurement ReO_3 should boil or sublime at 614°C ; this seems a surprisingly low temperature for such a material and it seems likely that this result is the effect of dissociation to the dioxide and the heptoxide. Chemically, ReO_3 is inert. It is insoluble in water, in hot hydrochloric acid and in dilute sodium hydroxide, but it dissolves in concentrated nitric acid to give perrhenic acid, and it is reduced by acidified potassium iodide to the dioxide. Concentrated

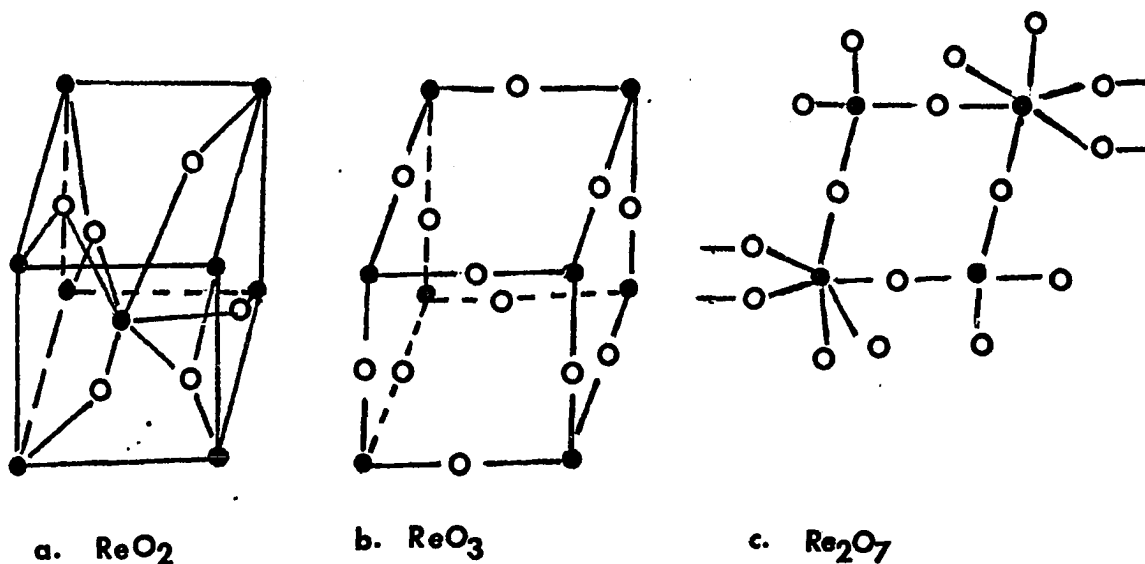
alkali induces dismutation to perrhenate and dioxide, so that it is impossible to prepare rhenates (VI) in aqueous solution.

ReO_3 is cubic, and no phase transformations are known in the range 1-300°K; the material disproportionates to ReO_2 and Re_2O_7 in the neighborhood of 400°C⁵⁷ when heated alone in vacuo.

Rhenium dioxide is made by partial reduction of ammonium perrhenate or of rhenium heptoxide with hydrogen at 300°C, or by the reduction of the heptoxide with metallic rhenium at 600°C. Alternatively, the hydrated oxide $\text{ReO}_2 \cdot n\text{H}_2\text{O}$, got from the aqueous hydrolysis of halogenorhenates(IV), is dehydrated at up to 650°C under a high vacuum.⁵⁴ When strongly heated in a stream of hydrogen, rhenium dioxide is reduced to the element which may remain in a pyrophoric condition, reigniting if brought into the air while still warm. At above 750°C in absence of O_2 and best in a vacuum, it breaks up into Re and Re_2O_7 .²³

Rhenium dioxide forms a dark brown or black powder which is slightly paramagnetic. Structurally, rhenium dioxide resembles most other transition metal dioxides in having a modified rutile lattice like molybdenum dioxide; this implies six-coordination of the rhenium atom.⁵⁴ ReO_2 is polymorphous, and when it is synthesized below 300°C the structural modification (α) is that of monoclinic MoO_2 type; above 300°C, this oxide transforms irreversibly to an orthorhombic form (β) with a structure characterized by zigzag chains of Re atoms propagating along the c axis of the unit cell. It is also possible to directly synthesize the high temperature form, and the material is stable in the range 300-1050°C. Resistivity data indicate that $\beta\text{-ReO}_2$ is metallic and most probably the low temperature modification is also metallic.⁵⁷

The structures of ReO_2 , ReO_3 , and Re_2O_7 are depicted in Fig. 3.⁶⁷



● Rhenium

○ Oxygen

Fig. 3. The structure of ReO_2 , ReO_3 , and Re_2O_7 .

The outstanding catalytic property of rhenium is high selectivity, particularly in hydrogenation reactions. Rhenium also displays unusually high resistance to such catalyst poisons as nitrogen, sulfur, and phosphorous.

In activity, rhenium generally surpasses tungsten, molybdenum, cobalt and other metals usually employed as oxides and sulfides and approaches nickel and platinum.²⁰

Research to date indicates that rhenium should be considered as the possible principal active metal in new catalysts for selective hydrogenation of fine chemicals, hydrocracking, and the disproportionation of olefins.

In hydrogenation, the selectivity and activity of the catalyst depend, to some extent, on its chemical composition and method of preparation. For example, the higher oxides of rhenium, Re_2O_7 and ReO_3 , are less effective than the lower oxides, ReO , ReO_2 and Re_2O_3 , in saturating aromatics.²⁰

On the disproportionation of olefins, only the highest oxide has been used and there is no report on the activity with respect to the oxidation state of rhenium.

Despite the high volatility of the heptoxide, rhenium on alumina can be regenerated with oxygen at 550°C for 12 hours without detection of rhenium heptoxide in the exit gas. Apparently, the rhenium oxides are strongly adsorbed on the alumina base.²⁰

E. Catalyst Support:

Both alumina and silica are widely used as catalyst supports. The mechanical function of a support is to act as a base or framework for the catalytic component. Other possible desirable effects of a support include:

- (1). Giving a larger exposed surface or active agent and thereby greater catalytic activity in cases in which this agent by itself has low surface area.
- (2). Increasing catalyst stability by keeping fine crystals of the active constituent too far apart for sintering to occur.
- (3). Favorably modifying the catalytic activity or selectivity, poison resistance, etc., of the active constituent. In some cases surface compounds complex formation may take place between the support and the supported materials given a complex which has better catalytic properties per unit area than the latter.

- (4). Improving activity by increasing the accessibility of the active surface.
- (5). Catalyzing one of the steps where there is a dual action mechanism.
- (6). Helping to dissipate heat and prevent local overheating which would cause sintering with result of loss in active surface.

The adsorptive and catalytic properties of alumina have been studied for many years.⁴² Many studies were devoted to developing reliable methods for the determination of "activity", which was found to differ considerably not only from the various known adsorptive or catalytic processes but also from the many natural and synthetic alumina products available. It was shown that the important variable for the adsorptive and catalytic activities such as crystal structure, pore texture, and the chemical nature of the surface were largely determined by rather detailed points in the preparation of the alumina.

Active alumina is prepared mostly by a thermal dehydration procedure. According to the temperature at which the aluminas were obtained from the hydroxides, two groups of alumina can be distinguished:

- (a). low-temperature aluminas: $\text{Al}_2\text{O}_3 \cdot n\text{H}_2\text{O}$, in which $0 < n < 0.6$; obtained by dehydrating at temperatures not exceeding 600°C (call γ -group).
- (b). high-temperature aluminas: nearly anhydrous Al_2O_3 , obtained at temperatures between 900 and 1000°C . (called δ -group).

To group (a) belong: ρ , χ , η -and γ - alumina, and to group (b) belong: κ , θ -and δ - alumina.⁴²

Recently, Krischner proposed a classification based upon a more profound knowledge of the crystallographic structures of the aluminas. Three series - α , β , and γ - were classified. The only representation of

the α - series is $\alpha\text{-Al}_2\text{O}_3$, either in the form of the stable corundum or as the decomposition product of diaspore. The β -series consists primarily of the alkali or alkaline earth oxides containing β -alumina, and the decomposition products of gibbsite (χ and κ alumina) which have a related structure. The γ -series consist of the decomposition products of the hydroxides bayerite, nordstrandite and boemite, and can be divided into a γ or low-temperature group (η - and γ - alumina), and a δ - or high temperature group (δ - and θ -alumina).

There is little doubt that γ -alumina has a lattice closely related to that of spinel (MgAl_2O_4). The unit cell of spinel is formed by a cubic close packing of 32 oxygen atoms with 16 aluminum atoms in half of the octahedral interstices and eight magnesium atoms in tetrahedral holes. In γ - alumina only $21\frac{1}{3}$ Al-atoms have to be distributed over these 24 cation positions. Verwey deduced that the unit cell of γ -alumina has two and two-thirds vacancies on the octahedral positions and that eight aluminum atoms are distributed over the tetrahedral holes, corresponding with the notion $\text{Al}_8(\text{Al}_{13\frac{1}{3}}\square_{2\frac{2}{3}})\text{O}_{32}$.

Active alumina adsorbs water, either as hydroxyl ions or as water molecules on the surface, depending upon the temperature. When exposed to water vapor at about room temperature alumina adsorbs water as undissociated molecules bonded with strong hydrogen bonds to the underlying surface. At higher water vapor pressures more water is bonded in a multi-layer physical adsorption process, but this water can be removed easily in a drying procedure at about 120°C . Peri and Hannan presented infrared spectroscopic evidence for the occurrence of undissociated water molecules at low temperatures and showed that during heat drying water molecules not form surface hydroxyl groups. This reaction is completed at about 300°C .

At higher temperatures these OH^- -ion, are gradually expelled as H_2O but even at $800\text{--}1000^\circ\text{C}$ and vacuum some tenths of a percent of water are still retained in the alumina.

Silica has found many applications: as an adsorbent, a catalyst, a catalyst-carrier, and a filler. Electron micrographs of silica shows that the physical structure can be described as a coherent aggregate of elementary particles of roughly spherical shape, with a diameter of the order of 100\AA . The pore system within this aggregate is formed by the open spaces between the elementary particles. The porous texture of silica - as characterized by the specific surface area, the pore volume, and the pore diameters - depends on the size of the packing of the elementary particles. X-ray examination reveals that silica is not crystalline. An elementary particle consists of an irregular three dimensional network of SiO_4 tetrahedra, each silicon atom being linked to four oxygens and each oxygen being linked to two silicons. At certain sites the elementary particles may be linked together by Si-O-Si bridges. The particle surface is covered with OH groups which are responsible for the hydrophilic nature of normal silica.

According to de Boer and Vleeskens, a silica dried at 120°C under atmospheric conditions has lost all physisorbed water and still contains all surface hydroxyles. Heating at higher temperatures partially depletes the surface of OH groups.

The reducibilities of WO_3 supported on γ -alumina and on silica have been studied by Biloen and Pott.⁶ An X-ray photoelectron spectroscopy study has indicated that calcination of $\text{WO}_3/\gamma\text{-Al}_2\text{O}_3$ leads to formation of tungstate. Proof has been obtained that $\text{WO}_3/\gamma\text{-Al}_2\text{O}_3$ can not be appreciably reduced in hydrogen at 550°C , whereas WO_3/SiO_2 is reduced to lower valence

states and unsupported WO_3 is completely reduced to tungsten metal under these conditions. Apparently, there is stronger interaction between the transition metal oxide and the γ -alumina.

F. Adsorption of Ethylene:

Adsorption of reactant molecules on a solid surface is universally accepted as the first step in the overall process of catalysis. Without adsorption there is no catalysis. This is why studies of the adsorption process itself and of the chemistry of the adsorbed state assume a dominant role in all investigations seeking a more fundamental understanding of catalytic phenomena.

Brunauer et al.¹¹ have classified adsorption isotherms according to five types. These are shown in Fig. 4.

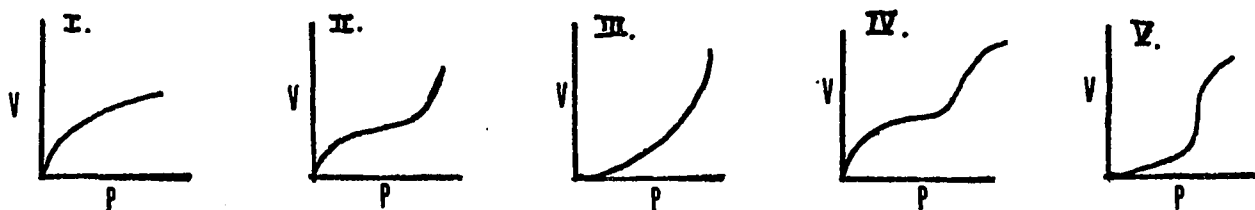


Fig. 4. Five types of isotherms according to Brunauer et al..

Type I is often referred to as the Langmuir type because it corresponds to experimental isotherms of monolayer adsorption. The rest of the curves are associated with multilayer adsorption. Since chemisorption never exceeds a monolayer, its isotherms are restricted to type I.

Type IV, and V are obtained in multilayer adsorption on highly porous adsorbents and the flattening of the isotherms at near saturation pressure is attributed to capillary condensation phenomena. Type II is the common S-shaped isotherm with an asymptotic approach to saturation

pressure. Type III, and V are rare.

Three theoretical isotherms, those of Langmuir, Freundlich and Temkin, are important.⁶² Each is characterized by certain assumptions, in particular as to the manner in which the differential heat of adsorption varies with adsorbed amount, and each is applicable to certain experimental systems.

The Langmuir isotherm is based on the simplest model, the fundamental assumptions being: (1) the adsorption is immobile, (2) each site accommodates only one adsorbed particle, and (3) the adsorption energy of all sites is the same and is unaffected by adsorption on neighboring sites. Although the first two assumptions on the basis of which this isotherm is developed may sometimes be valid, it is doubtful whether the third is true except in rare cases. The Langmuir isotherm, despite its very wide application, therefore contains a fundamental weakness.⁷

The Freundlich isotherm originated as an empirical relation between surface coverage (θ), and pressure (p): $\theta = k \times p^{1/n}$, where k and n are constants at a given temperature, both decreasing with increasing temperature, and n is always greater than unity. The isotherm has been derived theoretically on the basis of an exponential decrease in heat of adsorption with coverage. When the isotherm holds it may suggest an energetically heterogeneous surface.

The Temkin isotherm is based on the supposition that the heat of adsorption falls linearly with increasing surface coverage.

The Freundlich and Temkin relationships are more acceptable than that of Langmuir in that they make allowance for the generally observed dependence of heat of adsorption on coverage: of the two, the Temkin

isotherm treats the most usually encountered case.

Trapnell⁶² has described the application of these isotherms to a wide variety of experimental results. Before it can be asserted that a particular isotherm accurately describes a given system, three conditions must be met. (i) The monolayer volume must be independent of temperature. Quite frequently the Langmuir isotherm is obeyed, but this requirement is not fulfilled. (ii) The results must conform to the isotherm over the greater part of the range of coverages. (iii) It must be confirmed that the heat of adsorption varies with coverage in a manner consistent with that assumed in deriving the isotherm.

There are two distinct types of adsorption. In the first type, termed physical adsorption, the adsorbed molecule is held to the surface by weak van der Waals or dispersion forces. In the second type, termed chemisorption, there is a chemical reaction between the molecule being adsorbed and the adsorbent. There is no doubt that of the two the latter is of vastly greater relevance to catalysis.

Experimentally, it is frequently possible to distinguish between the two types of adsorption, but in some instances the distinction is so ill defined that several criteria have to be employed before a decision can be reached.⁶¹ The magnitude of the heat of adsorption forms the basis of one, and probably the best, of these criteria. During physical adsorption the heat liberated is generally in the range of 2-6 Kcal/mole of gas adsorbed, but values as large as 20 Kcal/mole have been reported. Seldom does the heat of physical adsorption exceed the heat of liquefaction of the gas in question by more than a factor of two or three. During chemisorption large values for the heat of adsorption are usually encountered.

Generally, heats of chemisorption are rarely less than 20 Kcal/mole, but values as low as those associated with physical adsorption are known, and evidence has recently come to light to demonstrate the occurrence of endothermic adsorption.

A second criterion used is the rate at which the process occurs. It is argued that since physical adsorption simulates liquefaction, the same dispersion forces being at work, it should, like liquefaction, require no activation and therefore occur very rapidly. Chemisorption, on the other hand, like most chemical processes, require activation. But it can be misleading if it alone is the sole criterion used. Physical adsorption on a porous solid, such as hydrocarbons on a silica-supported alumina catalyst, may take place very slowly, if diffusion of the adsorbate along the pore is the rate-determining step. This could easily be mistaken for activated chemisorption.

As well as the rate of adsorption, the rate of desorption is frequently a useful guide in deciding which type of adsorption obtained.

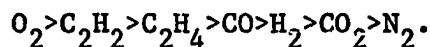
Another useful criterion is based on the temperature range over which the adsorption occurs. Physical adsorption is impossible much above the critical temperature of the gas,⁷ and is unlikely to be of significance at temperatures much above its boiling point. Chemisorption is capable of occurring at temperatures well above the boiling point of the adsorbate. But this test can also prove misleading if the adsorbent is highly porous. On such a solid, physical adsorption may be quite extensive even though the temperature is very much in excess of the boiling point of the adsorbate.

A fourth criterion is based on the extent of specificity in gas-solid interaction. The chemical potentials of the interacting surfaces

and of the possible surface products govern the feasibility of the chemisorption. Physical adsorption is the process whereby condensation of gas occurs, the adsorbate being capable of building up to one or many layers on an inert solid.

Although no single foolproof test is available to assess the type of adsorption in any given system, the above-mentioned criteria, taken collectively leave little doubt as to the type which prevails.

The strength of adsorption in any system depends both on the gas and on the adsorbent. In case the adsorbent is a metal, it is found possible to place a number of gases in a sequence such that any one is more strongly adsorbed by any metal than the ones succeeding it. For the gases which have been most thoroughly studied, the sequence is⁶²



Metals and semi-metals can then be classified into groups depending on the number of gases adsorbed at room temperature, in the manner shown in Table 2.⁷

This classification, due originally to Trapnell,⁶² has been slightly modified to incorporate more recent work.

Metals having a filled d-band (except copper and gold) are unable to adsorb any other gas than oxygen. The highest adsorption potential is shown by the d-metals. Saturated hydrocarbons are only adsorbed by transition metals, and the process is activated.

The oxides differ as adsorbents from the metals in two important respects.⁶² The first is that they possess two types of adsorption center and the same gas is often chemisorbed in two different ways. Second, the term active surface need not mean a surface free of adsorbed gas.

Table 2. Classification of Metals and Semimetals Based on Adsorption Properties.⁷ (A indicates Adsorption, NA No Adsorption)

Group	Metals	O ₂	C ₂ H ₂	C ₂ H ₄	CO	H ₂	CO ₂	N ₂
A	Ca, Sr, Ba, Ti,	A	A	A	A	A	A	A
	Zr, Hf, V, Nb,							
	Ta, Cr, Mo, W,							
	Fe, (Re)							
B ₁	Ni, (Co)	A	A	A	A	A	A	NA
B ₂	Rh, Pd, Pt, (Ir)	A	A	A	A	A	NA	NA
C	Al, Mn, Cu, Au	A	A	A	A	NA	NA	NA
D	K	A	A	NA	NA	NA	NA	NA
E	Mg, Ag, Zn, Cd,	A	NA	NA	NA	NA	NA	NA
	In, Si, Ge, Sn,							
F	Pb, As, Sb, Bi.	NA	NA	NA	NA	NA	NA	NA
	Se, Te							

(): Metal probably belong to this group, but the behavior of films is not known.

Quite often, chemisorption of one gas creates surface sites suitable for chemisorption of a second. Partly on this account active oxide surfaces are more easily prepared than active metal surfaces. However, chemisorption on oxides has only been studied using powders. These are very porous and it is easy to confuse slow chemisorption and slow diffusion to interior surfaces.

Hydrogen may be adsorbed reversibly on metal ions or irreversibly on oxygen ions as hydroxide, when it is desorbed only as water. Hydrocarbon chemisorption at room temperatures probably takes place on metal ions, and the activation energy probably small.⁶²

The adsorptions of hydrogen, ethylene, and ethane on zinc oxide have been studied by Kokes and Dent.³⁷ Initial adsorption of hydrogen at room temperature is rapid, and then slow adsorption continues for days. It was shown that hydrogen chemisorption is operationally of two types: Type I chemisorption which is removed by evacuation for 15 minutes at room temperature, and type II chemisorption which is not removed by evacuation at room temperature even after several hours. The type I chemisorption appear to be independent of the amount of type II chemisorption. Subsequent study of the infrared spectrum shows that OH and ZnH species are involved in the chemisorption and only type I chemisorption gives rise to these two species.

Ethylene adsorption on zinc oxide at room temperature is rapid and reversible. Even after prolonged exposure to the catalyst, the ethylene is recoverable as such by brief evacuation. The adsorption is relatively weak, and it would seem that this adsorption is, in part, physical adsorption. Adsorption of ethylene (boiling point -104°C) was

compared to that of ethane (boiling point -89°C). By traditional criteria physical adsorption of ethane should be greater than that of ethylene, and the comparison of the relative adsorption should let us assay what fraction of the ethylene adsorption is physical. At 0°C and 1 torr, ethylene adsorption is about two orders of magnitude greater than that for ethane. The initial heat of adsorption of ethylene is about 14 Kcal/mole, a value about four times the heat of liquefaction (3.2 Kcal/mole); by way of contrast, the heat of adsorption for ethane is about 5 Kcal/mole, only slightly greater than the heat of liquefaction (3.5 Kcal/mole). Thus, by the usual criteria, ethylene adsorption is chemical at low coverage. Plots of the heat of adsorption versus coverage for ethylene show that the value is roughly constant at low coverage, falls precipitously at about 0.25 ml/gm and reaches values consistent with physical adsorption at coverage above about 0.3 ml/gm. If we assume the physically adsorbed component of the ethylene to be similar to that found for ethane, we would expect the physically adsorbed ethylene to be roughly proportional to the pressure, whereas the chemically adsorbed ethylene is nearly independent of pressure above about 25 torr.

G. $\text{C}_2\text{H}_3\text{D}$ Disproportionation over $\text{MoO}_3/\text{Al}_2\text{O}_3$ Catalyst:

The disproportionation of monodeuterated ethylene on $\text{MoO}_3/\text{Al}_2\text{O}_3$ catalyst has been studied recently.⁴⁰

445 ml of $\text{C}_2\text{H}_3\text{D}$ is passed over 10 ml of Al_2O_3 for 25 minutes at 155°C . Analysis of the mass spectra of the reactant and the product shows no change in the relative peak heights. In other words, there is no reaction after contacting with the support Al_2O_3 alone. 450 ml of $\text{C}_2\text{H}_3\text{D}$

is then passed over 10 ml of 10% $\text{MoO}_3/\text{Al}_2\text{O}_3$ catalyst for 25 minutes at 155°C . Analysis of the product shows that 4.4% $\text{C}_2\text{H}_2\text{D}_2$ is formed. The disproportionation reaction does occur for ethylene, and the reaction rate is much less than that of the disproportionation of propylene as ethylene is a more stable molecule.

CHAPTER III

THEORETICAL BACKGROUND

A. Adsorption Isotherms:

The relation between the amount of substance adsorbed by an adsorbent and the equilibrium pressure at constant temperature is called an adsorption isotherm. There are a number of well-known isotherms, those of Langmuir, Freundlich, and Temkin, are important.

It is essential for us to become acquainted with the salient features of these isotherms before we can begin to appreciate the kinetic interpretation of heterogeneous catalyzed reactions. The isotherms can often be represented by simple equations which express directly how the concentration of the adsorbate varies with the gas pressure. The equations of some isotherms⁶¹ are presented in Table 3.

If, on adsorption, the adsorbed molecule dissociates into n entities each of which occupies a surface site, then the Langmuir equation becomes:

$$\theta = \frac{(bP)^{1/n}}{1 + (bP)^{1/n}}, \text{ or } \frac{P^{1/n}}{v} = \frac{1}{b^{1/n} v_m} + \frac{P^{1/n}}{v_m}$$

Should all points of $P^{1/n}/v$ ($n = \text{integer}$) against P at various temperatures yield straight lines, and the v_m 's are constant then the Langmuir equation is valid for this particular adsorbate-adsorbent system.

Table 3. A Selection of Adsorption Isotherms.⁶¹

Isotherm	Equation	Applicability
Langmuir	$v/v_m = \theta = \frac{bP}{1 + bP}$	Physical Adsorption,
	or $P/v = 1/(bv_m) + P/v_m$	Chemisorption.
Freundlich	$v = k P^{1/n}, (n > 1)$	Physical Adsorption,
	or $\ln(v) = \ln(k) + 1/n \ln(P)$	Chemisorption.
Temkin	$v/v_m = \theta = 1/a \ln C_o P$ or $v = v_m/a (\ln C_o + \ln P)$	Chemisorption,
Henry	$v = k P$	Physical Adsorption, Chemisorption,
B E T	$\frac{P}{v(P_o - P)} = \frac{1}{v_m c} + \frac{(c-1) P}{v_m c P_o}$	Physical Adsorption. (multilayer)

v : volume adsorbed (ml/gm at STP)

v_m : volume of monolayer (ml/gm at STP)

θ : fraction of surface coverage

P : equilibrium pressure

P_o : saturated vapor pressure of the adsorbate

a, b, c, C_o, k, K : constants

In testing whether a set of experimental data obeys the Freundlich isotherm, it is customary to plot $\ln v$ against $\ln P$. If the Freundlich isotherm, is followed, the plot of $\ln v$ versus $\ln P$ should be linear with the slope proportional to the absolute temperature.

To test the applicability of Temkin equation it is necessary to plot v against $\ln P$. If they all give straight lines with the slope proportional to the absolute temperature, then the Temkin equation is followed.

The B E T equation is mainly used for the estimation of the surface area of the adsorbent, and is only applied to multilayer physical adsorption.

B. Heat of Adsorption:

From adsorption isotherms at various temperatures the isosteric heat of adsorption, q_i , can be calculated by means of the Clausius-Clapeyron equation:

$$q_i = RT^2 \left(\frac{d \ln P}{dT} \right)_v$$

$$, \text{ or } q_i = RT_1 T_2 (\ln P_2 - \ln P_1) / (T_2 - T_1)$$

The true differential heat of adsorption, q_d , is related to the isosteric heat as follows:

$$q_i = q_d + RT$$

The difference between the two heats is usually too small to warrant distinction.

C. Entropy of Adsorption:

The entropy of adsorption may sometimes be obtained from the equation $-\Delta S = (\Delta G - \Delta H)/T$, where ΔG is the free energy change, and $-\Delta H$ the differential heat of adsorption. If adsorption is reversible ΔG may be calculated from the equation $\Delta G = RT \ln(P/P_0)$, where P is the equilibrium pressure in the gas phase, and P_0 is the pressure in the adsorbed layer. In calculating ΔG , it is customary to define a standard surface state for which P_0 is equal to one atmosphere. Thus, $-\Delta S = (-\Delta H/T) + R \ln(P/P_0)$.

When ΔS and ΔH are functions of surface coverage θ , then,

$$-\Delta S(\theta) = (-\Delta H(\theta)/T) + R \ln(P/P_0).$$

Hence, from two isotherms at temperature T_1 and T_2 , and from the equilibrium pressure P_1 and P_2 corresponding to the same degree of surface coverage θ ,

$$-\Delta S(\theta) = R \frac{T_2 \ln(P_2/P_0) - T_1 \ln(P_1/P_0)}{(T_1 - T_2)}$$

The mobility of the adsorbed layer can be followed by comparing the experimental value of the entropy of adsorption for the loss of various degree of freedom.

The translation entropy of a perfect gas of molecular weight M at one atmosphere pressure in three dimensions is:

$${}^3S_{\text{trans}} = R \ln(M^{3/2} T^{5/2}) - 2.30 \quad (\text{cal/deg./mole})$$

In two dimensions the translational entropy is:

$${}^2S_{\text{trans}} = R \ln(M T A) + 65.80 \quad (\text{cal/deg./mole})$$

where A is the area occupied by each molecule.

Immobile layers possess a configurational entropy which arises because the molecules may be distributed over the surface in a number of different ways. For single site adsorption,¹⁶

$$S_{\text{config.}} = -R (\ln \theta + (1-\theta)/\theta \ln(1-\theta)).$$

The degree of translation freedom perpendicular to the surface which is lost on adsorption is replaced by a vibration. For a vibration of frequency ν , the entropy is :

$$S_{\text{vib.}} = R \left(\frac{h \nu}{k T} \left(e^{h\nu/kT} - 1 \right)^{-1} - \ln \left(1 - e^{-h\nu/kT} \right) \right).$$

In chemisorption, ν will be high, and the vibrational entropy at ordinary temperatures is small and less than about 3 e.u..

The quantity $(S_{2\text{trans}} - S_{3\text{trans}})$ is the minimum entropy loss which may be expected for mobile layers, and the quantity $(S_{\text{config.}} - S_{3\text{trans}})$ is the minimum loss for immobile layers.⁶²

D. Mass Transfer Effects:

One of the objects of this investigation is to establish the steady state kinetics of the olefin disproportionation. To ensure that kinetic data obtained in an experiment reflect only chemical events, both interphase and intraparticle mass transfer effects must be virtually eliminated.

A common empirical test for the possible influence of interphase transport limitations, which consists of checking the effect of flow rate on conversion at constant space velocity, has been discussed in the literature.^{38,58} Interphase mass transfer theory suggests that each catalyst particle is enclosed within a boundary layer across which both

reactants and products must diffuse. When reactions are limited by the interphase mass transfer, an increase in the linear gas velocity reduces the boundary layer thickness and causes an increase in the reaction rate.

Empirical criteria are well established to evaluate the effects of intraparticle mass transport. The criterion is based on determining the reaction rate at progressively smaller particle sizes.

If the rate of reaction is unaffected by the particle size reduction, the resistance to pore diffusion is negligible. If we are operating in the region of strong pore diffusion the rate of reaction will vary inversely with particle size.

E. Reaction rate and Reaction Mechanism:

In heterogeneous catalysis, the rate of reaction is usually expressed as follows:

$$r_i = - \frac{1}{W} \frac{d N_i}{d t} = \frac{\text{Moles of } i \text{ disappeared}}{(\text{unit mass of catalyst}) (\text{time})}$$

Rates of reaction in differential reactors are found in a straightforward manner since integration of the plug flow design equation becomes trivial.

$$r_{\text{ave.}} = V (X_{\text{out}} - X_{\text{in}})$$

where $r_{\text{ave.}}$ is the average reaction rate in gm mole/gm catalyst/hour, V is the space velocity of the reactant in gm mole/gm catalyst/hour, and X is the conversion.

A differential reactor presents a number of attractive features. It is easier to evaluate the reaction rate, and also easier to keep isothermal condition. It is most widely used for the study of the reaction

kinetics. Since the conversion is low, the method of analysis for the reaction products must be very accurate.

The foregoing discussion has been concerned with the experimental aspects of surface reactions. Consideration must now be given to the interpretation of the molecular mechanisms by which surface reactions occur.

The mechanistic model must be capable of describing adequately the basic physical and chemical steps that take place with a process. Adsorption of the reactant molecules in the first step for the contact catalysis. The application of the more exact adsorption laws, taking account of surface inhomogeneity and interactions, is much more difficult, and not too much progress has yet been made along these lines. In the past, two types of reaction mechanisms have been used for widely varying reactions with great success. They are generally referred to as the Langmuir-Hinshelwood mechanism, and the Rideal mechanism.

According to the Langmuir-Hinshelwood mechanism the reactants are considered to be in adsorptive equilibrium with the surface, and reaction then involves the adsorbed molecules. The quantitative treatment of reactions occurring by this mechanism therefore involves obtaining an expression, using the adsorption isotherms, for the concentrations of reactant molecules on the surface, and then expressing the rate of reaction in terms of these surface concentrations; this rate of reaction can then be expressed in terms of the concentrations of gaseous reactants.

In the Rideal mechanism, the reaction occurs between a gas molecule and an adsorbed molecule. It appears that this type of mechanism is not of very general applicability.

For the catalytic disproportionation of propylene with the rate controlled by a dual-site surface reaction (Langmuir-Hinshelwood mechanism), the complete rate equation is given by:

$$r = k_s \theta_p^2 = \frac{k_s K_p^2 P_p^2}{(1 + K_e P_e + K_p P_p + K_b P_b)^2} \quad (2 \text{ C}_3\text{H}_6 \rightleftharpoons \text{C}_2\text{H}_4 + \text{C}_4\text{H}_8)$$

$\begin{matrix} P_p & P_e & P_b \end{matrix}$

At low conversion,

$$r = \frac{k_s K_p^2 P_p^2}{(1 + K_p P_p)^2}, \text{ or } \frac{P_p}{\sqrt{r}} = \frac{1}{\sqrt{k_s} K_p} + \frac{P_p}{\sqrt{k_s}}$$

Thus a plot of P_p/\sqrt{r} versus propylene partial pressure should be linear if the Langmuir-Hinshelwood mechanism is followed.

If the Rideal mechanism is true then,

$$r = k_s \theta_p P_p = \frac{k_s K_p P_p^2}{(1 + K_p P_p + K_e P_e + K_b P_b)}$$

at low conversion,

$$r = \frac{K_s K_p P_p^2}{1 + K_p P_p}, \text{ or } \frac{P_p^2}{r} = \frac{1}{k_s K_p} + \frac{P_p}{k_s}$$

A plot of P_p^2/r versus propylene partial pressure should yield a straight line.

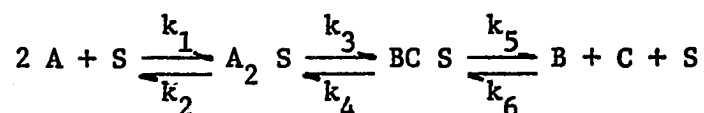
For the disproportionation of monodeuterated ethylene, the result is similar to that of the above discussion.

F. Mechanistic Equations:

In the disproportionation of olefin, a detailed picture of the intermediate surface complex has been proposed in both heterogeneous¹⁹ and homogeneous¹² systems. Two olefin molecules are assumed to form pi-complexes on a surface transition metal atom or ion. Interaction occurs through switching of the roles of the olefin bonding and anti-bonding pi-orbitals in the presence of the d-orbitals of the transition metal.

On the disproportionation of monodeuterated ethylene, if the isotope effect is neglected, the reaction mechanism can be depicted in the following ways under certain conditions.

(a). Uniform surface with two molecules adsorbed on each site:



where S represents surface site and A is reactant, and B,C are products.

If the isotope effect is neglected and a 50% conversion is assumed, then

$$k_1 = k_6 = k_a \quad (\text{adsorption constant})$$

$$k_2 = k_5 = k_d \quad (\text{desorption constant})$$

$$k_3 = k_4 = k_s \quad (\text{reaction rate constant}).$$

Therefore,

$$\text{the rate of adsorption} \quad r_a = k_a P_A^2 (1 - \theta_{AA} - \theta_{BC}) - k_d \theta_{AA}$$

$$\text{the rate of reaction} \quad r_s = k_s \theta_{AA} - k_s \theta_{BC}$$

$$\text{the rate of desorption} \quad r_d = k_d \theta_{BC} - k_a P_B P_C (1 - \theta_{AA} - \theta_{BC})$$

at steady state

$$r_a = r_s = r_d.$$

If no rate limiting steps,

$$r = \frac{k_a k_s k_d (P_A^2 - P_B P_C)}{(2 k_a k_s + k_a k_d) P_A^2 + (k_a k_d + 2 k_a k_s) P_B P_C + (2 k_d k_s + k_d^2)}$$

At low conversion, $P_A \gg P_B P_C$

then,

$$r = \frac{P_A^2}{P_A^2 (2/k_d + 1/k_s) + (2/k_a + k_d/(k_a k_s))}$$

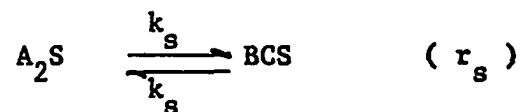
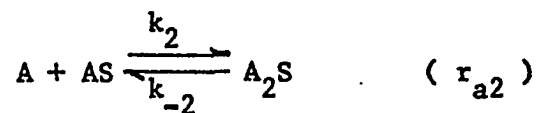
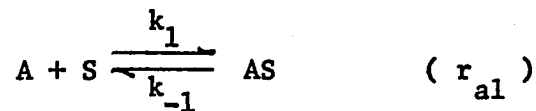
or,
$$P_A^2 / r = (2/k_d + 1/k_s) P_A^2 + (2/k_a + k_d/(k_a k_s))$$

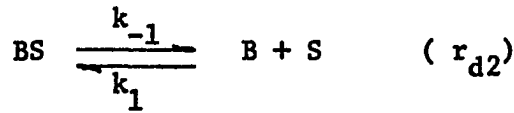
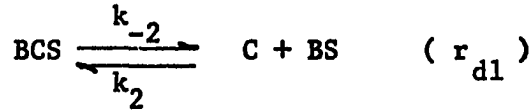
A plot of P_A^2/r versus P_A^2 should yield a straight line with positive slope and intercept.

(b). Stepwise adsorption with each site capable of adsorbing two molecules:

Neglecting isotope effect and assuming equilibrium conversion of

50%,





At steady state,

$$r = r_{a1} = r_{a2} = r_s = r_{d1} = r_{d2}$$

where

$$r_{a1} = k_1 P_A (1 - \theta_A - \theta_{AA} - \theta_{BC} - \theta_B) - k_{-1} \theta_A$$

$$\cong k_1 P_A (1 - \theta_A - \theta_{AA}) - k_{-1} \theta_A \quad (\text{at low conversion})$$

$$r_{a2} = k_2 P_A \theta_A - k_{-2} \theta_{AA}$$

$$r_s = k_s \theta_{AA} - k_s \theta_{BC}$$

$$r_{d1} = k_{-2} \theta_{BC} - k_2 P_C \theta_B = k_{-2} \theta_{BC} - k_2 P_B \theta_B \quad (\because P_C = P_B)$$

$$r_{d2} = k_{-1} \theta_B - k_1 P_B (1 - \theta_A - \theta_{AA} - \theta_{BC} - \theta_B)$$

$$\cong k_{-1} \theta_B - k_1 P_B (1 - \theta_A - \theta_{AA}) \quad (\text{at low conversion})$$

Solving the four equations and the final expression for r is:

$r = N / M$, where

$$N = C_1 P_A^3 + C_2 P_A^2 + C_3 P_A P_B + C_4 P_B^2$$

$$M = C_5 P_A^2 P_B^2 + C_5 P_A^3 P_B + C_6 P_A^3 + C_7 P_A^2 P_B + C_8 P_A P_B^2 + C_9 P_A^2 + C_{10} P_A P_B$$

$$+ C_{11} P_B^2 + C_{12} P_A + C_{13} P_B + C_{14}$$

C_1, C_2, \dots, C_{14} are constants involving k_1, k_{-1}, k_2, k_{-2} , and k_s .

It is clear that the expression is too complicated to be tested, even though some simplifications have already been made.

G. Reaction Rate Versus The Amount of Adsorption:

In the disproportionation of deuterated ethylene, the steady state kinetics obtained is at adsorption equilibrium. The surface concentration of the reactant is known during the reaction. Therefore it is interesting to correlated the rate of reaction with the amount of adsorption.

Assume b_1 is the probability of a molecule being adsorbed on one site, and b_2 is the probability of two molecules being adsorbed on one site with $b_2 = b_1 \cdot b_1$.

Then,

$V_1 \propto b_1$ where V_1 is the amount of gas adsorbed with one molecule on one site,

$V_2 \propto b_2 = b_1^2 \propto V_1^2$ where V_2 is the amount of gas adsorbed with two molecules on one site.

$V_2 = k V_1^2$ and k is a proportionality constant.

Hence $V_t = V_1 + V_2$ where V_t is the total amount of gas adsorbed.

$$kV_1^2 + V_1 - V_t = 0$$

$$V_1 = (-1 + \sqrt{1 + 4kV_t}) / 2k, \text{ and } V_2 = (1 + 2kV_t - \sqrt{1 + 4kV_t}) / 2k.$$

Suppose $4kV_t \leq 1$, then

$$\begin{aligned}\sqrt{1 + 4kV_t} &= 1 + \frac{1}{2}(4kV_t) - (1/8)(4kV_t)^2 + (1/16)(4kV_t)^3 - (5/128)(4kV_t)^4 + \dots \\ &= 1 + 2kV_t - 2(kV_t)^2 + 4(kV_t)^3 - 10(kV_t)^4 + \dots\end{aligned}$$

Therefore,

$$V_2 = kV_t (1 - 2kV_t + 5k^2V_t^2 + \dots)$$

If the rate of reaction is proportional to V_2 , then

$$R = k_s V_2 = k_s k V_t^2 (1 - 2kV_t + 5k^2V_t^2 + \dots)$$

and

$$\ln(R) = \ln(k_s k) + 2 \ln(V_t) + \ln(1 - 2kV_t + 5k^2V_t^2 + \dots)$$

The last term on the righthand side of the above equation is very small since $(1 - 2kV_t + 5k^2V_t^2 + \dots)$ approaches 1.

Therefore the plot of $\ln(R)$ versus $\ln(V_t)$ will approximately be linear with a slope close to 2.

CHAPTER IV

EXPERIMENTAL APPARATUS

The adsorption of ethylene on the supported catalysts is determined volumetrically, that is, the amount of gas adsorbed on the catalyst surface is calculated from the pressure change within a constant volume.

A conventional high vacuum adsorption system has been constructed, and is shown in Fig. 5. The pyrex glassware is mounted on a rigid aluminum framework. To avoid the transmission of vibrations to manometers, the mechanical forepump is placed on the floor, and linked with a short length of thick-walled rubber tubing. A Welch Duo-Seal vacuum pump is used as the forepump. High vacuum is obtained through the use of a two-stage mercury-vapor diffusion pump. The diffusion pump was purchased from Kontes Glass Company, and has a pumping speed of 6 liter per second to an ultimate vacuum of 10^{-7} torr. Generally, high vacuum ($<5 \times 10^{-6}$ torr) can be reached within one hour. The system pressure is read from a double-scaled McLeod gage which has a lowest reading of 5×10^{-6} torr. Two liquid nitrogen traps are installed, one before the diffusion pump, and the other before the McLeod gage, to eliminate the contamination by mercury vapor and to achieve high vacuum. Six greaseless stopcocks, and four Teflon glass valves are used in the apparatus to assure no grease and metal in contact with the gases. The

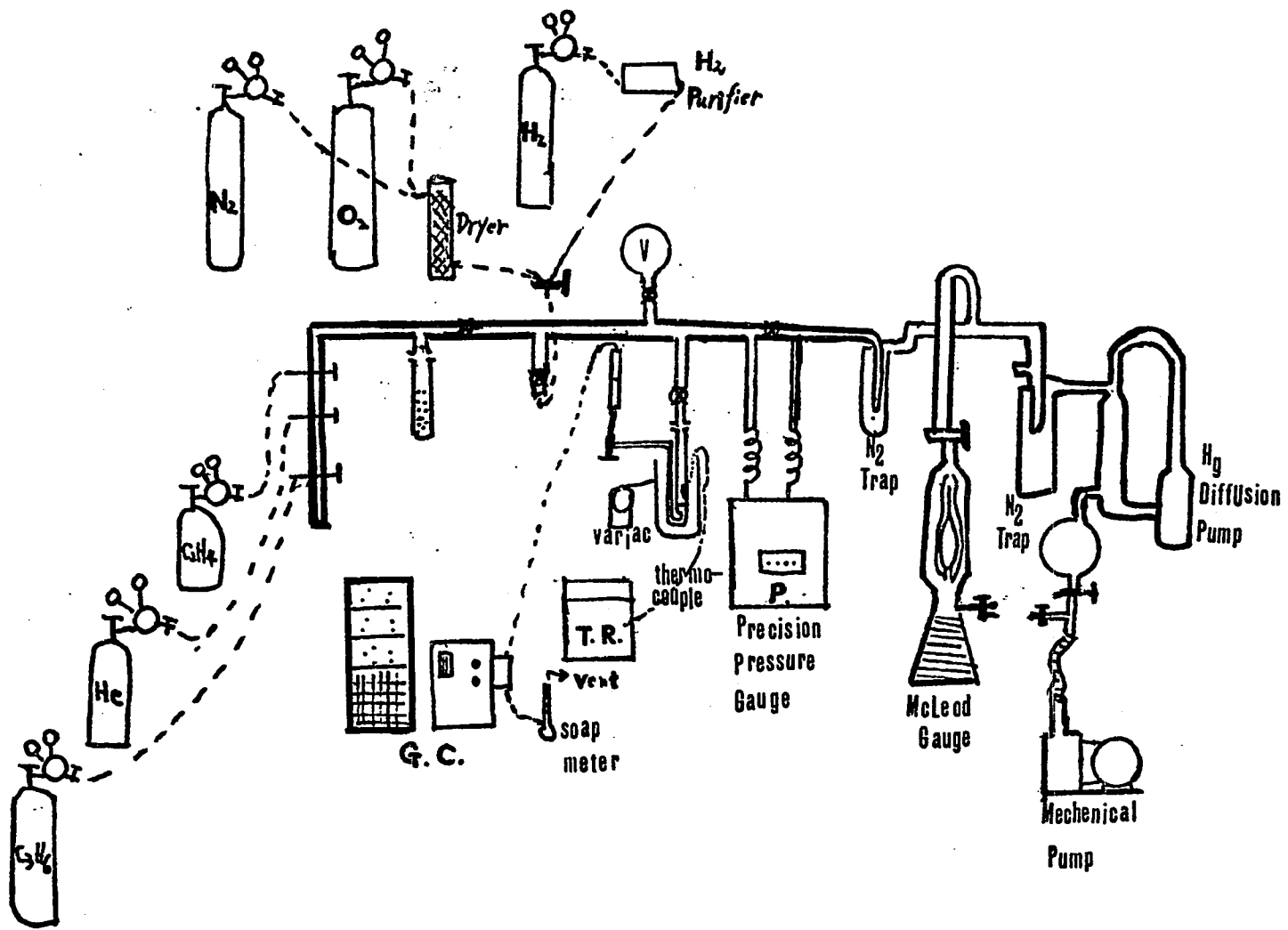


Fig. 5. Apparatus for the Adsorption of Ethylene and the Disproportionation of Propylene.

undesirability of greases and metals is well-known, particularly in the field of heterogeneous catalysis, so too are the many disadvantages of "mercury cut offs" sometimes used in lieu of a greased stopcock. The greaseless stopcock employs a fluorocarbon (Viton A) diaphragm, and can be used under high vacuum conditions to the order of 10^{-6} torr, and within the temperature range 60 - 450°F with satisfaction. It is also suitably employed under conditions of positive pressure.

In order to adjust the gaseous flow rate Teflon glass valves are used in the gas inlet ports. The valve consists of a Teflon stem with two Viton O-ring seals operating in a precision bore threaded glass tube. When the valve is opened fluid passes through an annular orifice formed by the end of the Teflon stem and glass tube. Flow regulation is quickly and accurately achieved by rotating the threaded stem in the threaded glass tube.

The adsorption cell is connected to the system via a ball and socket joint with a Viton O-ring located near the midpoint of the ground surface. The adsorbent is supported by a sealed-in fritted disc. A thermocouple well extended to the center of the cell is made for the accurate measurement of the temperature of the adsorbent. Because of the heavy weight of the greaseless stopcock, a Teflon glass valve is used at the end of the side tube of the adsorption cell.

In order to obtain the gas volume adsorbed, it is essential to know how much gas is used in filling the evacuated portions of the apparatus. These are called the dead spaces, and are determined using a pre-calibrated constant volume bulb.

The pressure change during adsorption is measured through a

Model 145 Precision Pressure Gage manufactured by Texas Instruments, Inc. The gage consists basically of two parts - the capsule containing the fused quartz pressure sensitive element, and the read-out unit. Bourdon tube deflection is measured directly by optical means so that no fragile force balance linkages are required. Optical coupling between pressure sensor and readout eliminates reactive and frictional forces on the sensor, assuring optimum repeatability. Accuracy is unaffected by the operator's technique. Neither mercury nor oil is required, problems concerning corrosive media or chemical interaction with the metric fluid are completely eliminated. A servo - nulling readout unit with a built in proportional capsule temperature control enable the user to achieve optimum accuracy. The fused quartz bourdon capsule is a differential type with maximum reading of 300 torr. The accuracy of the pressure reading is within ± 0.003 torr. The gage is connected to the system via two Kovar to Pyrex seals. Swagelock fittings are used for the connection.

The compressed gases are discharged through the two-stage pressure regulators. Flow rates are controlled by adjusting the needle valves. Soap bubble flow meters, and metal float metering tube are used to measure the flow rates. The connecting lines are 1/4" copper tubing with Swagelok fittings. Pyrex to Kovar seals are used to connect the tubings to the glass valves.

Oxygen and nitrogen are passed through a drying column filled with Drierite (anhydrous calcium sulfate). Hydrogen is purified through a Serfass Hydrogen Purifier manufactured by Milton Roy Company.

High temperature pretreatment is required to activate the catalyst. The heater is constructed by wrapping a flexible heating tape over a stainless steel pipe of 1-1/4" diameter. The heating tape is

insulated with Samox fibers and can be used at temperatures up to 1600°F or 870°C. Heating rates are controlled through a variac.

A Chromel-Alumel thermocouple is inserted into the thermocouple well in the adsorption cell. Temperature is read from a Sargent Model S.R. Recorder designed and manufactured by E.H. Sargent & Co..

In the kinetic studies, compressed propylene is discharged through a pressure/flow controller, and passed through a gas washing bottle filled with pre-dried silica gel. The reaction products are analyzed with a F & M Model 810 Analytical Gas Chromatograph. The chromatograph is a versatile, sensitive dual column instrument equipped with both thermoconductivity and flame ionization detectors. Its automated features permit the analyst to obtain the maximum benefit from programmed temperature or isothermal operation. The chromatograph peaks are recorded on a Honeywell Electronik 15 Strip Chart Chromatograph Recorder. Helium is used as the carrier gas. The stainless steel column, 1/8 inch in diameter by 14 foot in length, are packed with 20% bis-2-methoxy ethyl adipate on chromosorb P.

A gas sampling valve is equipped with the chromatograph for the injection of the gas sample of constant volume.

The analysis is done at room temperature using thermoconductivity detector. A sample can be analyzed within 5 minutes with a carrier gas flow rate of 25 ml/min.

Due to the very high cost of the deuterated ethylene, the volume of the apparatus for the kinetic measurements has to be minimized. The arrangement is shown in Fig. 6.

The same adsorption cell is used as the reactor. A Matheson No. 610 low flow flowmeter is used to maintain an extremely accurate

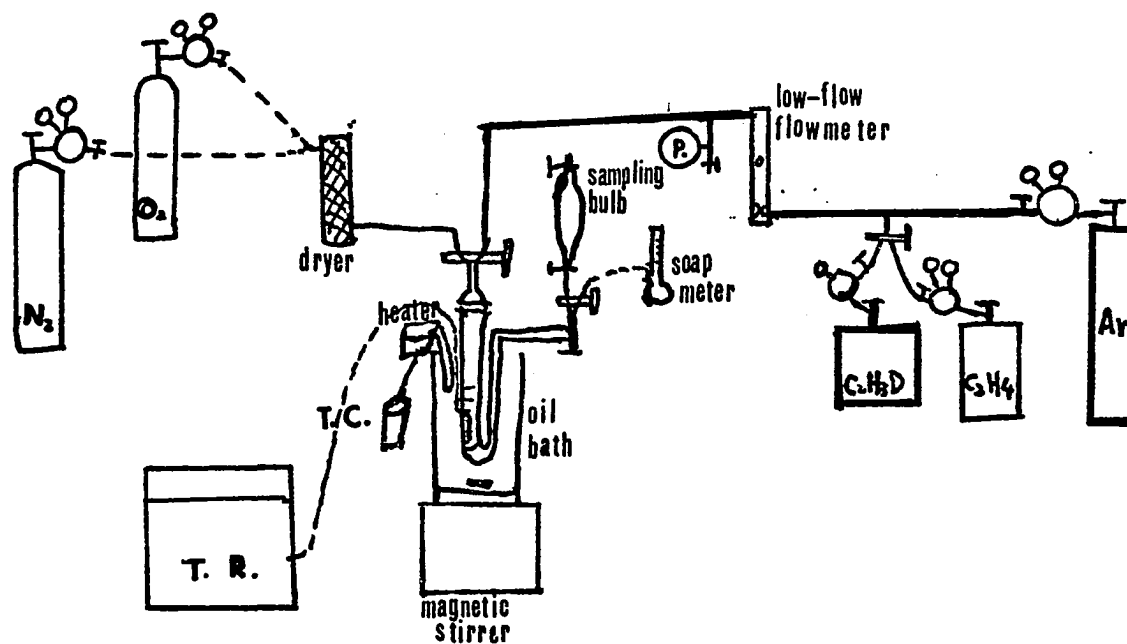


Fig. 6. Apparatus for the Disproportionation of Deuterated Ethylene.

control of the flow rate. The range of flow rate which the flowmeter can be operated is from 1/3 to 100 ml/min. of air at 1 atm and 70°F.

The reaction products are collected in a glass sampling bulb, and analyzed with a Hitachi Mass Spectrometer (Model RMU-7E) manufactured by Hitachi Ltd., Tokyo, Japan. This mass spectrometer has a minimum detectability of 0.05 ppm. It requires a minimum sample size of 0.1 c.c. NTP for gas, and 0.1 mg for liquid and solid. Quantitative analysis is performed using low ionizing voltage. The method of determination of the composition of the deuterated ethylene mixture is provided in the literature.

CHAPTER V

EXPERIMENTAL PROCEDURE

A. Preparation of the Supported Rhenium Oxide Catalysts:

(a). Materials Used:

1. Ammonium perrhenate (NH_4ReO_4) - 99% pure, supplied by Apache Chemicals, Inc., Rockford, Illinois. The solubility in water at 20°C is 0.227 moles/liter, or 0.61 gm/10 ml.
2. γ -Alumina - 99% Al_2O_3 , supplied by the Harshaw Chemical Company, Cleveland, Ohio. Type 0104, 1/8 inch tablets. The apparent bed density is 0.7-1.0, the surface area 80-100 m^2/gm , and the pore volume 0.28-0.33 cm^3/gm .
3. Silica gel - Grade 59, 3-8 mesh, supplied by Davison Chemical Division of W.R. Grace & Co., Baltimore, Maryland. The surface area is 345 m^2/gm .

(b). Method of Preparation:

The supported catalyst is prepared by impregnation. Dissolve completely x grams of ammonium perrhenate in distilled water and mixed with y grams of alumina or silica of 40-60 mesh. The paste is dried in oven at 110°C for at least 20 hours. The catalyst dry weight z is then measured, and the desired amount transferred to the adsorption cell.

The weight percentage of Re_2O_7 is calculated as follows:

$$\text{wt.}\% \text{ of } \text{Re}_2\text{O}_7 = (0.8939^* x/z) \cdot 100$$

$$\begin{aligned} * : 1 \text{ gm } \text{NH}_4\text{ReO}_4 \text{ (99\% pure)} &= 1 \times 0.99 \times \frac{186.2(\text{Re})}{268.4(\text{NH}_4\text{ReO}_4)} \times \frac{484.4(\text{Re}_2\text{O}_7)}{186.2 \times 2(\text{Re}_2)} \\ &= 0.8939 \text{ gm } \text{Re}_2\text{O}_7 \end{aligned}$$

B. Activation of the Catalyst:

The catalyst is activated in a mixture of dry oxygen and nitrogen at 500°C for two hours followed by a one hour nitrogen or helium purge at the same temperature, and then cooled to the desired temperature in nitrogen or helium.

C. Procedure of Ethylene Adsorption:

(1). Determination of the Volume of the Constant-Volume Bulb:

Both mercury and water are used to determine the volume of the bulb. The contained water or mercury is weighed in air with brass weights, and the coefficient of cubic expansion for glass is taken into consideration. According to the literature, the true capacity of the bulb is calculated by the following formula:⁶⁹

$$V = Wt \times Gw = Mt \times Gm ,$$

where V is the volume of the bulb in c.c., Gw is the weight of water in gram, Gm is the weight of mercury in gram, Wt=1.003271 at 22°C, and Mt=0.0738450 at 22°C.

The volume obtained by mercury is 103.756 c.c., and by water is 103.735 c.c. The agreement is good.

(2). Measurement of the Adsorption of Ethylene:

After the catalyst has been properly activated, the adsorption system is evacuated for at least three hours under a pressure of less

than 5×10^{-6} torr. The volume of the dead space is determined by the expansion of a known quantity of high purity helium pre-introduced in the constant-volume bulb. After the dead space volume is determined, the system is evacuated again. Matheson research grade ethylene (99.98% minimum) is then admitted successively, and the equilibrium pressures are recorded. Usually, equilibrium is reached rapidly on the unreduced catalysts.

When the adsorption is carried out other than at room temperature, the adsorption cell is immersed in a constant temperature oil bath. The temperature is maintained by an immersion heater with a built-in adjustable time proportional thermostatic control. The adsorption is then conducted as that of at room temperature, and helium is then admitted successively to obtain the correction of temperature effect.

D. Procedure of the Measurement of the Reaction Rates:

(1). On the Disproportionation of Propylene:

Propylene of polymerization grade (99 mol %) is obtained from Phillips Petroleum Company. The gas is discharged through a pressure/flow controller and passed through a drying bottle filled with silica gel, and then passed through the activated catalyst at the desired flow rate. Helium is used as diluent and to make up a total pressure of 1 atmosphere. The reaction products are analyzed with the gas chromatograph via the gas sampling valve. The reaction rate is obtained by multiplying the space velocity with the conversion of propylene determined from the chromatogram.

(2). On the Disproportionation of Deuterated Ethylene:

Mono-deuterated ethylene is purchased from Merck & Co., Inc., Quebec, Canada. The compressed gas is discharged through a needle valve

which incorporated with a cylinder pressure gage. The flow rate is further adjusted by the low-flow flowmeter. High purity argon is used as diluent, and to make up a total pressure of 1 atmosphere.

The deuterated ethylene is passed through the activated catalyst for at least 20 minutes to make sure that steady state is reached, and the products are collected in the gas sampling bulb for analysis.

The reaction rate is calculated the same way as that of propylene disproportionation.

CHAPTER VI

RESULTS AND DISCUSSION

A. Adsorption of Ethylene on the Supported Rhenium Oxide Catalysts:

(i). Blank Test:

At first, the adsorption of ethylene at room temperature with the blank adsorption cell is measured. The ideal gas law is used to calculate the amount of adsorption. The dead space volume is determined by using helium. The results for the adsorption of ethylene with the blank cell is shown in Table 4. As can be seen there is no detectable adsorption by the adsorption cell alone, and the maximum cumulative error is less than 0.0015 ml at STP for pressures up to 260 torr.

(ii). Unreduced Catalysts:

(1). Adsorption at Room Temperature on Alumina and Alumina-supported Catalysts:

The results for the adsorption and desorption of ethylene at room temperature on the unreduced alumina and alumina-supported catalysts of varying rhenium content are presented in Fig. 7.

The adsorption is reversible with the amount of ethylene adsorbed tending to zero as the ethylene pressure tends to zero. The amount increases with the increase of Re_2O_7 content to about 5%, then decreases with further increase of the rhenium content which may be due to the blocking of the pores.

Table 4. The Adsorption of Ethylene at Room Temperature
With the Blank Adsorption Cell.

Equilibrium Pressure (torr)	Moles of Gas Adsorbed	ml at STP of Gas Adsorbed
0.9946	-0.00000002	-0.00038453
2.0783	-0.00000006	-0.00139082
5.5728	-0.00000005	-0.00105892
13.4347	-0.00000004	-0.00095636
36.4890	-0.00000004	-0.00091300
54.4901	0.00000000	0.00002914
74.5338	-0.00000003	-0.00069795
88.3278	-0.00000003	-0.00069947
120.084	0.00000002	0.00034594
141.969	0.00000000	0.00005104
166.700	0.00000004	0.00089423
212.865	0.00000002	0.00055783
249.871	-0.00000004	-0.00081333
260.084	-0.00000004	-0.00082666

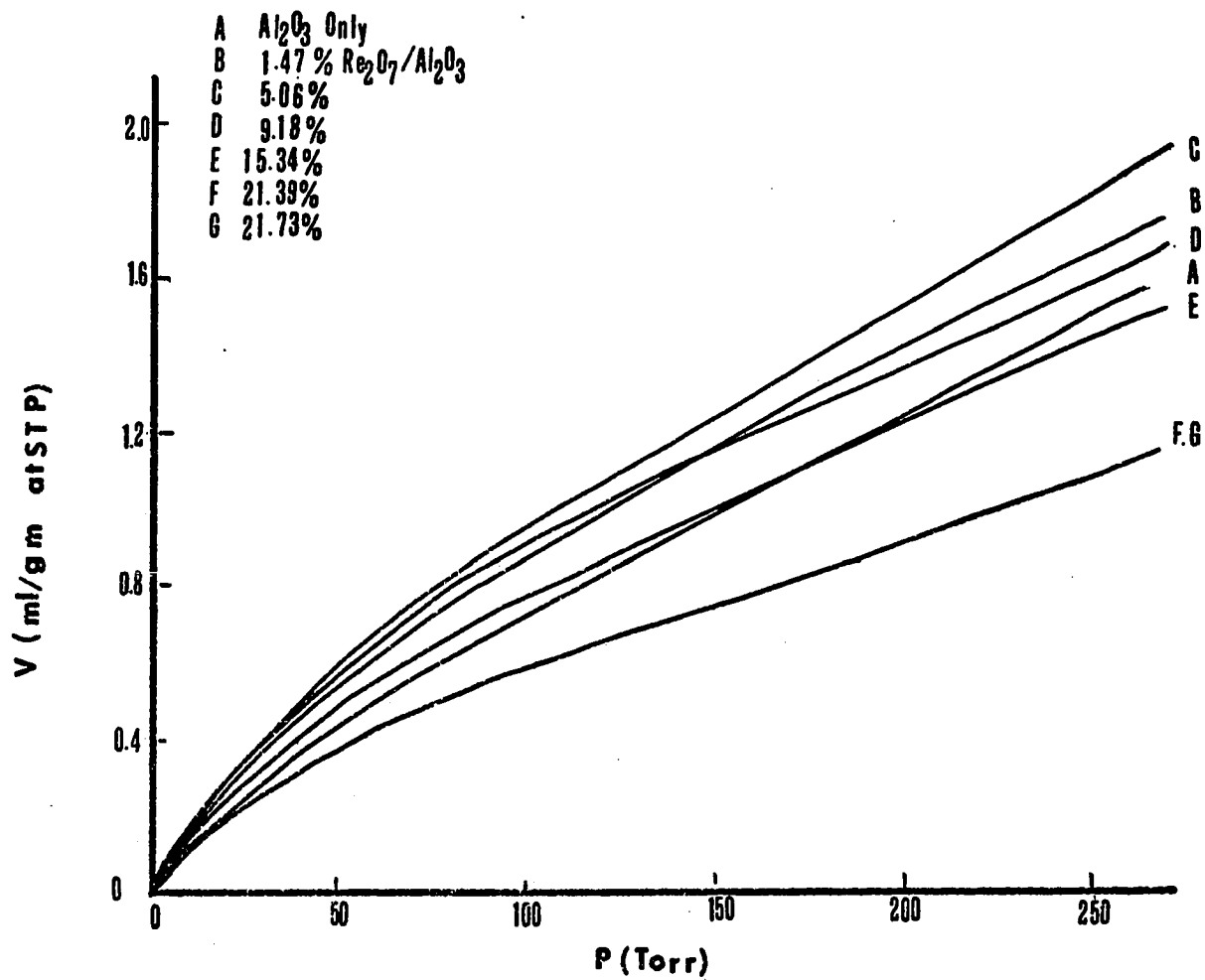


Fig. 7. Adsorption of Ethylene at Room Temperature on the Unreduced Alumina-Supported Catalysts.

(2). Adsorption at Room Temperature on Silica-supported Catalysts:

For the silica-supported catalysts, the results of adsorption and desorption of ethylene are presented in Fig. 8.

The amount of ethylene adsorbed decreases with the increase of rhenium content. The adsorption is reversible and the amount adsorbed for the supported catalyst never exceeds that of the support alone.

On the 5% catalyst supported on silica, the amount of adsorption is essentially the same as that of silica alone, but on the alumina supported catalyst there is an adsorption maximum. Silica has higher surface area than that of alumina, the dispersion of rhenium oxides on the silica support will be expected higher. Probably, interactions occur between the promoter- Re_2O_7 , and the support- Al_2O_3 , and more surface sites are activated. Since the difference of the amount of adsorption between the supported catalyst and the support is small, it may be that one rhenium site blocks one alumina site, and when rhenium content is high some pores are blocked and make some sites inaccessible by the adsorbate and therefore reduce the amount of adsorption.

For the adsorption of ethylene on silica supported catalysts, at higher pressures there is a slight color change of the catalyst. Originally, the catalyst is snow white, but as the adsorption proceeds a purple color is gradually developed. It is known that ReO_3 is purple, and Re_2O_7 is white or yellow, hence reduction occurs very slowly. On the alumina supported catalysts there is no color change observed. It gives further indication that interaction occurs between rhenium oxide and alumina, making it more resistant to reduction.

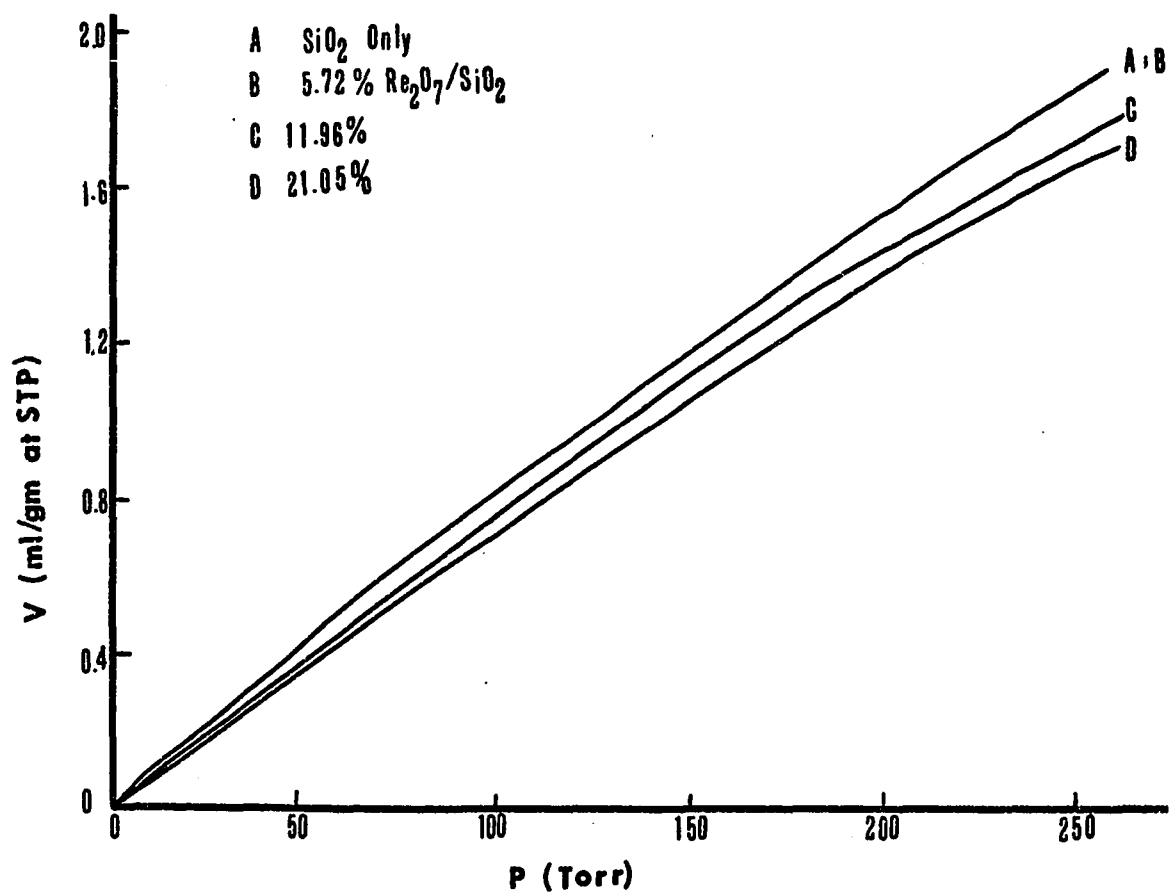


Fig. 8. Adsorption of Ethylene at Room Temperature on the Unreduced Silica-Supported Catalysts.

(3). Adsorption of Ethylene at Various Temperatures:

The results for the adsorption of ethylene at various temperatures on alumina and on 10% $\text{Re}_2\text{O}_7/\text{Al}_2\text{O}_3$ are shown in Fig. 9.

The results for the adsorption of ethylene at 1°C and room temperature on 11% $\text{Re}_2\text{O}_7/\text{SiO}_2$ catalyst are shown in Fig. 10.

In all cases the amount of adsorption decreases with increasing temperature. The heat of adsorption, and the entropy of adsorption are presented in Table 5, 6, 7, and 8 for alumina, 10.95% $\text{Re}_2\text{O}_7/\text{Al}_2\text{O}_3$, 10.81% $\text{Re}_2\text{O}_7/\text{Al}_2\text{O}_3$, and 11% $\text{Re}_2\text{O}_7/\text{SiO}_2$ respectively.

From the calculated results, the heats of adsorption of ethylene on the catalysts are all between the latent heat of liquefaction (3.5 Kcal/mole) and the maximum heat of physical adsorption in the first layer (8 Kcal/mole) as given by Trapnell.⁶² Since the heat of adsorption is low and the adsorption is reversible, it may be that most portion of the adsorption is physical.

The calculated entropies of adsorption are larger than the quantity (${}_2S_{\text{trans.}} - {}_3S_{\text{trans.}}$), that means the adsorption of ethylene on the catalysts is somewhat mobile.

- A. Al_2O_3 only (0°C)
- B. Al_2O_3 only (25°C)
- C. 10.95% $\text{Re}_2\text{O}_7/\text{Al}_2\text{O}_3$ (5.1°C)
- D. 10.95% (25°C)
- E. 10.81% (75°C)
- F. 10.81% (95°C)

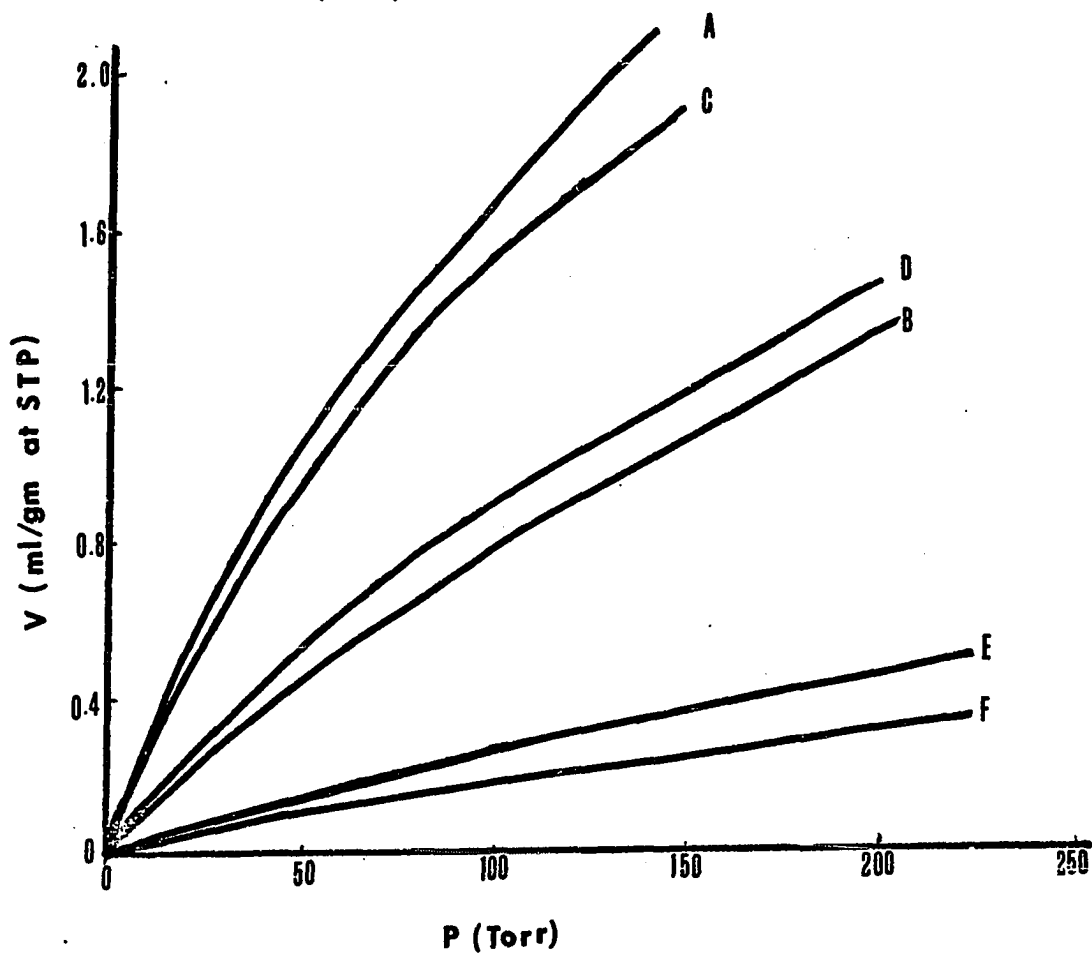


Fig. 9. Adsorption of Ethylene at Various Temperatures on the Unreduced Alumina-Supported Catalysts.

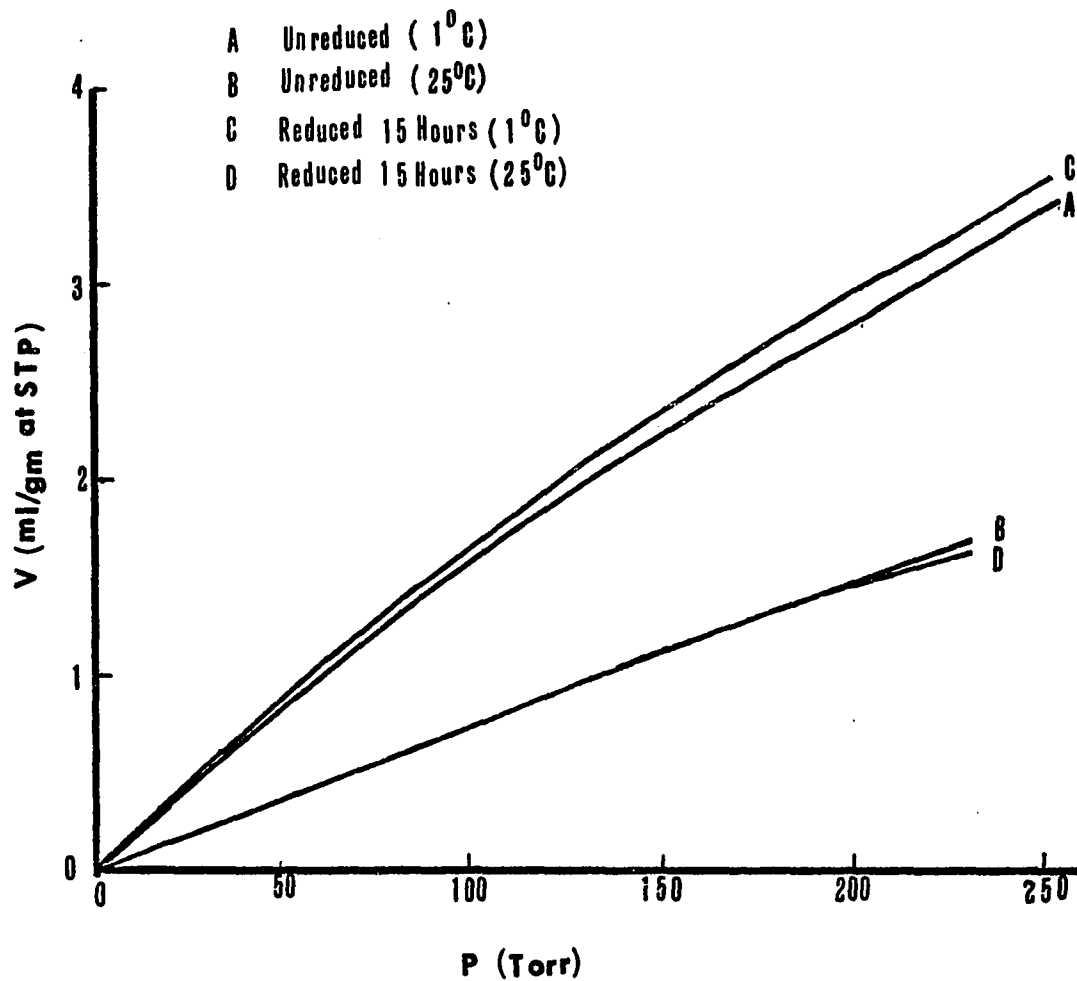


Fig. 10. Adsorption of Ethylene at 1°C and 25°C on the Unreduced and the Reduced 11.06% $\text{Re}_2\text{O}_7/\text{SiO}_2$ Catalyst.

Table 5. The heats of Adsorption and the Entropies of
Adsorption of Ethylene on Alumina

V (ml/gm @STP)	0.3	0.6	0.9	1.2	1.5	
Equilibrium Pressure(torr) (0°C)	10	23	41	61	85	
Equilibrium Pressure(torr) (25°C)	31	74	124	178	245	
$-\Delta H$ (Kcal/mole)	7.603	7.853	7.437	7.196	7.114	7.441(ave.)
$-\Delta S$ (e.u.)	19.23	21.80	21.43	21.33	21.69	21.10 (ave.)
$(2S_{trans} - 3S_{trans})$ at 300°K	: -20.60 e.u.					
$(S_{config.} - 3S_{trans})$	-28.9 e.u.					

Table 6. The Heats of Adsorption and the Entropies of
Adsorption of Ethylene on 10.95% Re_2O_7/Al_2O_3
Catalyst

V (ml/gm @ STP)	0.3	0.6	0.9	1.2	1.5	
Equilibrium Pressure (torr) at 5.1°C	10	24	46	70	103	
Equilibrium Pressure (torr) at 25°C	24	58	102	150	215	
$-\Delta H$ (Kcal/mole)	7.206	7.263	6.554	6.273	6.057	6.672(ave.)
$-\Delta S$ (e. u.)	17.31	19.26	18.00	17.83	17.82	18.04 (ave.)

Table 7. The Heats of Adsorption and the Entropies of Adsorption
of Ethylene on 10.81% $\text{Re}_2\text{O}_7/\text{Al}_2\text{O}_3$ Catalyst

V (ml/gm @ STP)	0.05	0.1	0.15	0.2	0.25	0.30	0.35
Equilibrium Pressure (torr) at 75°C	18	38	61	85	110	136	161
Equilibrium Pressure (torr) at 95°C	28	65	102	139	178	218	259
$-\Delta H$ (Kcal/mole)	5.621	6.821	6.540	6.257	6.123	6.003	6.048 6.203(ave.)
$-\Delta S$ (e. u.)	8.716	13.673	13.78	13.63	13.76	13.83	14.30 13.10(ave.)

Table 8. The Heats of Adsorption and the Entropies of Adsorption
of Ethylene on 11.06% $\text{Re}_2\text{O}_7/\text{SiO}_2$ Catalyst

A. Unreduced Catalyst:

V (ml/gm @ STP)	0.3	0.6	0.9	1.2	1.5
Equilibrium Pressure (torr) at 1°C	16	35	54	74	95
Equilibrium Pressure (torr) at 25°C	38	75	118	160	202
$-\Delta H$ (Kcal/mole)	5.883	5.183	5.316	5.244	5.131 5.352(ave.)
$-\Delta S$ (e. u.)	13.78	12.78	14.13	14.49	14.57 13.95(ave.)

B. 15 Hours Reduced Catalyst:

V (ml/gm @ STP)	0.3	0.6	0.9	1.2	1.5
Equilibrium Pressure (torr) at 1°C	12	28	46	65	84
Equilibrium Pressure (torr) at 25°C	38	75	118	160	206
$-\Delta H$ (Kcal/mole)	7.801	6.668	6.375	6.096	6.071 6.602(ave.)
$-\Delta S$ (e. u.)	20.21	17.76	17.68	17.35	17.77 18.15(ave.)

(iii). Reduced Catalysts:

(1). Silica Supported Catalysts:

Rhenium has several oxidation states. Reduction occurs during the adsorption of ethylene on the unreduced silica supported catalysts. The adsorptions of ethylene on the hydrogen reduced catalysts supported on silica are shown in Fig. 11.

Reduction of the silica supported catalysts with hydrogen gives rise to a considerable amount of slow irreversible adsorption, which decreases with reduction temperature and reduction time. Upon 15 hours of reduction at 500°C, the adsorption becomes rapid and reversible again. The catalysts quickly become black after the introduction of hydrogen at temperatures above 400°C. The differences for the amounts of ethylene adsorbed between the 15 hours reduced and the unreduced catalysts are all very small with the unreduced catalysts adsorbing slightly more ethylene.

(2). Alumina Supported Catalysts:

Similarly, slow irreversible adsorption occurs on the alumina-supported catalysts which are reduced with hydrogen. But the amount of adsorption increases with reduction time, and reaches a constant value after about 15 hours. The results are shown in Fig. 12, and 13. Points on the ascending branch are taken at one hour intervals, and those on the descending branch every 10 to 15 minutes.

The adsorption of ethylene on alumina, which is reduced 15 hours with hydrogen at 500°C, is still reversible. Therefore, the irreversible adsorption must occur on the rhenium sites.

- A SiO₂ Only
 B 11.96% Re₂O₇/SiO₂ Reduced 2.5 Hours at 500° C
 C 11.96% Re₂O₇/SiO₂ Reduced 15 Hours at 500° C
 D 21.05% Re₂O₇/SiO₂ Reduced 15 Hours at 500° C

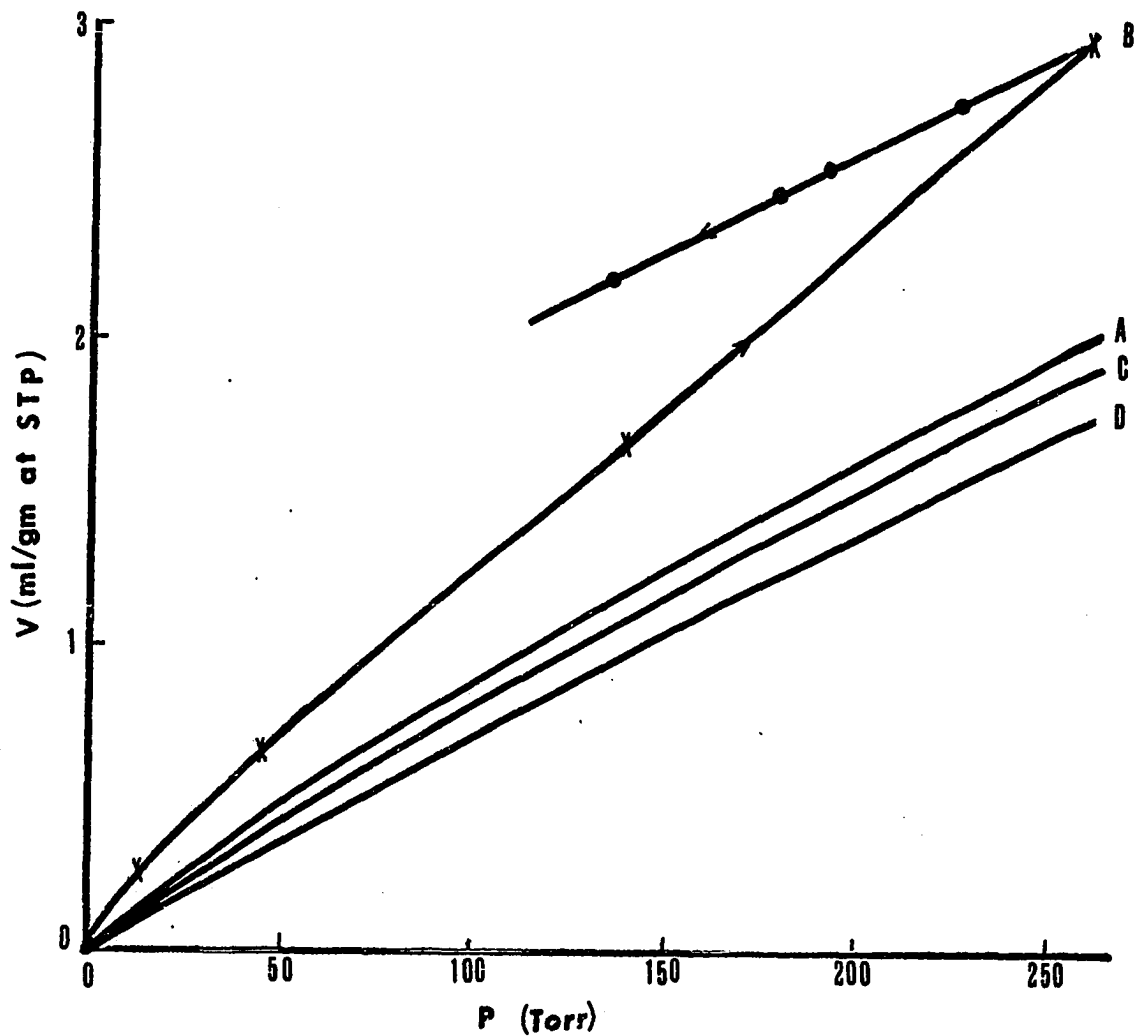


Fig. 11. Adsorption of Ethylene at Room Temperature on the Reduced Silica-Supported Catalysts.

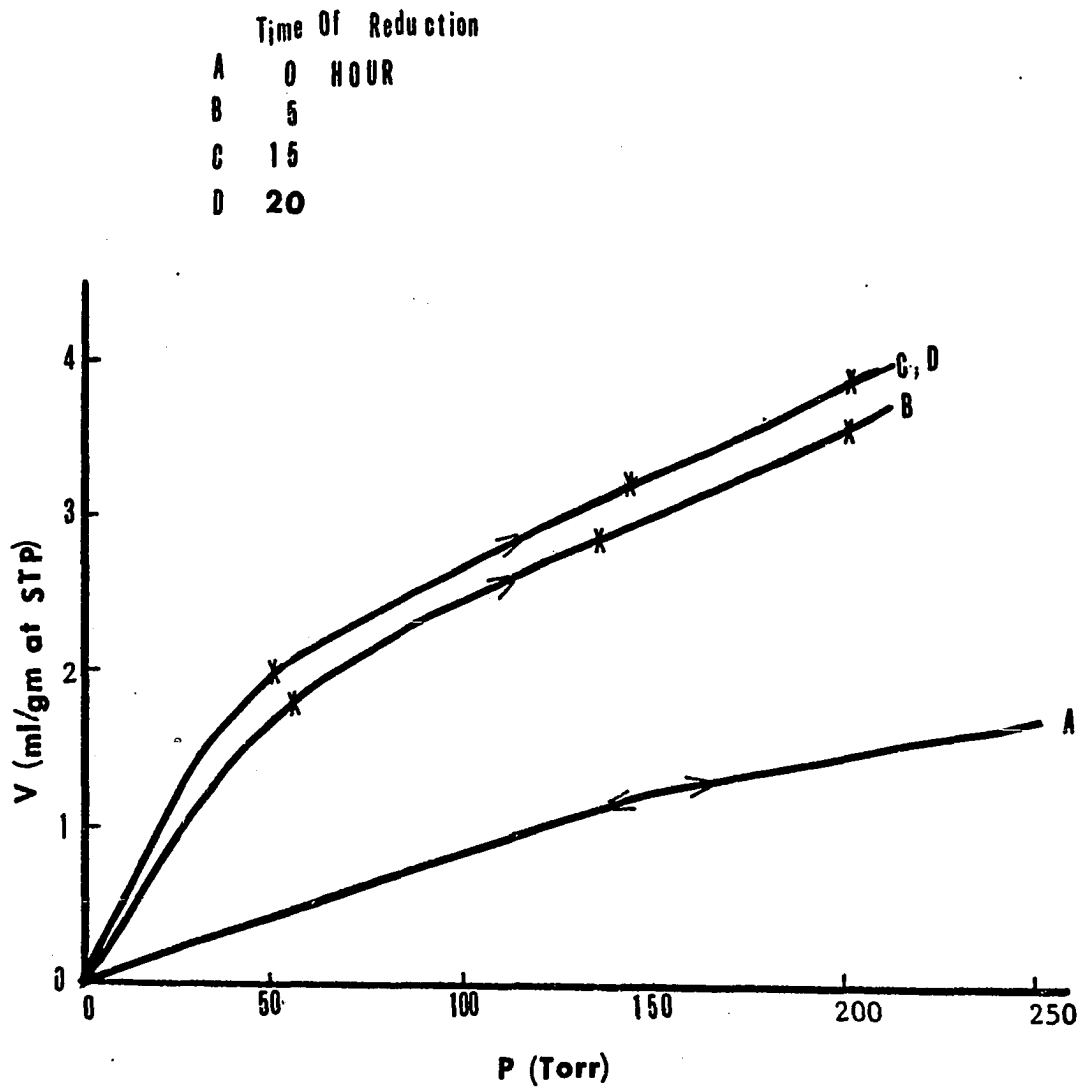


Fig. 12. Adsorption of Ethylene at Room Temperature on 10% $\text{Re}_2\text{O}_7/\text{Al}_2\text{O}_3$ Catalysts of Different Times of Reduction at 500°C.

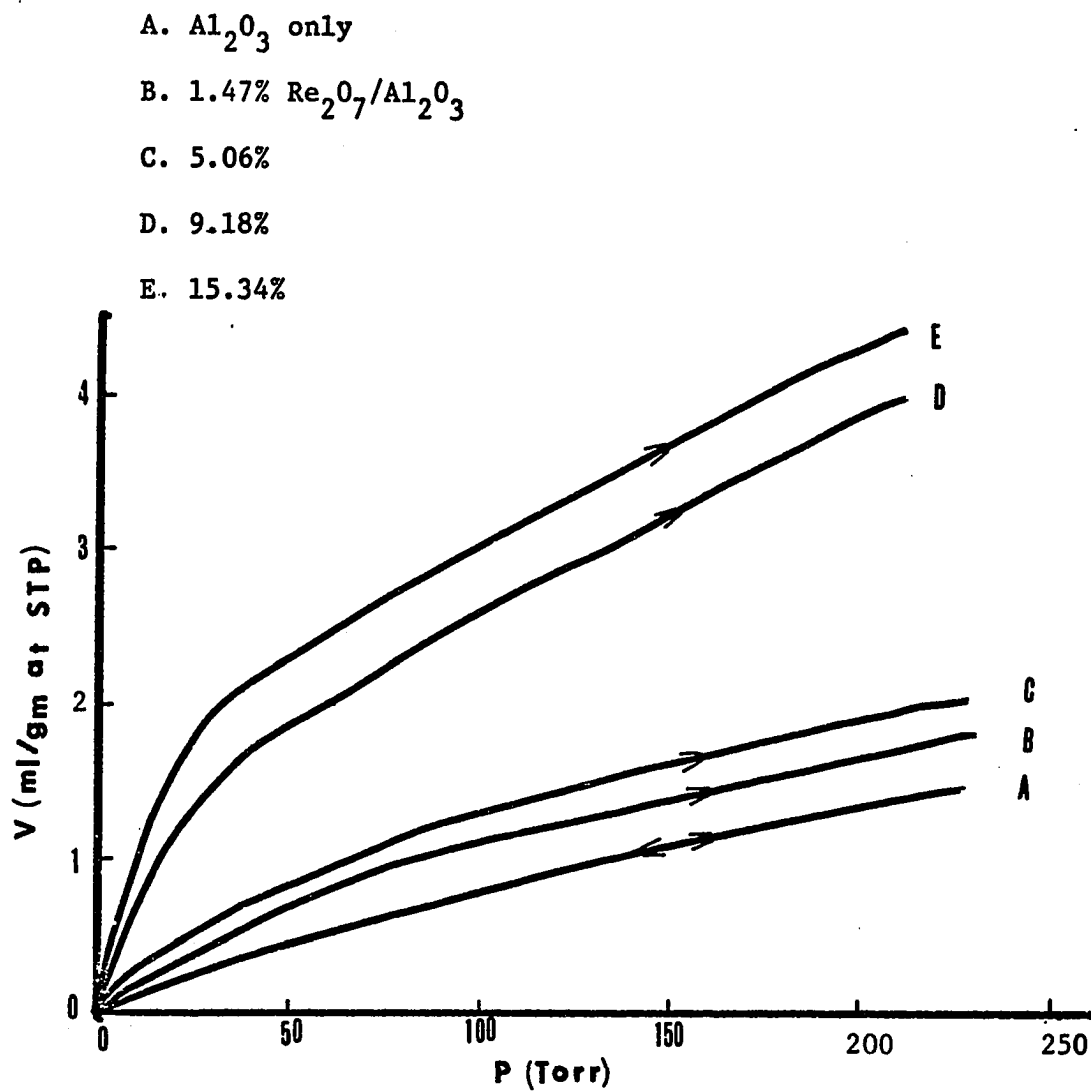


Fig. 13. Adsorption of Ethylene at Room Temperature on the 15 hours Reduced Alumina-Supported Catalysts.

The rate of adsorption of ethylene on 10.95% $\text{Re}_2\text{O}_7/\text{Al}_2\text{O}_3$ catalyst is shown in Fig. 14, with an initial pressure of about 536 torr. It is clear that it takes more than one day to reach the adsorption equilibrium.

On the reduced catalyst, the adsorbabilities keep decreasing after each regeneration but on the unreduced catalyst the adsorption is reproducible as shown in Table 9. It may be that very strong chemisorption occurs on some sites which can not be reactivated by 2.5 hours oxidation at 500°C.

After 25 hours of adsorption, the desorption of ethylene on the reduced catalysts has been measured. By extrapolating to zero pressure the amount of ethylene which is adsorbed irreversibly is presented in Table 10.

The kinetics and stoichiometry of reduction of $\text{MoO}_3/\text{Al}_2\text{O}_3$ catalysts was studied by Massoth⁴⁶ using microbalance reactor. Catalyst reduction was slower and different in character than those of bulk MoO_3 and $\text{Al}_2(\text{MoO}_4)_3$. Extent of reduction increased with increase in Mo content, time of reduction, and temperature. On the $\text{Re}_2\text{O}_7/\text{Al}_2\text{O}_3$ catalysts, the irreversible adsorptions increase with time of reduction but seem not depend strictly on the Re content. Rhenium has more oxidation states than molybdenum, and the state which adsorbs ethylene irreversibly is not clear at the present time, so that it is difficult to correlate the irreversible adsorption with the extent of reduction.

It was shown by Biloen and Pott⁶ that $\text{WO}_3/\text{Al}_2\text{O}_3$ can not be appreciably reduced in hydrogen at 550°C, whereas WO_3/SiO_2 is reduced to lower valence states, and unsupported WO_3 is completely reduced to tungsten metal within two hours by hydrogen at 1 bar pressure and 550°C.

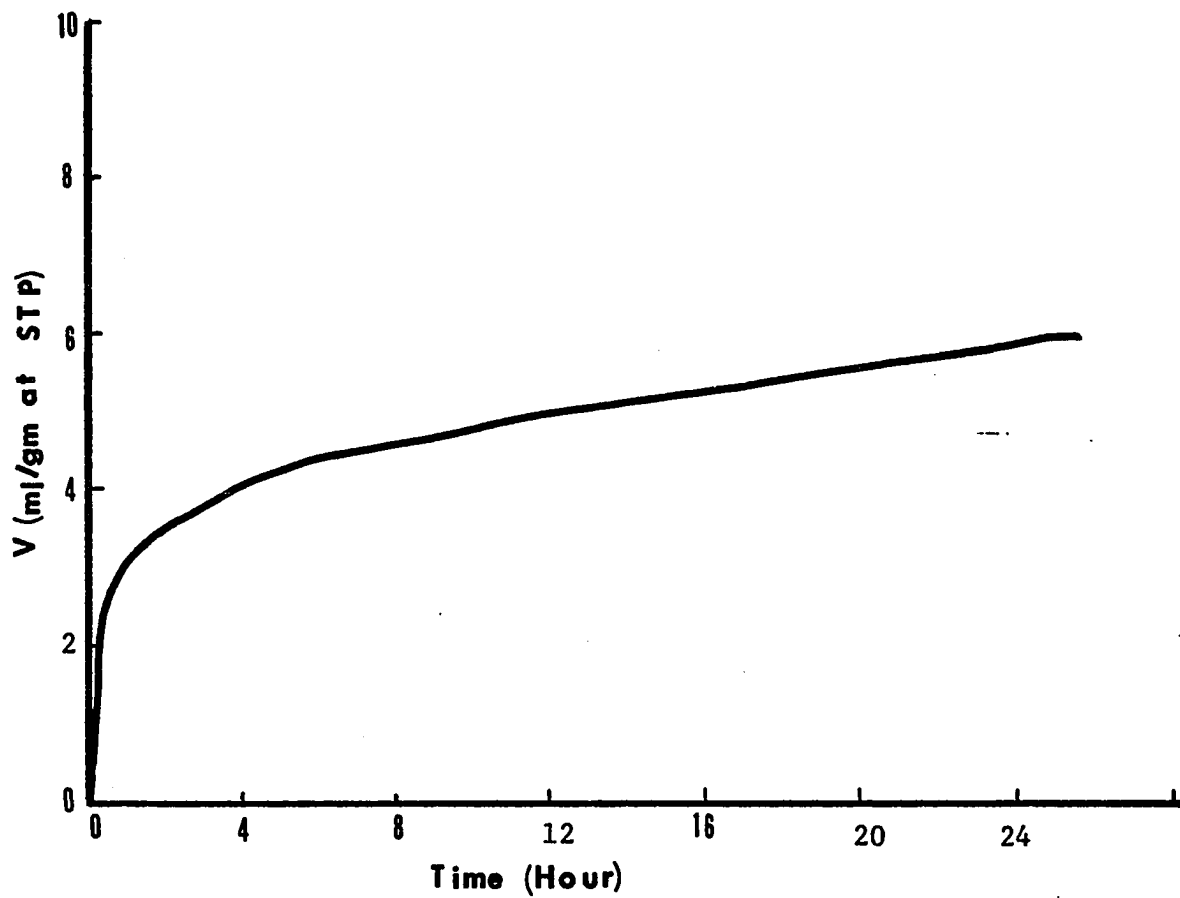


Fig. 14. The Rate of Adsorption of Ethylene at Room Temperature on the 15 Hours Reduced 10.95% $\text{Re}_2\text{O}_7/\text{Al}_2\text{O}_3$ catalyst.

Table 9. The Adsorbabilities of the Reused Catalysts.

(10.95% $\text{Re}_2\text{O}_7/\text{Al}_2\text{O}_3$)

Previous Regeneration Number	Time of Oxidation at 500°C	Time of Reduction at 500°C	Ethylene Admitted Initially. (ml/gm @STP)	Ethylene Adsorbed (ml/gm @STP)
7	2.5	16	11.22	3.08 after 2.5 hrs.
8	2.5	16	11.20	2.90 after 7.5 hrs.
9	2.5	16	11.28	2.03 after 22.5 hrs.
10	2.5	0	Two isotherms coincide.	
11	16	0		

Table 10. The Amount of Irreversible Adsorption of Ethylene
on the Alumina Supported Rhenium Oxide Catalysts

Catalyst Wt. %	Time of Reduction (hour)	Irreversible Adsorption of Ethylene (ml/gm @STP)	$\frac{\text{Moles of Re}}{\text{Moles of C}_2\text{H}_4}$
1.47	15	0.2	7
5.37	15	0.5	10
10.95	15	5.0	2
17.66	15	2.5	6

Whether the results obtained in the tungsten oxide system are applicable to the rhenium oxide system is not known, but from the experimental results of the adsorption of ethylene on the reduced rhenium oxide catalysts, it seems that the two systems behave similarly. It appears that an intermediate state of oxidation of rhenium oxide may exist on the surface, which adsorbs ethylene irreversibly, and is far more resistant to reduction on alumina than on silica.

Rhenium was added to the catalyst as perrhenate ion having Re in the +7 state. Calcination of perrhenic acid, or of lower oxides at an elevated temperature yields Re_2O_7 . Therefore, the Re in the calcined catalyst will be +7. If it were to be reduced to metal, seven atoms of hydrogen per atom of rhenium would be required. The data obtained by Johnson and LeRoy³⁵ showed that in a Pt/Re/ Al_2O_3 catalyst Re^{+7} is reduced to Re^{+4} by hydrogen at 482°C, because the ratio of hydrogen to rhenium is 3. Bulk Re_2O_7 is reduced to ReO_2 by hydrogen at 300°C, and to metal at 400°C.¹⁸ If the oxide is stabilized by incorporation into the alumina lattice, it would not be surprising to find that reduction to metal at 482°C is difficult. Further work is necessary to know whether rhenium in silica supported catalyst is reduced to metal.

Reversible adsorptions of ethylene on the reduced catalysts of different reduction times have been studied. After oxidation and different times of reduction, ethylene is passed over the catalysts for 4 hours at 1 atmosphere, and the irreversible sites are saturated. Then the system is evacuated and the adsorption-desorption experiment is performed. The results, as presented in Fig. 15, show that the reversible adsorption isotherms essentially coincide with each other.

Suppose two kinds of site exist on the surface, one called alumina site and the other rhenium site. On the unreduced form both sites adsorb ethylene reversibly. Upon reduction, it is known from experiment that alumina sites still adsorb ethylene reversibly. If no other kinds of sites are generated by reduction, and rhenium sites become irreversible sites then the reversible sites will be decreased more and more by longer reduction. Upon complete reduction only alumina sites are responsible for the reversible adsorption. Then one can know exactly the portions of ethylene adsorbed on rhenium sites and on alumina sites. But since the reversible adsorption is independent of the reduction time, another kind of site may be generated, and the irreversible adsorption occurs on these sites without affecting the reversible parts.

During hydrogen reduction, water is formed and the oxygen in the catalyst has been taken out thus creates some anion vacancies. Probably ethylene is held irreversibly on these anion vacancies. Of course there may be some other explanations, but this one seems to be the most straightforward. I R studies on the adsorbed species may be very useful to prove it.

(B). Disproportionation of Propylene:

(i). Unreduced Catalysts:

The kinetics of the disproportionation of propylene have been studied at various partial pressures of propylene and at various temperatures. Mass transfer effects are examined first to ensure that the data obtained only reflect the chemical events.

Catalysts supported on silica have no reactivity for the disproportionation of propylene at room temperature. The catalysts are reduced rather quickly by propylene. On a silica supported catalyst which is

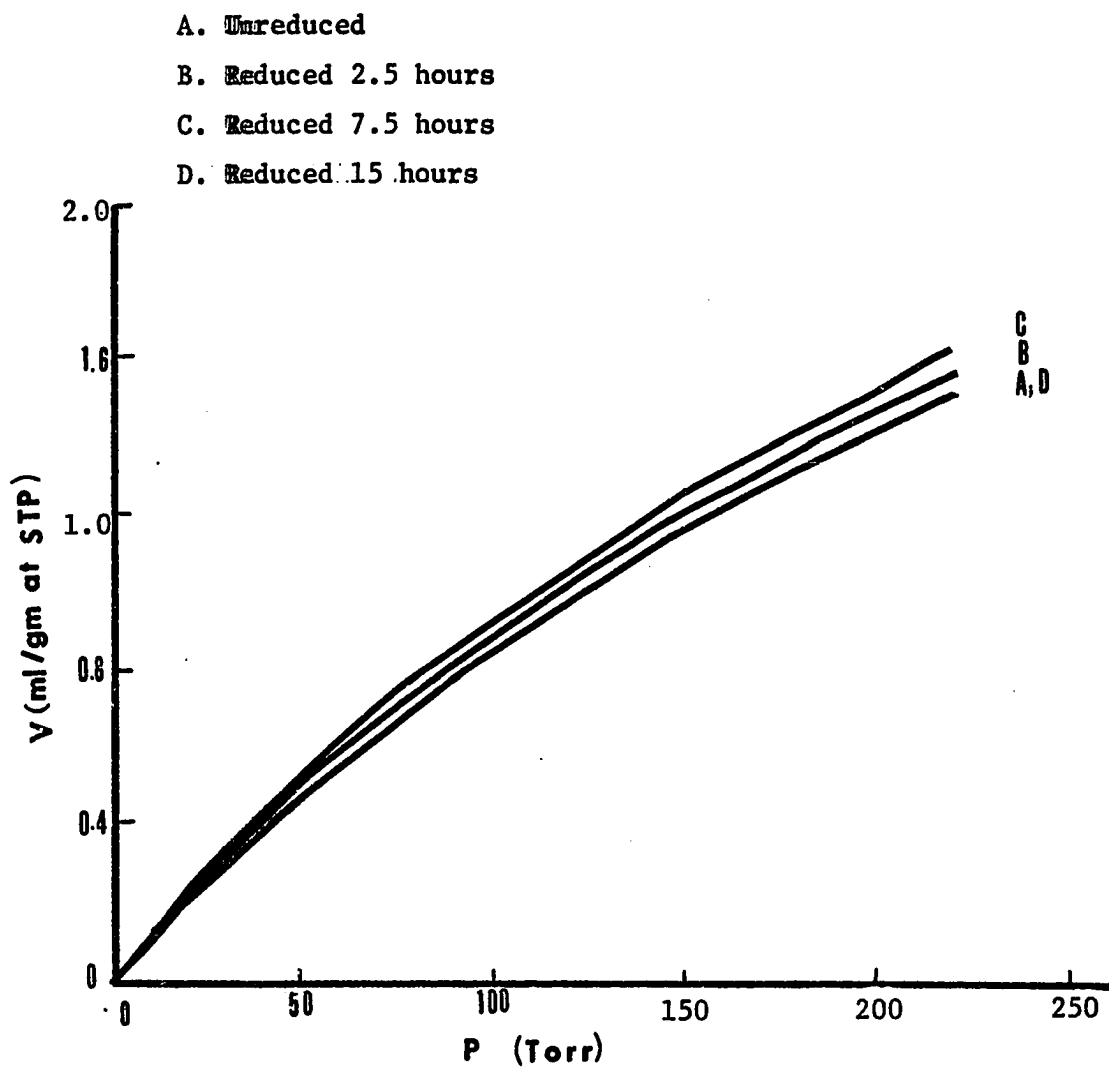


Fig. 15. Reversible Adsorption of Ethylene at Room Temperature on the Reduced 10.95% $\text{Re}_2\text{O}_7/\text{Al}_2\text{O}_3$ Catalysts.

reduced with hydrogen for 15 hours, there is still no reaction even up to 180°C.

The disproportionation of propylene is studied first using 21% $\text{Re}_2\text{O}_7/\text{Al}_2\text{O}_3$ catalyst. To examine whether an interphase mass transfer effect exists the reaction rates are measured on different weights of catalyst under the same space velocity. The results are shown in Table 11. The average rate for two grams of catalyst is 29.42×10^{-4} gm mole per gm catalyst per hour; for 4 grams is 38.99×10^{-5} . The rate increased more than 30% as the weight of the catalyst is doubled. That means the reaction rates increase with linear velocity, and an interphase mass transport limitation exists on the 21% catalyst in the flow ranges studied. A plot of conversion versus W/F is shown in Fig. 16. At 0.5°C and 1 atmospheric pressure the average rate for two grams catalyst is 1.28×10^{-3} , and for four grams catalyst is 1.17×10^{-3} . Since the rates did not increase with linear velocity, the interphase mass transfer problem disappeared at the lower temperature. The conversion versus W/F is also plotted in Fig. 16. As can be seen when W/F approaches zero the conversions all go to zero by extrapolation.

On 10% $\text{Re}_2\text{O}_7/\text{Al}_2\text{O}_3$ catalyst there is no interphase limitation at room temperature. The data are presented in Table 12, and are also plotted in Fig. 16. The average rate for 2 grams catalyst is 0.0024 gm mole per gm catalyst per hour, and 0.0022 for 4 grams catalyst.

The intraparticle mass transfer effect is studied using catalysts of different particle sizes. For catalyst of 10-28 mesh size (0.0787" to 0.0232") the reaction rate is 23.97×10^{-4} , and for catalyst of 40-60 mesh size (0.0165" to 0.0098") the rate is 24.89×10^{-4} . The results are shown in Table 12. There is essentially no pore diffusion limitation on these

Table 11. Results for the Disproportionation of Propylene at Room

Temperature and 1 Atmosphere on 21.39% $\text{Re}_2\text{O}_7/\text{Al}_2\text{O}_3$ Catalyst.

W (gm)	2.1090	2.1090	2.1056	2.1056	4.2178	4.2178	4.2178
F (ml/sec at 1 atm. 25°C)	1.15	2.222	0.625	2.222	1.16	2.38	4.444
W/F	1.834	0.949	3.369	0.948	3.636	1.772	0.949
WHSV ($\frac{\text{gm. C}_3\text{H}_6}{\text{gm. Cat. Hr.}}$)	3.43	6.63	1.87	6.64	1.73	3.55	6.63
Conversion (%)	3.73	1.72	7.43	1.85	10.35	4.64	2.48
Rate x 10^4 ($\frac{\text{gm mole}}{\text{gm Cat. Hr}}$)	29.91	26.65	32.43	28.71	40.06	38.50	38.42
	Average: 29.42				Average: 38.99		

Table 12. Results for the Disproportionation of Propylene at Room

Temperature and 1 Atmosphere on 9.94% $\text{Re}_2\text{O}_7/\text{Al}_2\text{O}_3$ Catalyst.

W (gm)	2.4994	2.0750	2.0750	4.1503	4.1503	4.1503
F (ml/sec at 1 atm. 25°C)	0.83	1.0	1.0	2.0	1.0	0.625
W/F	3.019	2.075	2.075	2.075	4.150	6.64
WHSV ($\frac{\text{GM C}_3\text{H}_6}{\text{gm Cat. Hr}}$)	2.07	3.03	3.03	3.03	1.52	0.95
Conversion (%)	5.11	3.21	3.57	3.26	6.17	9.00
Rate x 10^4 ($\frac{\text{gm mole}}{\text{gm Cat. Hr}}$)	24.89	22.47	25.34	23.08	21.84	19.89
	Average: 24.23			Average: 21.60		

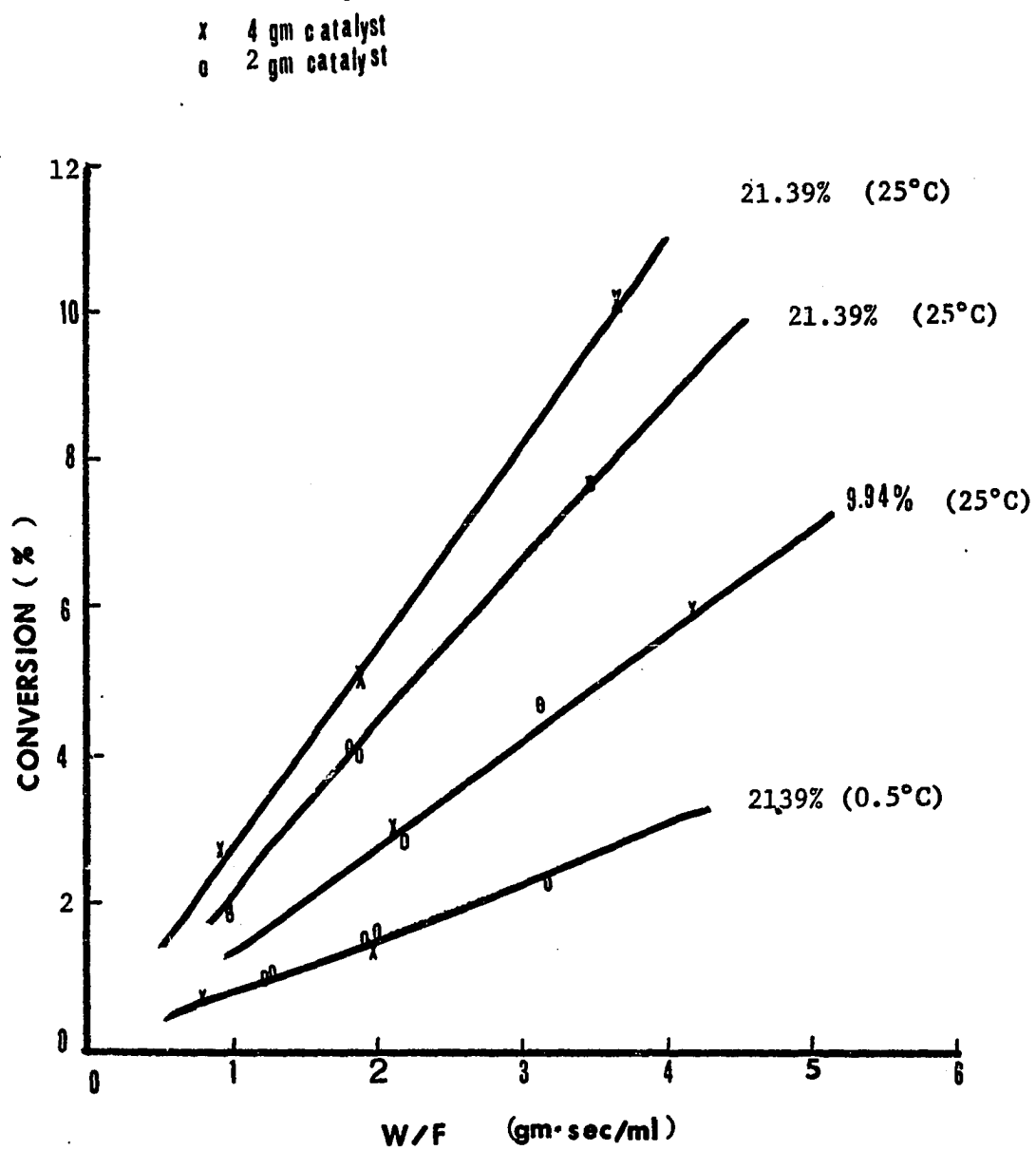


Fig. 16. Percent Conversion of Propylene vs W/F for 21.37% and 9.94% $\text{Re}_2\text{O}_7/\text{Al}_2\text{O}_3$ Catalysts.

catalysts of small particle sizes. In the studies of adsorption and reaction kinetics all the catalysts used are of 40-60 mesh size unless specified particularly.

Since there is a slight mass transfer problem on the 20% catalyst at room temperature, only 10% catalyst supported on alumina is used for the study of the reaction kinetics of the disproportionation of propylene and deuterated ethylene.

The activities of the 10.95% catalyst in propylene stream are measured for four hours at room temperature and 1 atmospheric pressure. The reaction rate versus time is shown in Table 14. As to be expected, the activity decays rather slowly because the reaction temperature is not high, and coke formation is not likely.

On WO_3/SiO_2 catalyst there is a break-in period during which activity increases with time in the propylene stream. In the present system there is no such phenomenon.

Equal moles of ethylene and 2-butenes are produced. There is no appreciable change in the ratio of trans to cis 2-butene with time. Higher olefins are not detected. At higher flow rates of propylene the trans to cis ratio is lowered, and in all cases this ratio is lower than the equilibrium value. Cis-2-butene may be the more favorable product of disproportionation, and trans-2-butene is formed mainly by the isomerization of the cis form, as trans form is favorable thermodynamically and alumina is a known catalyst for isomerization. More proof is found on the reduced catalyst as to be discussed later.

The results for the disproportionation of propylene on 10.95% Re_2O_7/Al_2O_3 catalyst at various temperatures and various propylene

Table 13. Effect of Catalyst Particle Size on Reaction Rate (9.94% $\text{Re}_2\text{O}_7/\text{Al}_2\text{O}_3$ Catalyst at 1 Atmosphere and 25°C).

Mesh Size	W (gm)	F (ml/se)	W/F	Conversion(%)	Rate $\times 10^4$
10 - 28 (0.0787"-0.0232")	2.4836	0.776	3.199	5.21	23.97
40 - 60 (0.0165" -0.0098")	2.4994	0.830	3.019	5.11	24.89

Table 14. Activities of the 10.95% $\text{Re}_2\text{O}_7/\text{Al}_2\text{O}_3$ Catalyst Versus Time in Propylene Stream.

Time (minute)	10	20	30	60	90	120	150
Rate $\times 10^4$ (gm mole/gm/hr.)	19	19.5	20	20	18.5	16.5	15.5
Time			180	210	240		
Rate $\times 10^4$			15	14.5	13		

partial pressures are presented in Table 15, 16, and 17. Helium is used as diluent to make up the total pressure of 1 atmosphere. The results using least square fitting to different reaction models are shown in Table 18.

The rate of reaction is proportional to the partial pressure of propylene to the 1.4th power for pressures equal to or less than one atmosphere. As can be seen, the Langmuir Hinshelwood model fits the data better than the Rideal model which is in agreement with other studies using both $\text{Co-MoO}_3/\text{Al}_2\text{O}_3$ and WO_3/SiO_2 catalysts. The deviation using the Rideal model is twice of that of the Langmuir Hinshelwood model.

The activation energy is 11 Kcal/mole, which is very close to the value obtained by Moffat and Clark of 10 Kcal/mole on $\text{Co-MoO}_3/\text{Al}_2\text{O}_3$ catalyst.

(ii). Reduced Catalysts:

On the reduced catalysts supported on alumina, the rate of reaction of propylene shows a substantial increase initially, then the rate drops gradually with time. The initial rate depends upon the time of reduction with hydrogen at 500°C. The effect of time of reduction on the initial rate obtained by extrapolation is shown in Table 19.

Upon 15 hours of reduction at 500°C of the freshly prepared catalyst, the initial rate is about three times of that of the unreduced fresh catalyst.

The reaction rates on the reused catalysts both unreduced and 15 hours reduced have been followed for 4 hours. The results are shown in Fig. 17, and 18. On the 15 hours reduced catalyst the rates drop rather rapidly in the first hour, and after 2 hours the rate is essentially equal to the rate of the unreduced catalyst.

Table 15. Rates of Reaction of Propylene Disproportionation on 10.95% $\text{Re}_2\text{O}_7/\text{Al}_2\text{O}_3$ at 25°C, and 1 Atmosphere Pressure.

$P_{\text{C}_3\text{H}_6}$ (atm)	1.0	0.816	0.754	0.342	0.187	0.163	0.151
Rate $\times 10^4$ (gm mole/gm/hr.)	23.81	20.85	19.53	5.71	2.18	1.97	1.96

Table 16. Rates of Reaction of Propylene Disproportionation on 10.95% $\text{Re}_2\text{O}_7/\text{Al}_2\text{O}_3$ at 40°C, and 1 Atmosphere Pressure.

$P_{\text{C}_3\text{H}_6}$ (atm)	1.0	0.843	0.494	0.361
Rate $\times 10^4$ (gm mole/gm/hr)	67.23	42.75	25.90	14.25

Table 17. Rates of Reaction of Propylene Disproportionation on 10.95% $\text{Re}_2\text{O}_7/\text{Al}_2\text{O}_3$ at 68°C, and 1 Atmosphere Pressure.

$P_{\text{C}_3\text{H}_6}$ (atm)	1.0	0.854	0.792	0.784	0.340	0.244	0.130
Rate $\times 10^4$ (gm mole/gm/hr.)	220.6	217.4	156.99	144.45	42.17	28.29	12.40

Table 18. Results of the Least Square Fitting of the Rate Data for
Propylene Disproportionation on 10.95% $\text{Re}_2\text{O}_7/\text{Al}_2\text{O}_3$ Catalyst.

Temperature(°C)	25	40	68
Power Law	$\ln R = -5.931 + 1.427 \ln P$	$\ln R = -5.082 + 1.393 \ln P$	$\ln R = -3.792 + 1.455 \ln P$
$\left \frac{E-C}{E} \right _{\text{ave.}}$	0.00956	0.016703	0.016662
L.H. Model*	$P/\sqrt{R} = 10.152 + 9.884P$	$P/\sqrt{R} = 7.548 + 5.251P$	$P/\sqrt{R} = 3.754 + 3.042P$
K_p (atm^{-1})	0.9736	0.6957	0.8102
K_r (gm mol/gm/hr)	0.010235	0.036268	0.108085
$\left \frac{E-C}{E} \right _{\text{ave.}}$	0.03902	0.0445	0.059893
Rideal Model**	$P^2/R = 85.701 + 306.7P$	$P^2/R = 46.94 + 115.97P$	$P^2/R = 12.82 + 32.27P$
K_p (atm^{-1})	3.5794	2.4708	2.5182
K_r (gm mol/gm/hr)	0.003259	0.008623	0.03098
$\left \frac{E-C}{E} \right _{\text{ave.}}$	0.07505	0.08994	0.107104

$$* \quad P/\sqrt{R} = 1/(\sqrt{K_r} K_p) + P/\sqrt{K_r}$$

$$** \quad P^2/R = 1/(K_r K_p) + P/K_r$$

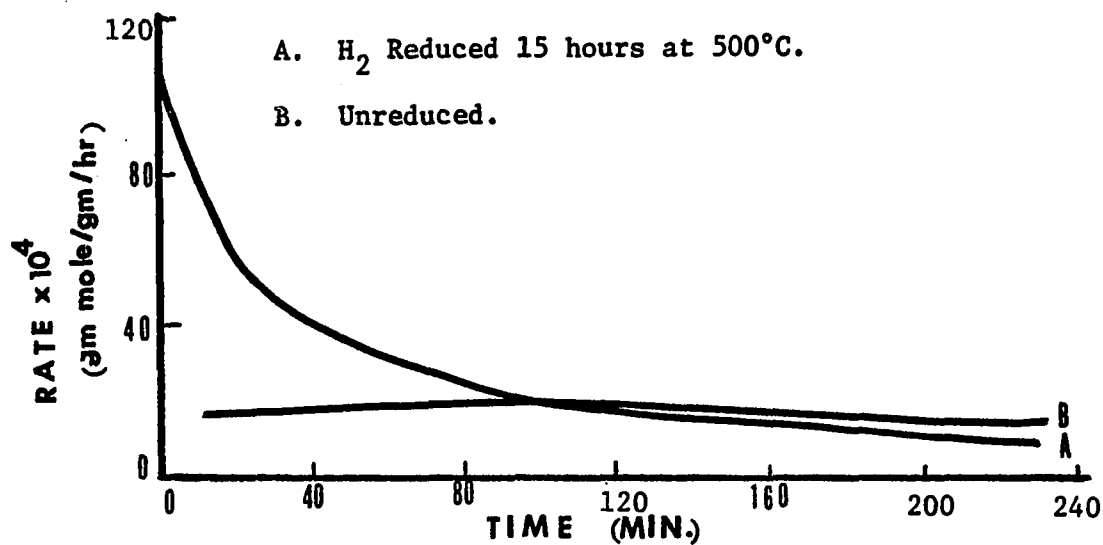


Fig. 17. The Rate of Propylene Disproportionation vs. Time on 10.95% Re₂O₇/Al₂O₃ Catalyst.

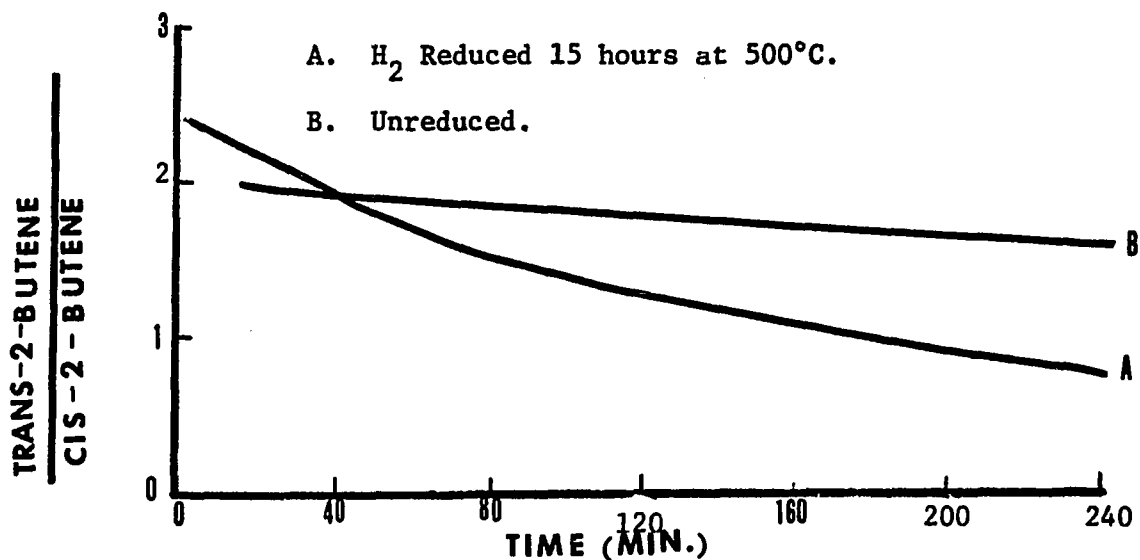


Fig. 18. The Ratio of trans-2-butene to cis-2-butene vs. Time for the Disproportionation of Propylene on 10.95% Re₂O₇/Al₂O₃ Catalyst.

From the results of ethylene adsorption it is known that slow irreversible adsorption occurs on the reduced catalysts. The decay of activities of the reduced catalyst may be due to this slow irreversible adsorption, and the rates on the reduced catalysts decrease to the constant value for unreduced catalysts, as the irreversible sites are filled.

Like the unreduced catalysts, the ratio of the product trans-2-butene to cis-2-butene is lower than the equilibrium value, but it decreases continuously with time. It also depends upon the flow rate of propylene. The trans to cis ratio is lowered by increasing the flow rate. The irreversible adsorption may poison the sites for isomerization in a great extent.

(iii). Reduced Catalysts with Pre-adsorption of Ethylene: —

On the 15 hours reduced catalyst, the effect of pre-adsorption of ethylene on the rate of propylene disproportionation is shown in Table 20. After 15 hours reduction the catalyst is purged with helium for 1.5 hours, then the system is evacuated, and approximately 12.4 ml/gm @ STP of ethylene is admitted for a desired period then the system is evacuated again for two hours and propylene is then introduced.

The initial rate of propylene disproportionation decreases with the time of exposure to ethylene of the catalyst. This gives a proof that the irreversible adsorption causes the decrease in reaction rates, and also the rate of isomerization of cis-2-butene to trans-2-butene.

Table 19. Effect of Time of Reduction on The Initial Rate of the Disproportionation of Propylene
(10.95% $\text{Re}_2\text{O}_7/\text{Al}_2\text{O}_3$ at 25°C, and 1 atm.)

Time of H_2 Reduction (hour)	Initial Rate (gm mole/gm/hr)	% with respect to the Unreduced Catalyst
0	0.00260	100
2.5	0.00600	180
5	0.00220	65
10	0.0110	317
15	0.0130	360

Table 20. Effect of Pre-adsorption of Ethylene on the Initial Rate of the Disproportionation of Propylene at Room Temperature
(11.2% $\text{Re}_2\text{O}_7/\text{Al}_2\text{O}_3$ Fresh Catalysts Reduced 15 Hours)

Time of Exposure to Ethylene (hour)	Initial Rate of Propylene Disproportionation (gm mole/gm/hr)	Initial Ratio of Trans-2-butene to Cis-2-butene
2.5	0.0081	2
7.5	0.0075	2
15.5	0.0021	1.5
22.5	0.0006	1.0

(C). Disproportionation of Deuterated Ethylene on Unreduced Catalysts:

The disproportionation of monodeuterated ethylene was investigated by Lewandos⁴⁰ using $\text{MoO}_3/\text{Al}_2\text{O}_3$ catalyst at 155°C. It was found that alumina alone will not cause any composition change by passing monodeuterated ethylene over it at a gas hourly space velocity of 107 (ml per ml catalyst per hour). While at the same GHSV, disproportionation occurs over the supported catalyst with 8.8% conversion of monodeuterated ethylene. Also, there is no C_2HD_3 or C_2D_4 been detected, that means there is no scrambling effect.

In this work, the disproportionation of monodeuterated ethylene is first investigated at room temperature using 10% $\text{Re}_2\text{O}_7/\text{Al}_2\text{O}_3$ catalyst. $\text{C}_2\text{H}_3\text{D}$ is passed over two grams of catalyst at a flow rate of 7.21 ml/min. Analysis of the mass spectra of both reactant and product shows no change in composition. Then the experiment is conducted again under static conditions. After 10 minutes of contact time, there is still no reaction observed. It is indicated that the reaction is extremely slow at room temperature. Finally, a 46% conversion of $\text{C}_2\text{H}_3\text{D}$ is reached after 20 hours of contact time with equal amounts of C_2H_4 and $\text{C}_2\text{H}_2\text{D}_2$ formed. No C_2HD_3 , C_2D_4 , or cyclobutane is detected, in other words, there is no scrambling effect during the reaction.

The kinetics of the disproportionation of $\text{C}_2\text{H}_3\text{D}$ and the adsorption of C_2H_4 were then investigated at 95° and 75°C subsequently.

The isotope effect on the adsorption of ethylene at 22°C was also measured. The results are shown in Table 21, and 22.

Table 21. Adsorption of C_2H_4 and C_2H_3D at $22^\circ C$ on 10.81% Re_2O_7/Al_2O_3 Catalyst

C_2H_4		C_2H_3D	
Equilibrium Pressure	Volume Adsorbed	Equilibrium Pressure	Volume Adsorbed
(torr)	(ml/gm @ STP)	(torr)	(ml/gm @ STP)
18.88	0.2360	18.92	0.2596
39.62	0.3931	44.15	0.4902
89.60	0.6857	89.89	0.8138
129.00	0.9909	129.79	1.0592
158.75	1.1406	162.66	1.2185
206.57	1.3265	207.03	1.4305
255.43	1.5304	255.51	1.6367

$$V_{C_2H_4} = 0.027126 P^{0.730923}$$

(by least square fitting)

$$V_{C_2H_3D} = 0.033077 P^{0.708066}$$

(by least square fitting)

Table 22. Isotope Effect on the Adsorption of Ethylene at $22^\circ C$

Pressure (atm)	Pressure (torr)	$\frac{V_{C_2H_3D}}{V_{C_2H_4}}$
1.0	760	1.0478
0.826	628	1.0524
0.600	456	1.0601
0.435	331	1.0679

The amount of adsorption of C_2H_3D is somewhat higher than that of C_2H_4 , but as the pressure increases the ratio of C_2H_3D adsorbed to C_2H_4 adsorbed keeps decreasing. Therefore the isotope effect is not significant at higher pressures.

The equilibrium compositions of the disproportionation of C_2H_3D over 10.81% Re_2O_7/Al_2O_3 catalyst at 23°, 75°, and 95°C are shown in Table 23. The equilibrium products are obtained after 20 hours or more of contact time under static condition. No cyclobutane is detected.

The kinetic data at 75° and 95°C are shown in Table 24. The Least Square method is used to fit the data to the various kinetic models as discussed in Chapter 3, and the results are shown in Table 25.

Similar to the results obtained from the disproportionation of propylene, the average deviation for the Rideal model is about twice of that of the Langmuir Hinshelwood model. A plot of P^2/R versus P^2 shows the largest deviation implying that the assumption of a uniform surface with each site adsorbing two molecules is not a good one. The empirical power law fits the rate data best.

In this reaction adsorption equilibrium is established if the isotope effect is neglected. As discussed in Chapter 3, the rate of reaction can be correlated with the amount of adsorption. If the amount of adsorption of ethylene at the reaction temperature is known then one can check the validity of the correlation.

The adsorption isotherms of C_2H_4 at 75°, and 95°C are measured, and the results are shown in Table 26 and 27 respectively.

Table 23. The Compositions of the Equilibrium Products of the Disproportionation of C_2H_3D on 10.81% Re_2O_7/Al_2O_3 .

Temperature	C_2H_4	Mole % C_2H_3D	$C_2H_2D_2$	% Conversion of C_2H_3D
23°C	23.25	53.63	23.12	46.37
75°C	24.97	50.41	24.62	49.59
95°C	24.41	49.49	26.10	50.51

Table 24. Results for the Disproportionation of C_2H_3D over Unreduced 10.81% Re_2O_7/Al_2O_3 Catalyst at 75°C, and 95°C.

T (°C)	$P_{C_2H_3D}$ (atm)	C_2H_3D Flow Rate (ml/min @ 1atm 23°C)	Catalyst Wt. (gm)	% Conversion of C_2H_3D (%)	Rate $\times 10^4$ (gm mol/gm/hr)
75	1.0	7.21	3.1157	11.14	6.20
	0.826	4.10	3.1157	13.78	4.36
	0.667	2.54	3.1034	15.68	3.09
	0.435	2.67	3.1034	6.81	1.41
95	1.0	7.21	1.9841	7.94	6.94
	0.826	4.78	1.9787	8.51	4.94
	0.640	3.64	1.9787	7.04	3.11
	0.580	2.53	1.9726	8.86	2.74

Table 25. Results of the Least Square Fitting of the Rate Data for the Disproportionation of C_2H_3D on 10.81% Re_2O_7/Al_2O_3 Catalyst at 75°C, and 95°C.

T (°C)	$P_{C_2H_3D}$ (atm)	Rate x 10^4 (gm mol/gm/hr)	Relative Deviation (E-C/E)			
			Power Law	L.H. Model	Rideal Model	Uniform Surface with each Site Adsorbing 2 Molecules
75	1.0	6.20	0.000014	-0.004280	-0.007502	0.011408
	0.826	4.36	0.001764	0.009045	0.01721	0.024604
	0.667	3.09	0.002559	-0.004844	0.011029	-0.00151
	0.435	1.41	0.001279	-0.000046	0.000805	-0.01013
			Average 0.001279	0.004554	0.009137	0.012582
Power Law: $\ln(R) = 7.3857 + 1.7709 \ln(P)$;			L.H. Model: $P/R = 33.783 + 6.557 P$			
Rideal Model: $P^2/R = 1121.79 + 503.786P$;			Uniform Surface with 2 molecules on 1 site: $P^2/R = 1290.13 + 346.07 P^2$			
95	1.0	6.94	-0.000832	-0.003905	-0.007077	-0.008923
	0.826	4.94	0.000363	0.003931	0.007117	0.01301
	0.640	3.11	0.002920	0.012101	0.023590	0.024038
	0.580	2.74	0.002471	-0.012468	-0.025009	-0.029947
			Average: 0.001646	0.008101	0.015699	0.018980
Power Law: $\ln(R) = -7.2791 + 1.7322 \ln(P)$;			L.H. Model: $P/R = 31.8416 + 6.2661 P$			
Rideal Model: $P^2/R = 992.363 + 458.757 P$;			Uniform Surface with 2 molecules on 1 site: $P^2/R = 1168.56 + 285.224 P^2$			

Table 26. Adsorption of C_2H_4 at $75^\circ C$ on $10.81\% Re_2O_7/Al_2O_3$.

Equilibrium Pressure (torr)	Volume Adsorbed (ml/gm @ STP)
16.37	0.0463
55.15	0.1238
131.09	0.2626
211.14	0.4079
255.47	0.4857
311.43	0.5928
371.40	0.7046
427.62	0.7912
473.27	0.8753
518.16	0.9415
551.99	1.0147
634.38	1.1403
737.41	1.2788
769.07	1.3566

By the least square fitting for 10 data points:

(1). Langmuir Isotherm: $P/V = 435.15 + 0.204739 P$

$$V_m = 4.88 \text{ ml/gm @ STP. } K_p = 0.000471 (\text{torr}^{-1}).$$

(2). Freundlich Isotherm: $\ln(V) = -5.60401 + 0.885458 \ln(P)$

V: ml/gm @ STP; P: torr.

Table 27. Adsorption of Ethylene at 95°C on 10.81% Re₂O₇/Al₂O₃.

C_2H_4		C_2H_3D	
Equilibrium P. (torr)	Volume Adsorbed (ml/gm @ STP)	Equilibrium P. (torr)	Volume Adsorbed (ml/gm @ STP)
56.68	0.0471	30.89	0.0501
137.26	0.222	119.75	0.191
227.19	0.360	182.09	0.283
269.48	0.400	249.51	0.383
368.50	0.533	305.14	0.470
419.08	0.587	355.09	0.535
492.74	0.689	400.50	0.587
535.44	0.727	468.13	0.638
615.82	0.846	506.35	0.678
667.61	0.903	533.65	0.729
701.92	0.947	562.43	0.743
750.98	1.041	632.40	0.808
781.06	1.105	692.54	0.886
		743.21	0.953
		770.15	0.998

By the least square fitting for 11 data points:

(1). Langmuir Isotherm

$$P/V = 0.199737P + 601.906$$

$$V_m = 5.006 \text{ ml/gm}; K_p = 0.000332$$

(2). Freundlich Isotherm

$$\ln(V) = 0.903152 \ln(P) - 5.96367$$

$$C_2H_3D$$

$$P/V = 0.255464P + 597.811$$

$$V_m = 3.914; K_p = 0.000427$$

$$C_2H_3D$$

$$\ln(V) = 0.922629 \ln(P) - 6.10285$$

The maximum differential pressure can be read from the precision pressure gage is 300 torr, but the kinetic data obtained are all above 300 torr. It is desirable to have the adsorption data at the pressure where the reaction kinetics are measured. A threeway stopcock is installed just above the reference port of the bourdon capsule of the pressure gage. Argon is introduced to get the fixed pressure at the reference port, and the adsorption is carried out up to one atmosphere. The adsorption of C_2H_3D at $95^\circ C$ is also measured. The results are also shown in Table 27. It is clear that the amount of adsorption of C_2H_3D at $95^\circ C$ is essentially the same as that of C_2H_4 , that is, the isotope effect is negligible at high temperatures.

The results of the reaction rates versus the amounts of adsorption are shown in Table 28, and 29 for temperatures of 75° and $95^\circ C$ respectively. As can be seen, the rate is proportional to the square of the volume of gas adsorbed. In Chapter 3, a correlation based on the assumption that one or two molecules may be adsorbed on one site and that the reaction occurs only on those sites upon which two molecules are adsorbed, predicts that the rate should be proportional to the square of the total amount of gas adsorbed. The agreement between the experimental value and the theoretical value is good. Further proof that one site is capable of adsorbing two molecules is necessary. But in the present system it is very difficult to get this information, because the catalyst support also adsorbs ethylene, and the results obtained so far do not indicate that the amount of gas adsorbed exceeds the total number of available surface sites. For the adsorption of ethylene on $5.06\% Re_2O_7/Al_2O_3$ at room temperature, if the Langmuir isotherm is followed, a monolayer volume of 3.5 ml/gm @ STP is obtained.

Table 28. Correlation of the Reaction Rate of the Disproportionation of C_2H_3D with the Amount of Adsorption at $75^\circ C$ on 10.81% Re_2O_7/Al_2O_3 .

P(C_2H_3D) (atm)	Rate $\times 10^4$ (gm mol/gm/hr)	V(C_2H_4) (ml/gm @STP)	Relative Deviation (E-C)/E	
			Plot of lnR vs. lnV	Plot of ln(R/P) vs. lnV
1.0	6.20	1.3343	-0.000731	-0.000318
0.826	4.36	1.1302	0.002942	0.002331
0.667	3.09	0.9249	-0.002978	-0.002885
0.435	1.41	0.6285	0.000705	0.000859
		Ave.	0.001852	0.001598

$$\ln(R) = -7.95391 + 1.95113 \ln(V) \quad \frac{1.95113-2}{2} = -2.44\%$$

$$\ln(R/P) = -7.63305 + 0.849196 \ln(V) \quad \frac{0.849196-1}{1} = -15.08\%$$

Table 29. Correlation of the Reaction Rate of the Disproportionation of C_2H_3D with the Amount of Adsorption at $95^\circ C$ on 10.81% Re_2O_7/Al_2O_3 .

P(C_2H_3D) (atm)	Rate $\times 10^4$ (gm mol/gm/hr)	V(C_2H_3D) (ml/gm @ STP)	Relative Deviation (E-c)/E	
			Plot of $\ln(R)$ vs. $\ln(V)$	Plot of $\ln(R/P)$ vs. $\ln(V)$
1.0	6.94	0.981	0.003106	0.000928
0.826	4.94	0.804	-0.005517	-0.002154
0.64	3.11	0.657	0.001267	0.002305
0.58	2.74	0.617	0.001120	-0.001089
Average:			0.002753	0.001619

$$\ln(R) = -7.21145 + 2.03308 \ln(V) \quad \frac{2.03308-2}{2} = +1.65\%$$

$$\ln(R/P) = -7.24976 + 0.86197 \ln(V) \quad \frac{0.86197-1}{1} = -13.80\%$$

If there are 10^{15} surface sites per square centimeter, a monolayer volume of 3.5 ml/gm @ STP only corresponds to 10% of the total sites available. The experimental results show that proper interaction between the promoter (Re_2O_7) and the support (Al_2O_3 or SiO_2) is necessary for the disproportionation reaction to occur. Therefore, measurement of the adsorption of ethylene on the promoter Re_2O_7 alone still does not mean much as far as the reaction is concerned. Upon reduction, irreversible sites are generated and these sites are very likely the anion vacancies, and it is still impossible to distinguish the amount of adsorption on the support and on the promoter. Further, alumina sites may enter the reaction mechanism as feeder sites to the Rhenium sites upon which reaction actually occurs.

On the disproportionation of olefins, there are numerous references exploring the detailed reaction mechanism, and looking into the formation of the surface complex in terms of the molecular orbital transformation. It appears consistent that the reaction occurs through a four center intermediate with two olefins forming a surface complex with a catalytic site. That is the Langmuir-Hinshelwood type of mechanism is more likely than the Rideal mechanism, since the Rideal mechanism requires only one adsorbed molecule to react with the molecule in gas phase.

In the Langmuir Hinshelwood mechanism, $\text{Rate} = k\theta^2 = k(V/V_m)^2$, and rate is proportional to V^2 . In the Rideal mechanism, $\text{Rate} = k'P\theta = k'PV/V_m$, and rate is proportional to the product of P and V. If V is proportional to P to the first power, then there will be no difference in the slopes on the plots of $\log(R)$ versus $\log(V^2)$ and $\log(R)$ versus $\log(PV)$.

If the Langmuir Hinshelwood mechanism is true, a plot of $\log R$ versus $\log V$ should yield a straight line with slope of 2. At 75°C the slope is 1.95113 and at 95°C it is 2.03345. The relative deviations are -2.44% and +1.65% respectively.

If the Rideal mechanism is true, a plot of $\log(R/P)$ versus $\log V$ should yield a straight line with slope of 1. At 75°C the slope is 0.849196 and at 95°C it is 0.86197. The relative deviations are -15.08% and -13.80% respectively.

Obviously the Langmuir Hinshelwood mechanism fits the rate data better than the Rideal mechanism at both 75° and 95°C.

In general, the reaction rate can be expressed as a product of a temperature-dependent term and a composition-dependent term, or $R = k \times f(\text{composition})$. The temperature-dependent term, the reaction rate constant, has been found in practically all cases to be well represented by Arrhenius' law: $k = k_0 e^{-E/RT}$, where k_0 is called the frequency factor and E is called the activation energy. Thus the activation energy can be obtained from the slope of the plot of $\log k$ versus $1/T$. Now we have the rate data at two temperatures, namely 75° and 95°C, so we can calculate the activation energy. In the Langmuir Hinshelwood mechanism, $R = k\theta^2$, and $k = k_0 e^{-E/RT}$, a value of E of 9.5 Kcal. is obtained. In the Rideal mechanism, $R = k'P \theta$, and $k' = k'_0 e^{-E'/RT}$, a value of E' of 4.9 Kcal. is obtained. In the power law, $R = k'' p^n$ ($n \approx 1.75$), and $k'' = k''_0 e^{-E''/RT}$, a value of E'' of 1.3 Kcal. is obtained.

The following will show that all activation energies are consistent - merely corrected for heat of adsorption.

(i). Langmuir Hinshelwood mechanism:

$$R = k \theta^2 = k_0 e^{-E/RT} \theta^2 \quad E = 9.5 \text{ Kcal (experimental)}$$

(ii). Rideal mechanism:

$$R = k' P \theta = k'_0 e^{-E'/RT} P \theta \quad E' = 4.9 \text{ Kcal (experimental)}$$

Let $\theta = KP$ where K is the adsorption constant, and

$$K = e^{\Delta S/R} e^{-\Delta H/RT}$$

$$\text{Thus, } R = k' P \theta = (k'/K) \theta^2 = (k'_0 / e^{\Delta S/R}) e^{-(E' - \Delta H)/RT} \theta^2$$

Therefore, $E = E' - \Delta H$

From the previous result $E = 9.5$ Kcal, and from the adsorption isotherms
 $-\Delta H \cong 6.2$ Kcal.

So, the apparent activation energy $E' = E + \Delta H = 9.5 - 6.2 = 3.3$,
 as compared to the experimental value of 4.9.

(iii). Power law:

$$R = k'' P^n = k''_0 e^{-E''/RT} P^n \quad E'' = 1.3 \text{ Kcal (experimental).}$$

Let $\theta = KP$

$$\text{Then } R = (k''/K^n) \theta^n = (k''_0 / e^{n\Delta S/R}) e^{-(E'' - n\Delta H)/RT} \theta^n$$

$$E'' - n \Delta H = E = 9.5$$

$$n \cong 1.75$$

$E'' = 9.5 - 1.75 \times 6.2 = 1.3$ Kcal, as compared to the experimental
 value of 1.3 Kcal.

In the determination of a reaction mechanism, people usually assume that the reaction is in adsorption equilibrium but can not give any proof. In the present case, the adsorption equilibrium is reached within the limit of isotope effect which is relatively small. It is important to emphasize the establishment of adsorption equilibrium because it is dangerous to make assumptions without justification, and the final result may be misleading.

Incidentally, in determining the reaction mechanism, people usually assume a Langmuir type of isotherm but really don't have any idea what the true isotherm is. In this work the adsorption isotherm is measured, and no assumption is necessary, therefore, the result is much more reliable.

CHAPTER VII

CONCLUSIONS AND RECOMMENDATION

In this work, the adsorption and disproportionation of ethylene over supported rhenium oxide catalysts have been studied.

Adsorption of ethylene on the supports, and on the supported catalysts at various temperatures has given the following information:

1. Both unreduced and reduced supports (silica or alumina) adsorb reversibly.
2. Unreduced catalysts supported on silica or alumina adsorb reversibly.
3. Catalysts supported on alumina which is reduced 15 hours at 500°C adsorb reversibly and irreversibly. Catalysts supported on silica which is reduced 15 hours at 500°C adsorb reversibly, but in an intermediate state of reduction the adsorption is partially irreversible. Namely, catalysts supported on alumina are more resistant to reduction than catalysts supported on silica.
4. Reversible adsorption is constant and independent of reduction time.
5. Irreversible adsorption occurs on anion vacancies.
6. For the unreduced catalysts, the heats of adsorption calculated from the adsorption isotherms are in the range of physical adsorption.
7. Isosteric entropies indicate some mobility on unreduced catalysts.
8. In general, the Freundlich isotherm fits the data best.

Studies of the kinetics of propylene disproportionation have yielded the following information:

1. Both unreduced and reduced catalysts supported on silica have no activity for propylene disproportionation at temperatures below 180°C.
2. Interaction between the promoter and the support is necessary for the disproportionation reaction to occur.
3. Reaction on 20% $\text{Re}_2\text{O}_7/\text{Al}_2\text{O}_3$ catalyst is bulk diffusion limited at room temperature.
4. Rates on unreduced catalysts supported on alumina decay slowly with time. At 1 atmosphere pressure or below the rate is proportional to the propylene partial pressure to the 1.4th power at temperatures between 25° and 68°C.
5. Rates on reduced catalysts decrease to the constant value for unreduced catalysts, as the irreversible sites are filled.
6. Cis-2-butene is the more favorable product of disproportionation and the isomerization sites are poisoned by the irreversible adsorption.
7. The Langmuir-Hinshelwood mechanism fits the data better than the Rideal mechanism, and the empirical power law fits the data best.

Studies of the adsorption and the disproportionation of mono-deuterated ethylene have given the following information:

1. The reaction proceeds efficiently with no scrambling effects.
2. No cyclobutane is found during the reaction.
3. The isotope effect is small at high ethylene pressures, and at high temperature.
4. About 50% conversion is obtained at equilibrium.

5. The reaction rate is proportional to the square of the amount of adsorption.
6. The Langmuir-Hinshelwood mechanism fits the rate data better than the Rideal mechanism.

In order to have a better understanding of the catalyst and this catalytic reaction, following are some suggestions which might be worth trying:

1. Infrared spectroscopic study on the irreversibly adsorbed species.
2. Measurement of hydrogen consumption at high temperature and pressure on the silica supported catalysts to gain information regarding the oxidation state of rhenium.
3. Carry out the adsorption up to the saturation point to determine the volume of a monolayer.
4. Calorimetric study on the adsorption of ethylene at very low coverage.
5. Flash desorption study on the ethylene saturated, 15 hours reduced catalyst supported on alumina.
6. Measurement of the rate of adsorption as a function of the level of reduction.
7. Measurement of the ratio of trans-2-butene to cis-2-butene as a function of the propylene flow rate to get information on the rate of isomerization.
8. Kinetic study on the reaction rate as a function of the rhenium content of the catalyst.
9. Try other supports which will not adsorb ethylene yet have activity for disproportionation.

NOMENCLATURE

A	Area occupied by a molecule; Peak area of Chromatogram.
a	Constant in Temkin equation.
b	Constant in Langmuir equation.
b_1	Probability of a molecule been adsorbed on one site.
b_2	Probability of two molecules been adsorbed on one site.
C	Constant in B E T equation; Calculated value.
C_0	Constant in Temkin equation.
E	Activation energy; Experimental value.
F	Flow rate.
f	Substance-specific correction factor.
G	Gibb's free energy.
H	Enthalpy.
I	Intercept.
K	Constant in Henry equation; Adsorption constant.
K_b	Adsorption equilibrium constant for butene.
K_e	Adsorption equilibrium constant for ethylene.
K_p	Adsorption equilibrium constant for propylene.
k	Constant in Freundlich equation; Proportionality constant; Rate constant.
k_a	Adsorption constant.
k_d	Desorption constant.
k_r	Surface reaction rate constant.
k_s	Surface reaction rate constant.
M	Molecular weight.

N_i	Number of moles of component i.
n	Constant in Freundlich equation.
P	Equilibrium pressure.
P_o	Pressure in the adsorbed layer; Saturation vapor pressure.
P_b	Partial pressure of butene.
P_e	Partial pressure of ethylene.
P_p	Partial pressure of propylene.
q_i	Isosteric heat of adsorption.
q_d	Differential heat of adsorption.
R	Gas constant; Rate of reaction.
r_i	Rate of reaction of component i.
$r_{i\text{ave}}$	Average rate of reaction of component i.
r_a	Rate of adsorption.
r_d	Rate of desorption.
r_s	Rate of surface reaction.
r_{a1}	Rate of adsorption of a molecule on an empty site.
r_{a2}	Rate of adsorption of a molecule on a site which has already adsorbed one molecule.
r_{d1}	Rate of desorption of a molecule from sites which adsorbed two molecules.
r_{d2}	Rate of desorption of a molecule from sites which adsorbed only one molecule.
S	Entropy; Slope; Surface site.
3^S trans.	The translation entropy of a perfect gas in three dimensions.
2^S trans.	The translation entropy of a perfect gas in two dimensions.
S_{config}	Configurational entropy.

S_{vib}	Vibrational entropy.
T	Absolute temperature.
V	Volume of gas adsorbed.
V_1	Space velocity of component 1.
V_m	Monolayer volume.
V_t	Total amount of gas adsorbed.
V_1	Volume of gas adsorbed with one molecule on one site.
V_2	Volume of gas adsorbed with two molecules on one site.
W	Weight of catalyst.
x	Conversion
ν	Vibrational frequency.
θ	Fraction of surface coverage.

BIBLIOGRAPHY

1. Bailey, G. C. "Olefin Disproportionation" *Catalysis Reviews* 3 (1), 37 (1969)
2. Banks, R. L.; and Bailey, G. C. "Olefin Disproportionation - a New Catalytic Process" *I & E C Product R & D* 3, 170 (1964)
3. Banks, R. L.; and Bailey, G. C. "Four-Center Mechanism for Olefin Reactions" *Journal of Catalysis* 14, 276 (1969)
4. Begley, J. W.; and Wilson, R. T. "The Kinetics of Propylene Disproportionation" *Journal of Catalysis* 9, 375 (1967)
5. Biemann, K. "Mass Spectrometry - Organic Chemical Applications" McGraw-Hill Book Company, Inc. New York 1962
6. Biolen, P.; and Pott, G. T. "X-ray Photoelectron Spectroscopy Study of Supported Tungsten Oxide" *Journal of Catalysis* 30, 169 (1973)
7. Bond, G. C. "Catalysis by Metals" Academic Press, London 1962
8. Bradshaw, C. P. C.; Howman, E. J.; and Turner, L. "Olefin Dismutation: Reactions of Olefins on Cobalt Oxide-Molybdenum Oxide-Alumina" *Journal of Catalysis* 7, 269 (1967)
9. British Petroleum Co. Ltd. British Patent 1054864
10. British Petroleum Co. Ltd. British Patent 1096200
11. Brunauer, S.; Deming, L.S.; Deming, W. E.; and Teller, E. J. *Journal of American Chemical Society* 62 1723 (1940)
12. Calderon, N.; Chen, H. Y.; and Scott, K. W. *Tetrahedron Letters* 3727(1967); *Chemical Engineering News* 45, 51 (1967)
13. Calderon, N.; Ofstead, E. A.; Ward, J. P.; Judy, W. A.; and Scott, K. W. "Olefin Metathesis" *J. A. C. S.* 90 4133 (1968)
14. Cassar, L.; Eaton, P.; and Halpern, J. *Journal of American Chemical Society* 92, 6366 (1970)
15. Clark, A.; and Cook, C. "The Mechanism of Propylene Disproportionation" *Journal of Catalysis* 15, 420 (1969)

16. Clark, A. "The Theory of Adsorption and Catalysis" Academic Press, Inc. New York 1970
17. Clark, A. "The Chemisorptive Bond -Basic Concepts" Academic Press, Inc. New York 1974
18. Colton, R. "The Chemistry of Rhenium and Technetium" Interscience Publishers, New York 1969
19. Crain, D. L. "The Mechanism of Olefin Disproportionation" Journal of Catalysis 13, 110 (1969)
20. Davenport, W. H.; Kollinitsch, V.; and Kline, C. H. "Advances in Rhenium Catalysts" I & E C 60, 10 (1968)
21. Davie, E. S.; Whan, D. A.; and Kemball, C. "Reactions of Butenes on a supported Molybdenum Hexacarbonyl Catalyst" The Proceedings of the Fifth International Congress on Catalysis, No. 86, Page 1025, North-Holland Publishing Co. Amsterdam 1973
22. Dowden, D. A. Anles real Soc. espan. Fis. Quim. 61 326 (1965)
23. Druce, J. G. F. "Rhenium" Cambridge University Press London 1948
24. Greiner, J. D.; and Shanks, H. R. "The Magnetic Susceptibility of Rhenium Trioxide" Journal of Solid State Chemistry 5, 262 (1972)
25. Grubbs, R.H.; and Brunck, T. K. J. A. C.S. 94, 2358 (1972)
26. Heckelsberg, L. F.; Banks, R. L.; and Bailey, G. C. "A Tungsten Oxide on Silica Catalyst for Phillips' Triolefin Process" I & E C Product R & D 7, 29 (1968)
27. Hill H. C. "Introduction to Mass Spectrometry" Heyden & Son Ltd., London 1966
28. Heckelsberg, L. F.; Banks, R. L.; and Bailey, G. C. "Olefin Disproportionation Catalysts" I & E C, Product R & D 8, No. 3, 259 (1969)
29. Heckelsberg, L. F. Belgian Patent 713185
30. Hoffmann, R.; and Woodward, R. B. "The Electronic Mechanism of Electrocyclic Reactions" J. A. C. S. 87, 2045 (1965)
31. Hughes, W. B. "Stereochemistry of the Homogeneous Disproportionation of 2-Pentene" Chemical Communications 431 (1969)
32. Hughes, W. B. "Kinetics and Mechanism of the Homogeneous Olefin Disproportionation Reaction" J. A. C. S. 92, 532 (1970)
33. Hughes, W. B.; Zuech, E. A.; Kittleman, E. T.; and Kubicek, D. H. "Homogeneous Catalysts for Olefin Disproportionation"

34. Jeitschko, W.; and Sleight, A. W. *Journal of Solid State Chemistry* 4, 324 (1970)
35. Johnson, M. F. L.; and LeRoy, V. M. "The State of Rhenium in Pt/Re/ Al_2O_3 Catalysts" *Journal of Catalysis* 35, 434 (1974)
36. Kaiser, R. "Gas Phase Chromatography" Volume III. Butterworth & Co. Ltd., London, 1963
37. Kokes, R. J. and Dent, A. L. "Hydrogenation and Isomerization over ZnO " *Advances in Catalysis* 22. ; (1972)
38. Levenspiel, O. "Chemical Reaction Engineering" John Wiley & Sons, Inc. New York 1962
39. Lewandos, G. S.; and Pettit, R. "A Proposed Mechanism for the Metal Catalyzed Disproportionation Reaction of Olefins" *Tetrahedron Letters* No. 11, 789 (1971)
40. Lewandos, G. S. Ph.D. Thesis, The University of Texas at Austin 1972
41. Lewis, M. J.; and Wills, G. B. "Initial Rates of Propylene Disproportionation" *Journal of Catalysis* 15, 140 (1969)
42. Linsen, B. G. "Physical and Chemical Aspects of Adsorbents and Catalysts" Academic Press, London 1970
43. Luckner, R. C.; McConchie, G. E.; and Wills, G. B. "Initial Rates of Propylene Disproportionation over WO_3 on Silica Catalysts" *Journal of Catalysis* 28, 63 (1973)
44. Luckner, R. C.; and Wills, G. B. "Transient Kinetics of the Disproportionation of Propylene over a Tungsten Oxide on Silica Catalyst" *Journal of Catalysis* 28, 83 (1973)
45. Mango, F. D. "Molecular Orbital Symmetry Conservation in Transition Metal Catalysis" *Advances in Catalysis* 20, 291 (1969)
46. Massoth, F. E. "Studies of Molybdena-Alumina Catalysts, II. Kinetics and Stoichiometry of Reduction" *Journal of Catalysis* 30, 204 (1973)
47. Moffat, A. J.; and Clark, A. "Rate Temperature Maximum for the olefin Disproportionation Reaction" *Journal of Catalysis* 17, 264 (1970)
48. Moffat, A. J.; Johnson, M. M. and Clark, A. "Mass Transfer Effects in the Olefin Disproportionation Reaction" *Journal of Catalysis* 18, 345 (1970)

49. Moffat, A. J.; Clark, A., and Johnson, M. M. "Mass Transfer Effects in the Olefin Disproportionation Reaction. I. Promoter Concentration and Temperature Effects for Propylene on WO_3 -Silica Catalysts" *Journal of Catalysis* 22, 379 (1971)
50. Moffat, A. J. "Site-Localized Diffusional Effects" *Journal of Catalysis* 24, 170 (1972)
51. Mol, J. C.; Moulijn, J. A.; and Boelhouwer, C. "On the Mechanism of the Disproportionation of Olefins" *Journal of Catalysis* 11, 87 (1968)
52. Mol, J. C.; Moulijn, J. A.; and Boelhouwer, C. "Carbon-14 Studies on the Mechanism of the Disproportionation of Propene" *Chemical Communications* 633 (1968)
53. Orchin, M. and Jaffe, H. H. "The Hoffman-Woodward Rules for Electrocyclic Reactions" Chapter 5.
54. Peacock, R. D. "The Chemistry of Technetium and Rhenium" Elsevier Publishing Co. Amsterdam 1966
55. Pennella, F.; and Banks, R. L. "The Influence of Chelating Polyolefins on the Disproportionation of Propylene Catalyzed by WO_3 on Silica" *Journal of Catalysis* 31, 304 (1973)
56. Pennella, F.; Regier, R. B.; and Banks, R. L. "The Influence of Ligands on the Disproportionation of Olefins Catalyzed by Tungsten Oxide on Silica" *Journal of Catalysis* 34, 52 (1974)
57. Rao, C. N. R. "Transition Metal Oxides" from *Solid State Chemistry*" Marcel Dekker, Inc., New York 1974
58. Satterfield, C. N. "Mass Transfer in Heterogeneous Catalysis" MIT Press Cambridge, Mass. 1970
59. Schneider, V.; and Frolich, P. K. *I E C* 23, 1405 (1931)
60. Sidgwick, N. V. "The Chemical Elements and Their Compounds" Oxford University Press, London 1950
61. Thomas, J. M.; and Thomas, W. J. "Introduction to the Principles of Heterogeneous Catalysis" Academic Press, London 1967
62. Trapnell, B. M. W. "Chemisorption" Butterworths Scientific Publications, London 1955
63. Tribalat, S. "Rhenium and Technetium" Gauthier-Villars, Paris 1957
64. Zeuch, E. A. "Homogeneous Catalysts for Olefin Disproportionation" *Chemical Communications* 1182 (1968)

65. Zeuch E. A.; Hughes, W. B.; Kubicek, D. H.; and Kittleman, E. T. "Homogeneous Catalysts for Olefin Disproportionations from Nitrosyl Molybdenum and Tungsten Compounds" J. A. C. S. 92, 528 (1970)
66. Wang, J.; and Menapace, H. R.; Journal of Organic Chemistry 33, 3794 (1968)
67. Wells, A. F. "Structural Inorganic Chemistry" Oxford University Press, Amenhouse, London 1962
68. Woodward, R. B.; and Hoffmann, R.; J. A. C. S. 87, 2046 (1965)
69. Handbook of Chemistry and Physics. Page D-75

APPENDICES

APPENDIX A

Gas Chromatographic Analysis of the Products From The Disproportionation of Propylene

In order to determine the reaction rate, it is necessary to know the composition of the reaction products. Gas chromatographic separation of ethylene, propylene, and butenes was found to be a convenient method of analysis for this purpose.

Originally, two columns, 8' in length by 1/8" in diameter, packed with Porapak T were installed in the chromatograph used. The reaction products were passed through the column at 130°C, and a thermoconductivity detector at 30°C, and helium was used as carrier gas. The chromatogram was obtained within 6 minutes at a helium flow rate of 25 ml/min. The time of analysis is satisfactory but the resolution for trans-2-butene and cis-2-butene is no good. Therefore the Porapak T columns were changed to columns, 14' in length by 1/8" in diameter, packed with 20% bis-2-methoxy ethyl adipate on chromosorb P. The analysis was done at room temperature, and the chromatogram was obtained within 5 minutes at a helium flow rate of 25 ml/min. The peaks obtained were essentially symmetric, and the resolution for trans- and cis-2-butenes was much improved.

The quantitative result was obtained by determining the peak area. The area may be obtained by weighing, by planimetry, by approximations (peak height multiplied by peak width at half height or peak height

times the retention time), or by the use of an electronic integrator. The first three methods were tried, and compared, and the differences were small. Since measurements of the peak height and peak width at half height were the easiest one, the peak area was determined through this way.

The weight percent of substance 1 in the mixture was calculated by the following equation:³⁶

$$\text{Wt. \% of 1} = \frac{A_1 f_1 \times 100}{\text{Sum of all A f values}} \quad (\text{A-1})$$

where A_1 = peak area of substance 1.

f_1 = substance-specific correction factor for substance 1.

Equal amounts of different substances give rise to peak areas of different sizes in the gas chromatogram. The area multiplied by the appropriate f values have the same value for equal weights of different substances. In recent years a whole series of authors have contributed to the subject of substance-specific correction factors. These factors depend on the type of detector and the kind of carrier gas used. Correction factors show systematic properties in relation to the substance to be detected. The values, relative to benzene of 1.000, for some olefins are shown in Table 30. They are based on the work of Messner, Rosie, and Argabright. (Analytic Chemistry, 31 230, 1959)

After the peak areas were measured, the weight percent of each component was obtained using equation (A-1).

Table 30. Substance-Specific Correction Factors for Thermoconductivity
Cells Using Helium as Carrier Gas. (Benzene=1.000)

Substance	Correction Factor(f)
Ethylene	0.731
Propylene	0.816
Butene-1	0.867
Iso-butene	0.874
Trans-2-butene	0.841
Cis-2-butene	0.822
Butadiene 1,3	0.865

in general, $f_i = \frac{1.282 M_i}{1.20 M_i + 13.0}$

where M_i is the molecular weight of substance i .

APPENDIX B

Mass Spectrographic Analysis of the Products From the Disproportionation of Monodeuterated Ethylene.

Mass spectrometer has been widely used as an highly accurate analytic instrument for both quantitative and qualitative purposes. Its operating principles were described rather extensively in the literatures.^{5,29} It is especially useful for the quantitative determination of the extent of isotope incorporation.

Ethylene consists of carbon and hydrogen. The natural abundance for C^{12} to C^{13} is 1 to 0.0108, and for H^1 to H^2 (or D) is 1 to 0.00016. The theoretical isotopic abundance ratio for ethylene of mass 28, 29, and 30 is 100:2.23:0.01. Nitrogen and carbon monoxide also have masses of approximately 28, and which will result a overlap of the mass peak if high resolution mass spectrometer is not used. The mass spectrometer used in this work has a resolution of over 1100, and is capable of separating the ethylene and the nitrogen peaks, but in order to get rid of the interference the nitrogen content of the sample is kept to a minimum, i.e. air leak to the sample is kept as small as possible. Another encouraging fact is that at low ionization voltage the ionization of nitrogen is rather small as compared to ethylene or oxygen.

Ethylene has an appearance potential of 10.56 eV, that is if the ionization potential is equal to or less than 10.56 eV only molecular

ions will be produced. It is important that no fragmentation of the molecule is permitted in order to determine the composition of the deuterated products. The analysis is based on that the mass peak height is proportional to partial pressure of the corresponding component. At the usual operating pressures of the mass spectrometer, Dalton's law of partial pressure applies, and the peak heights are quantitatively additive. The composition can be calculated by solving the simultaneous linear equations. During this calculation it is assumed that the relative abundance of the peaks in the molecular ion group of each species is the same.²⁷

For the undeuterated ethylene molecule, the relative abundance of the peaks 28, 29, and 30 is determined first. Usually, the ratio is about 100:3:0. For the deuterated mixtures, the peaks are contributed to by each species as follows:

	Mass Peak	
Undeuterated	<u>28</u>	<u>29</u>
Monodeuterated	<u>29</u>	<u>30</u>
Dideuterated	<u>30</u>	<u>31</u>
Trideuterated	<u>31</u>	<u>32</u>
All-deuterated	<u>32</u>	<u>33</u>

The calculation of the percentage composition of the mixture is given by the following example.

Example:

The observed relative peak heights for the undeuterated ethylene are 100: 3.0154 : 0, for mass peaks 28, 29, and 30. There are no other peaks observed. If the observed peak heights for the deuterated mixture were

Mass Peak	<u>28</u>	<u>29</u>	<u>30</u>	<u>31</u>
Relative Height	6.5510	100	8.9686	0.00

the following reasoning could be applied.

Peak 28 is due solely to the undeuterated molecule. Its contribution to 29 is $6.5510 \times 0.030154 = 0.1975$. The 29 peak contains 100 minus the contribution from 28 ($100 - 0.1975 = 99.8025$) due to the monodeuterated species. The contribution to peak 30 from the monodeuterated species is $99.8025 \times 0.030154 = 3.0094$. So the contribution to peak 30 from the dideuterated species is $8.9686 - 3.0094 = 5.9592$. Since no peak was detected at 31, there would be no trideuterated or all-deuterated ethylene presented. The correct peak height for each species is therefore:

Nondeuterated	Monodeuterated	Dideuterated	Trideuterated
6.5510	99.8025	5.99592	0

The percentage composition of the mixture is:

Nondeuterated	Monodeuterated	Dideuterated
$\frac{6.5510}{6.5510+99.8025+5.952}$	$\frac{99.8025}{6.5510+99.8025+5.952}$	$\frac{5.9592}{6.5510+99.8025+5.9592}$
=5.8228%	=88.8613%	=5.3059%

APPENDIX C

Least Square Fitting of the Adsorption Data to the
Various Adsorption Isotherms.

As discussed in Chapter 3, three theoretical isotherms, those of Langmuir, Freundlich and Temkin are important. The isotherm equations, after rearrangement are as follows:

1. Non-dissociative Langmuir isotherm:

$$\frac{P}{V} = \frac{1}{b V_m} + \frac{P}{V_m} \quad (\text{plot } P/V \text{ vs. } P, \text{ slope}=1/V_m, \text{ intercept}=1/(bV_m))$$

2. Dissociative Langmuir isotherm

$$\frac{\sqrt{P}}{V} = \frac{1}{\sqrt{b} V_m} + \frac{\sqrt{P}}{V_m} \quad (\text{plot } \sqrt{P}/V \text{ vs. } \sqrt{P}, \text{ slope}=1/V_m, \text{ intercept}=1/(\sqrt{b} V_m))$$

3. Langmuir isotherm with two molecules adsorbed on one site:

$$\frac{P^2}{V} = \frac{1}{b V_m} + \frac{P^2}{V_m} \quad (\text{plot } P^2/V \text{ vs. } P^2, \text{ slope}=1/V_m, \text{ intercept}=1/(bV_m))$$

4. Freundlich isotherm:

$$V = k P^{1/n} \quad \text{or} \quad \ln V = \ln K + \frac{1}{n} \ln P$$

(plot $\ln V$ vs. $\ln P$, slope = $1/n$, intercept = $\ln k$,
slope/absolute temperature = constant)

5. Temkin isotherm:

$$V = \frac{V_m}{a} \ln(C_0 P) \quad (\text{plot } V \text{ vs. } \ln P, \text{ slope}=V_m/a, \text{ intercept}=V_m \ln C_0/a,$$

slope/absolute temperature = constant)

where V =volume adsorbed (ml/gm at STP)

V_m = volume of monolayer (ml/gm at STP)

P = equilibrium pressure (torr)

a, b, C_0, k are constant.

The results of the least square fittings of the adsorption data to these isotherms are shown in the following tables. In these tables, S stands for slope; I, intercept; $\frac{E - C}{E}$ ave., average absolute relative deviation; and T, absolute temperature. The relative deviation is defined as the experimental value minus the calculated value obtained by least square method, then divided by the experimental value.

In general, Freundlich isotherm fits the data better than the other types of isotherm, especially at high temperatures. When the amount of adsorption is close to one ml/gm, the $\ln V$ value becomes very small, therefore a large relative deviation occurs, and in this case the average absolute relative deviation seems not to be a good criterion for the fitness of the isotherm.

	1. Non-disoc. Langmuir	2. Dissociati Langmuir	3. Two molecules On One Site	4. Freundlich	5. Temkin
25°C, Al ₂ O ₃ only, Unreduced, 10 data points.					
S	0.28264	=1.1388	0.60425	0.80588	0.46370
I	95.91455	26.71545	4623.179	-4.0021	-1.19649
$\frac{E-C}{E}$ ave.	0.03258	0.13183	0.61919	3.30513	0.36841
b	0.002984	0.001817	0.0001307	k 0.01827	V_m/a 0.4637
V_m	3.49355	-0.878054	1.65495	n 1.24088	lnC _o -2.5803
				S/T 0.002703	S/T 0.0015552
25°C, 1.47% Re ₂ O ₇ /Al ₂ O ₃ , Unreduced, 7 data points.					
S	0.30430	-1.38166	0.55350	0.80060	0.39595
I	76.83235	28.34995	3858.575	-3.8549	-0.74446
$\frac{E-C}{E}$ ave.	0.05962	0.21755	1.89401	0.10641	0.68655
b	0.003961	0.0023752	0.0001434	k 0.021195	V_m/a 0.39595
V_m	3.28626	-0.723767	1.80670	n 1.24907	lnC _o -1.88201
				S/T 0.00268513	X/T 0.00132797

	1.	2.	3.	4.	5.
25°C 5.06% Re ₂ O ₇ /Al ₂ O ₃ , Unreduced, 7 data points.					
S	0.28980	-0.86837	0.51710	0.76744	0.50132
I.	67.68445	20.77104	3278.902	-3.59097	-1.13674
$\frac{E-C}{E}$ ave.	0.04490	0.13537	0.90616	0.07279	0.37393
b	0.0042816	0.0017478	0.0001577	k 0.0275716V _m /a	0.501342
V _m	3.45065	-1.15158	1.93385	n 1.30303 lnC _o	-2.26748
				S/T 0.0025739	S/T 0.00168139

25°C, 9.18% Re₂O₇/Al₂O₃, Unreduced, 7 data points.

S	0.35988	-1.07034	0.57588	0.75317	0.38202
I	67.61873	24.23494	3436.708	-3.61267	-0.68786
$\frac{E-C}{E}$ ave.	0.07202	0.18143	2.06686	0.19108	0.57418
b	0.005322	0.0019505	0.00016757	k 0.02697797V _m /a	0.382015
V _m	2.77867	-0.934285	1.73647	n 1.32771 lnC _o	-1.80062
				S/T 0.0025261	S/T 0.00128124

	1.	2.	3.	4.	5.
25°C, 15.34% $\text{Re}_2\text{O}_7/\text{Al}_2\text{O}_3$, Unreduced, 7 data points.					
S	0.37607	-0.95551	0.63174	0.74640	0.40017
I	79.51282	23.97104	4137.109	-3.68726	-0.89140
$\frac{E-C}{E}$ ave.	0.05553	0.12441	1.02083	0.09930	0.35173
b	0.0047297	0.001589	0.0001527	k 0.02504	V_m/a 0.400168
V_m	2.65905	-1.04656	1.58293	n 1.33976	$\ln C_o$ -2.22756
				S/T 0.00250336	0.00134213

25°C, 21.39% $\text{Re}_2\text{O}_7/\text{Al}_2\text{O}_3$, Unreduced, 14 data points.					
S	0.50215	-1.52096	0.82884	0.75950	0.27348
I	108.0153	35.43057	5718.515	-4.05367	-0.55460
$\frac{E-C}{E}$ ave.	0.06688	0.18102	1.79277	0.17380	0.74699
b	0.00464886	0.0018428	0.0001449	k 0.17358	V_m/a 0.273475
V_m	1.99144	-0.657478	1.20650	n 1.31666	$\ln C_o$ -2.0280
				S/T 0.00254727	0.00091721

	1.	2.	3.	4.	5.
0°C, Al ₂ O ₃ only, Unreduced, 6 data points.					
S	0.24082	-0.70930	0.36819	0.74995	0.56819
I	31.635583	13.96070	1169.656	-2.95415	-0.78238
$\frac{E-C}{E}$ ave.	0.07749	0.21888	2.76654	0.10709	0.72726
b	0.0076123	0.0025813	0.00031479	k 0.05212	V_m/a 0.56819
V_m	4.15245	-1.40984	2.71598	n 1.33342	$\ln C_o$ -1.37697
				S/T 0.00274546	0.00208007

5.1°C, 10.95% Re₂O₇/Al₂O₃, Unreduced, 6 data points.

S	0.32207	-0.38792	0.41962	0.65044	0.48078
I	29.20781	11.31834	1330.385	-2.62464	-0.58728
$\frac{E-C}{E}$ ave.	0.13185	0.12776	4.14668	0.11494	0.49251
b	0.011027	0.00117468	0.0003154	k 0.0724654	V_m/a 0.48078
V_m	3.10487	-2.57785	2.38310	n 1.53743	$\ln C_o$ -1.22153
				S/T 0.00233742	0.0017277

	1.	2.	3.	4.	5.
1.1°C, 11.06% Re ₂ O ₇ /SiO ₂ , Unreduced, 7 data points.					
S	0.08761	-1.18561	0.29382	0.91177	0.79768
I	53.69946	20.52492	2154.036	-3.77457	-1.69798
$\frac{E-C}{E}$ ave.	0.01538	0.30141	1.09127	0.05338	0.9108
b	0.00163156	0.00333672	0.0001364	k 0.022947	V_m/a 0.797677
V_m	11.4137	-0.843448	3.40343	n 1.09676	$\ln C_o$ -2.12865
				S/T 0.00332437	0.00290837

1.1°C, 11.06% Re ₃ O ₇ /SiO ₂ , Reduced 15 hours, 6 data points.					
S	0.17010	-0.69767	0.28998	0.76632	0.67815
I	35.24725	13.81733	1719.907	-2.97935	-1.01484
$\frac{E-C}{E}$ ave.	0.13464	0.16305	3.68698	0.04454	0.76239
b	0.004826	0.0025495	0.0001686	k 0.050826	V_m/a 0.67816
V_m	5.87878	-1.43335	3.44849	n 1.30494	$\ln C_o$ -1.49649
				S/T 0.0027951	0.0024736

	1.	2.	3.	4.	5.
22°C, 10.81% Re ₂ O ₇ /Al ₂ O ₃ , Unreduced, 7 data points.					
S	0.33715	-0.70058	0.6167	0.73090	0.49548
I	85.82045	20.59294	4629.527	-3.60714	-1.35847
$\frac{E-C}{E}$ ave.	0.04572	0.05220	0.44069	0.79089	0.7601
b	0.00392856	0.0011574	0.00013321	k 0.027129	V_m/a 0.49548
V_m	2.96603	-1.42738	1.62154	n 1.36818	$\ln C_o$ -274173
				S/T 0.00247628	0.00167868

	1.	2.	3.	4.	5.
22°C, 10.81% Re ₂ O ₇ /Al ₂ O ₃ , Unreduced, 7 data points (C ₂ H ₃ D adsorption)					
S	0.34175	-0.56503	0.58090	0.70804	0.52294
I	74.28262	17.91171	4105.945	-3.40881	-1.40816
$\frac{E-C}{E}$ ave.	0.03732	0.05824	0.41069	0.08091	0.15092
b	0.0046007	0.0009951	0.00014148	k 0.03308	V_m/a 0.522943
V_m	2.92611	-1.76982	1.72147	n 1.41234	$\ln C_o$ -2.69276
				S/T 0.00239885	0.0017717

	1.	2.	3.	4.	5.
75°C, 10.81% Re ₂ O ₇ /Al ₂ O ₃ , Unreduced, 7 data points.					
S	0.55884	-4.44617	1.75568	0.87738	0.16409
I	365.7607	94.81708	19607.54	-5.51685	-0.46974
$\frac{E-C}{E}$ ave.	0.02901	0.12450	0.49276	0.00928	0.33523
b	0.0015279	0.0021989	0.00008954	k 0.0040185	V_m/a 0.1641
V_m	1.78943	-0.224913	0.56579	n 1.13976	$\ln C_o$ -2.8628
				S/T 0.002520	0.0004713

95°C, 10.81% Re ₂ O ₇ /Al ₂ O ₃ , Unreduced, 7 data points.					
S	0.56028	-7.6828	2.55628	0.91729	0.11229
I	609.3859	156.7211	32623.61	-6.14441	-0.33045
$\frac{E-C}{E}$ ave.	0.02253	0.13876	0.47920	0.00381	0.37959
b	0.009194	0.0024035	0.00007836	k 0.002145	V_m/a 0.112295
V_m	1.78483	-0.130153	0.391194	n 1.09017	$\ln C_o$ -2.94274
				S/T 0.0024916	0.00030502

	1.	2.	3.	4.	5.
25°C, SiO ₂ only, Unreduced, 10 data points.					
S	0.12585	-1.40483	0.48401	0.90507	0.59575
I	104.8853	5067.398	-4.36489	-1.67068	
$\frac{E-C}{E}$ ave.	0.01976	0.14958	0.50006	0.02809	0.42897
b	0.0011999	0.0023986	0.000095513	k 0.01716	V_m/a 0.59574
V_m	7.94594	-0.711832	2.06609	n 1.104488	$\ln C_o$ -2.80435
				S/T 0.0030355	0.0019981

25°C, 5.72% Re₂O₇/SiO₂, Unreduced, 7 data points.

S	0.11802	-2.54133	0.51212	0.93505	0.42817
I	106.5503	42.72853	4484.546	-4.51226	-0.88256
$\frac{E-C}{E}$ ave.	0.01926	0.35426	1.34367	0.26275	1.16379
b	0.0011076	0.0035374	0.0001142	k 0.01097	V_m/a 0.428175
V_m	8.47316	-0.393494	1.95265	n 1.06946	$\ln C_o$ -2.06121
				S/T 0.0031306	0.0014361

	1.	2.	3.	4.	5.
25°C, 5.72% Re ₂ O ₇ /SiO ₂ , Reduced, 5 data points.					
S	0.22837	-1.65051	0.522w1	0.83212	0.41042
I	81.91373	30.71545	3409.204	03.9614	00.76703
$\frac{E-C}{E}$ ave.	0.12135	0.18680	2.24259	0.08023	0.94702
b	0.0027879	0.0028875	0.0001532	k 0.019037	V_m/a 0.41042
V_m	4.37888	-0.605875	1.9494	n 1.20175	$\ln C_o$ -1.8689
				S/T 0.0027909	0.0013765

25°C, 11.96% Re₂O₇/SiO₂, Unreduced, 5 data points.

S	0.06456	-1.15311	0.47520	0.94049	0.76978
I	122.0964	25.70972	6994.246	-4.59167	-2.62138
$\frac{E-C}{E}$ ave.	0.01368	0.06211	0.18677	0.03543	0.16313
b	0.00052873	0.00251116	0.00006794	k 0.01014	V_m/a 0.76978
V_m	15.4904	-0.867222	2.10438	n 1.06327	$\ln C_o$ -3.4054
				S/T 0.0031543	0.00258176

	1.	2.	3.	4.	5.
25°C, 11.96% Re ₂ O ₇ /SiO ₂ , Reduced, 5 data points.					
S	0.13549	-0.96322	0.50397	0.88601	0.74628
I	111.8327	23.23357	6326.23	-4.31671	-2.51022
$\frac{E-C}{E}$ ave.	0.01440	0.05069	0.16324	0.01291	0.12979
b	0.00112212	0.00171879	0.00007966	k 0.0133437	V_m/a 0.746279
V_m	7.96874	-1.03818	1.98424	n 1.12866	$\ln C_o$ -3.36364
				S/T 0.00297158	0.002503

25°C, 21.05% Re₂O₇/SiO₂, Unreduced, 7 data points.

S	0.09228	-3.46025	0.51836	0.95861	0.37861
I	122.5585	56.61061	5334.925	-4.72244	-0.69496
$\frac{E-C}{E}$ ave.	0.00838	0.50829	1.9536	0.10100	1.83631
b	0.0007529	0.0037361	0.00009716	k 0.0088934	V_m/a 0.37861
V_m	10.8366	-0.288997	1.92918	n 1.04317	$\ln C_o$ -1.83558
				S/T 0.0032151	0.00126981

	1.	2.	3.	4.	5.
25°C, 21.05% Re ₂ O ₇ /SiO ₂ , Reduced, 7 data points.					
s	0.15723	-2.41174	0.58868	0.91808	0.40631
I	118.3404	43.30334	5035.64	-4.56761	-0.90004
$\frac{E-C}{E}$ ave.	0.01904	0.28710	1.00311	0.06510	0.84367
b	0.00132861	0.0031018	0.00011690	k 0.0103828	v_m/a 0.40631
v_m	6.36018	-0.414639	1.69872	n 1.089923	$\ln C_o$ -2.21518
				S/T 0.0030792	0.0013627